SYNTHESIS AND CHARACTERIZATION OF ALKYLZIRCONIUM COMPLEXES FOR THE FABRICATION OF LOW WORK FUNCTION MATERIALS AND SYNTHESIS OF HYDANTOINS AND DIHYDROURACILS FROM AMINO AMIDES

By

SETH MICHAEL DUMBRIS

A DISSERTATION PRESENTED TO THE GRADUATE SCHOOL
OF THE UNIVERSITY OF FLORIDA IN PARTIAL FULFILLMENT
OF THE REQUIREMENTS FOR THE DEGREE OF
DOCTOR OF PHILOSOPHY

UNIVERSITY OF FLORIDA

2010

To SDG and to my loving wife, Molly

ACKNOWLEDGMENTS

I would like to thank my parents, Alan and Linda Dumbris, and siblings for their encouragement over the years. I would also like to thank my colleagues whom I have worked with in the McElwee-White laboratories, especially Phillip Shelton, Ampofo Darko, and Jennifer Johns. I would also like to thank Dr. Khalil Abboud and Jürgen Kohler for their assistance with the X-ray crystallography and Dempsey Hyatt for computational assistance.

TABLE OF CONTENTS

page

LIST OF TABLES

LIST OF FIGURES

LIST OF ABBREVIATIONS

AA-MOCVD	aerosol-assisted metal-organic chemical vapor deposition
amu	atomic mass unit
Bn	benzyl group
Boc	*tert*-butyl carbonyl group
BtOH	1-hydroxy-1H-benzotriazole
Cat.	any catalyst
Cbz	carbobenzyloxy group
CDI	1,1-carbonyldiimidazole
CI-MS	chemical ionization mass spectrometry
Cmpd	compound
CVD	chemical vapor deposition
DABCO	1,4-diazabicyclo[2.2.2]octane
DBU	1,8-diazabicyclo[5.4.0]undec-7-ene
DCB	1,4-dichloro-2-butene
DCE	1,2-dichloroethane
DCM	dichloromethane
DMA	dimethylacetamide
DMAP	4-dimethylaminopyridine
DMDTC	dimethyl dithiocarbamate
DMF	dimethylformamide
DMP	DuPont-Merck Pharmaceuticals
DMSO	dimethyl sulfoxide
DPT	di-2-pyridylthiocarbonate
DPU	N,N′-diphenylurea

E_a	activation energy
EDCI	1-ethyl-3-(3-dimethylaminopropyl)carbodiimide
EI-MS	electrical ionization mass spectrometry
Equiv.	equivalent
Et	ethyl group
EtOAc	ethyl acetate
EtOH	ethanol
eV	electron volt
FEA	field emission array
FT-IR	Fourier transform infrared spectroscopy
GLC	gas-liquid chromatography
h	hour
HIV	Human Immunodeficiency Virus
HOMO	highest occupied molecular orbital
HPLC	high pressure liquid chromatography
^{i}Pr	isopropyl group
L	any ligand
LCMS	liquid chromatography mass spectrometry
LMCT	ligand-to-metal charge transfer
LUMO	lowest unoccupied molecular orbital
M	any metal
MAC	mixed anhydride coupling
Me	methyl group
MEM	methoxyethoxymethyl ether
MeOH	methanol

MO	molecular orbital
MOCVD	metal-organic chemical vapor deposition
MS	mass spectrometry
NMM	N-methymorpholine
NMP	N-methylpyrrolidinone
NMR	nuclear magnetic resonance spectroscopy
Np	neopentyl group
PG	protecting group
PVD	physical vapor deposition
Py.	pyridine
rt	room temperature
SEM	[β-(trimethylsilyl)ethoxy] methyl acetal
SPOC	solid phase organic chemistry
SPOS	solid phase organic synthesis
TFA	trifluoroacetic acid
THF	tetrahydrofuran
TLC	thin layer chromatography
TMAH	tetramethylammonium hydroxide
UHV	ultra high vacuum
X	any halide

Abstract of Dissertation Presented to the Graduate School
of the University of Florida in Partial Fulfillment of the
Requirements for the Degree of Doctor of Philosophy

SYNTHESIS AND CHARACTERIZATION OF ALKYLZIRCONIUM COMPLEXES FOR THE FABRICATION OF LOW WORK FUNCTION MATERIALS AND SYNTHESIS OF HYDANTOINS AND DIHYDROURACILS FROM AMINO AMIDES

By

Seth Michael Dumbris

May 2010

Chair: Lisa McElwee-White
Major: Chemistry

Alkylzirconium compounds have been studied as precursors for the chemical vapor deposition of ZrC for application as low work function materials in devices such as field emitter arrays. Tetraneopentylzirconium and trineopentylzirconium monochloride were synthesized to test the decomposition pathways using mass spectrometry to help further understand the thermal decomposition under deposition conditions. The initial decomposition step of tetraneopentylzirconium was determined to occur through a mixture of α- and γ-hydride elimination processes resulting in a complex mass spectrum.

The homoleptic alkylzirconium complex tetra-η^3(phenylpropargyl)zirconium was synthesized. It exhibited interesting bonding resulting in a D_{2d} symmetric, 16 electron complex that was characterized with X-ray crystallography. The bonding was further analyzed by computational analysis, which determined the HOMO-LUMO gap to be 5.2 eV and showed the highly delocalized bonding of the phenylpropargyl ligands to the zirconium center.

The synthesis of ureas has traditionally been accomplished using stoichiometric amounts of phosgene or its derivatives, which results in various environmental, safety, and health issues. Due to the prevalence of urea moieties in molecules of interest in the pharmaceutical industry, catalytic alternative routes that employ CO as the carbonyl source have been found. $W(CO)_6$-catalyzed oxidative carbonylation provides an alternative to using phosgene or isocyanates to yield ureas. A series of α- and β-amino amides were synthesized and successfully carbonylated using a $W(CO)_6/I_2$ system resulting in hydantoins and 5,6-dihydrouracils, respectively. The effects of sterics on the system are seen as steric bulk of the *N*-alkyl substituent increases, yield of the corresponding product decreases. Secondary amides also have been shown to afford the products in moderate to good yields.

CHAPTER 1
THIN FILM DEPOSITON OF ZrC FOR THE FABRICATION OF LOW WORK FUNCTION MATERIALS

Introduction

Metal carbide coatings have been of interest lately because their thermal and electrical conductivities are similar to those of pure metals. In addition, they possess high hardness values, high melting temperature, high strength at elevated temperature, and stability.[1] They have been incorporated into a number of applications including corrosion resistant materials, energy production applications, components for aircraft and rockets, high heat resistant materials, and wear-resistant technologies. Zirconium carbide (ZrC) has been of particular interest as it has been shown to enhance the corrosion resistance of carbon steels,[2] improve beam confinement and emission stability on the cathodes of field emitters,[3] and control wear and friction in engineering materials.[4] It is also used in atomic fuel particles due to its low neutron cross section[5] and used in high brightness electron sources.[6] Thin films of ZrC can be deposited on a variety of substrates through many methods that center around two main types; physical vapor deposition (PVD) and chemical vapor deposition (CVD). CVD itself can be further divided into two main types: conventional and metal-organic (MOCVD). While both PVD and CVD are successful in depositing ZrC in a controlled manner, there are intrinsic differences between the two methods that can result in differences in morphology, film thickness, rate of deposition, atomic ratio of Zr to C, and temperatures and pressures needed for deposition.

Physical Vapor Deposition (PVD) of ZrC

Physical vapor deposition is a method that employs vacuum to deposit thin films by the condensation of a gaseous form of a specific material onto a substrate. This is

conducted in a directional, line-of-sight manner through numerous methods, one of which is evaporative deposition. In this method, the material to be deposited is heated under vacuum on one side of the reactor and is distributed on the substrate opposite it. This can be assisted by an inert carrier gas to help transfer or not. The substrate is then coated on any surface that is exposed to the flow of gas/deposited material. Other PVD methods that have been successfully employed for the deposition of ZrC include e-beam bombardment,[6] pulsed laser ablation,[7] laser cladding,[8] and magnetron sputtering.[9] These methods have proven successful at depositing ZrC onto many substrates including steel, silica, molybdenum, tungsten, and graphite.

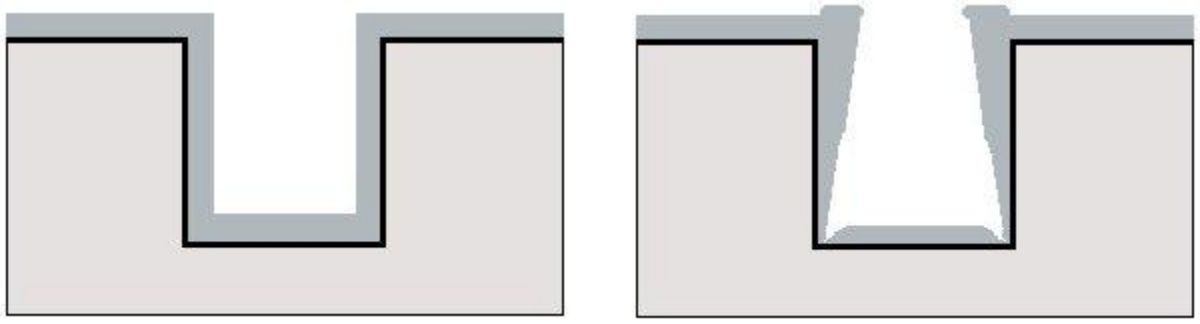

Figure 1-1. Comparison of conformal vs. non-conformal substrate coverage. Left) Conformal coverage of film on substrate. Right) Non-conformal coverage of film on substrate.

These methods also tend to be fairly mild to the substrate as the temperature needed often does not exceed 300 °C. This is not always the case, however, as laser cladding superficially melts the surface of the substrate.[8] While this generally does not affect the mechanical properties of the material, it could potentially affect the substrate if it has more than one layer. In addition as this is a line-of-sight deposition method at low pressure, a substrate that is not smooth will not have conformal coverage. Areas have thicker coverage on the direction facing the gas/deposited material flow while the face

opposite would receive less. Achieving conformal coverage on an inset substrate area would also not be viable (Figure 1-1).

Conventional Chemical Vapor Deposition (CVD) of ZrC

Conventional CVD uses binary metal halide precursors, such as $ZrCl_4$, and methane (CH_4) as the carbon source under a reducing H_2 atmosphere to achieve deposition of ZrC. The metal source, $ZrCl_4$, is heated under reduced pressure and is transported to the substrate, which is heated to 1000-2000 °C. The zirconium halide and CH_4 react to generate ZrC on the surface. As the reaction does not occur until the reactants reach the substrate, conformal coverage is much easier to obtain. Control parameters such as temperature, pressure, carbon source, and flux of gas precursors have been thoroughly examined.[10-12] An in-depth thermodynamic analysis predicted that, at equilibrium, it would be easy to manipulate the exact molecular composition of the solid deposited by controlling the input partial-pressure of CH_4 with a constant $ZrCl_4$ feed.[13] These pressure ranges at 1900 K are $5x10^{-3}$ torr < $P°_{CH4}$<10^{-2} torr and 10^{-2} torr <$P°_{ZrCl4}$<10^{-1} torr, where $P°_{CH4}$+ $P°_{ZrCl4}$+ $P°_{H2}$ = 1. Experimentally, obtaining the desired 1:1 stoichiometry of Zr to C has been achieved.[12]

A kinetic analysis of the deposition mechanism was sought to better help understand and control the ZrC deposition process.[14] It was found that at temperatures below 1523 K the activation energy (E_a) for deposition was 85 kJ/mol and at temperatures above 1523 K, E_a = 305 kJ/mol. This indicated a mechanistic change above that temperature, consistent with a surface kinetic driven process, which is strongly dependant on deposition temperature.[15] Previously, it was also determined that Zr and C appear to be deposited separately during the process and not simultaneously in this type of system.[16] This was significant because this $ZrCl_4$-CH_4-H_2

system's surface reaction kinetics should be dominated by deposition of Zr or C, or the reaction of the two to form carbide. Independently, the decomposition E_a of CH_4 was found to range from 280-380 kJ/mol in an experiment involving the deposition of pyrocarbon using CH_4 as the carbon source under similar experimental controls as in the ZrC system.[17] In addition, the pyrocarbon studies showed that gaseous hydrocarbons tend to decompose into a complex mixture of organic molecules in the form of liquid or plastic-like droplets.

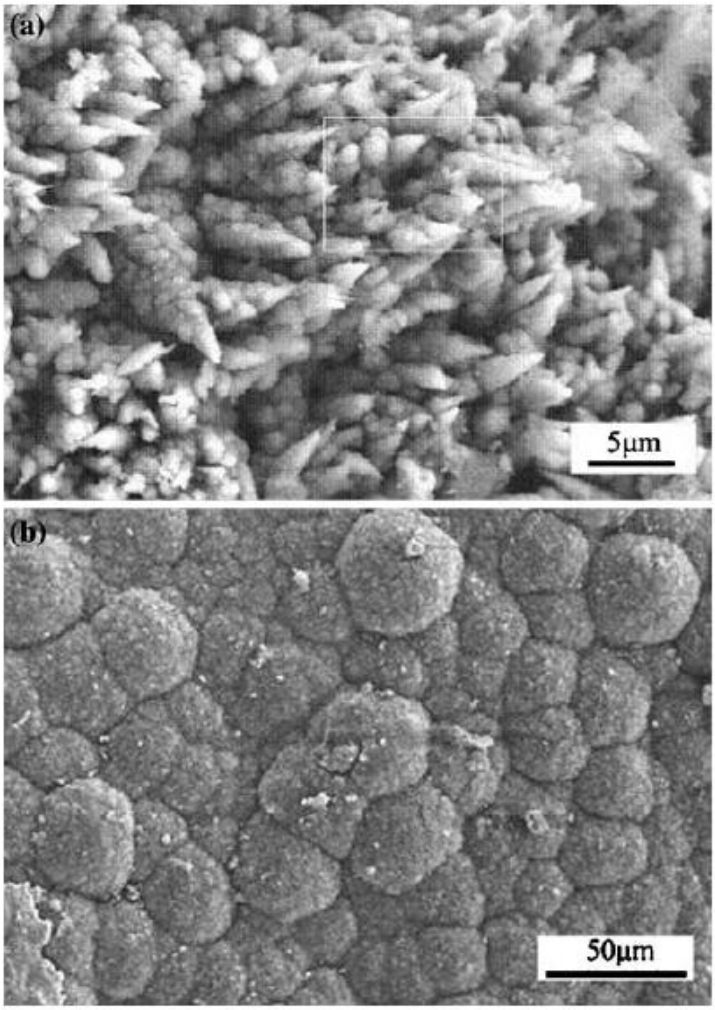

Figure 1-2. Morphologies of ZrC films deposited from a $ZrCl_4$-CH_4-H_2-Ar system. a) Film grown at 1573 K. b) Film grown at 1673 K.[14]

These studies help to explain the very different morphologies obtained from the deposition of ZrC (Figure 1-2). When the temperature is 1573 K or lower, the deposited films show columnar growth. Each column terminates in a tip and grows larger towards its base. In contrast, films grown at 1673 K show an isotropic cauliflower-like shape. The grain size of films grown above 1573 K are considerably larger than those which are grown below it.[14] This observation is consistent with morphologies of deposited carbon and its isotropic forms at these temperatures.[18] These observations seem consistent with others[19] that the growth rate of ZrC appears to be limited by the carbon deposition rate at temperatures above 1573 K.

The observed morphologies can more readily be understood using this model. At 1573 K the CH_4 first decomposed to form plastic-like droplets of C on the substrate surface. The droplets tend to be more dispersed as the temperature was not high enough for neighboring droplets to fuse together. This resulted in columnar growth as the zirconium or reduced $ZrCl_4$ then reacted at the carbon droplet. It was also believed that the needle tip of the column was then where more liquid droplets deposit, continuing the film growth at this temperature resulting in a slower growth rate. When the temperature is greater at 1673 K, CH_4 can decompose more readily and resulted in more plastic-like droplets per unit area on the substrate surface. Droplets could then also fuse together while some form of reduced zirconium dissolved and reacted in the droplets.

This was not a stepwise process, like atomic layer deposition. Both the decomposition of CH_4 and reaction of zirconium happened simultaneously. Particle sizes tend to enlarge as the film growth rate is much higher at elevated temperatures

resulting in more of the materials coming into contact with one another more quickly via an increased transport rate.[14] The results showed that the films grown from a $ZrCl_4$-CH_4-H_2 system can be made much more conformal in coverage at temperatures higher than 1523 K.

Conventional CVD of ZrC requires relatively high growth temperatures and thus limits the number of substrates that can tolerate such high temperature. One such example is silica, which is used to make high brightness electron sources. Its melting temperature is 1414 °C, too low for ZrC to be effectively deposited under conventional conditions.[20] In addition, $ZrCl_4$ or other halogen bearing sources of zirconium are most often utilized as the zirconium source. These halogens have a tendency to be incorporated into the film and can limit device efficiency.[21,22] Large amounts of acidic halide waste are also generated under these conditions, four equivalents of HCl for every mole of $ZrCl_4$ used, which can be hazardous on a large scale to humans, equipment, and the environment. Thus, an alternative approach was sought to overcome these limitations.

Metal-Organic Chemical Vapor Deposition (MOCVD) of ZrC

The use of a single source precursor that contains only the requisite metal, carbon, and hydrogen is advantageous for CVD. The precursor only contains the desired atoms, so problems associated with halide contamination are eliminated. In MOCVD, the precursor is carried through the deposition system either in a gaseous state or part as of an aerosolized mixture. The precursor is delivered to the substrate, which is heated to the requisite deposition temperature needed to decompose the precursor. The organic portion of the molecule then thermally decomposes, leaving only the desired film behind on the substrate. The decomposition reaction itself is

initiated at the substrate surface, which results in conformal coverage and does not have line-of-sight issues as in PVD. As with conventional CVD, growth rates are also a function of a variety of factors including identity of the precursor, deposition temperature, flow rate and carrier gas, and reactor design.

There are limitations on the metal-organic precursors that can be used for the deposition of ZrC. Alkyl ligands placed on the zirconium center cannot contain any β-hydrogen atoms as β-hydride elimination occurs readily at room temperature from early transition metals. Heteroatoms in the ligands are avoided, as they can be incorporated into the film. The compound must also be sufficiently stable to be handled. Tetramethylzirconium, $Zr(CH_3)_4$, meets the criteria of no β-hydrogens and no heteroatoms, however, it cannot be used for deposition of ZrC as it readily decomposes at -20 °C.[23] Tetraallylzirconium is also known and does have β-hydrogens, but does not have the necessary geometry to eliminate them. It is also unable to be utilized for CVD as it decomposes readily at temperatures above -20 °C. The most heavily studied alkylzirconium compound that meets the criteria above is tetraneopentylzirconium, $Zr[CH_2C(CH_3)_3]_4$ ($ZrNp_4$), Figure 1-3.[1,23-27]

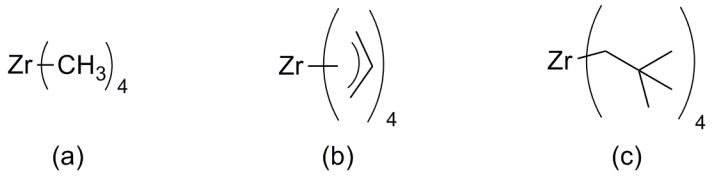

(a) (b) (c)

Figure 1-3. Tetraalkyl zirconium compounds.
a) Tetramethylzirconium. b) Tetraallylzirconium. c) Tetraneopentylzirconium.

ZrC has been successfully deposited from $ZrNp_4$ under various conditions. Deposition using ultra-high vacuum has been done with solid $ZrNp_4$ and applying heat and a base pressure of around 10^{-10} torr.[1] This was done as the vapor pressure of

$ZrNp_4$ itself is very low, which makes it difficult to volatilize. Another route to overcome low volatility is to dissolve the material in a high-boiling temperature organic solvent. The solvent can be nebulized and carried to the deposition reactor in a process called aerosol-assisted metal-organic CVD (AA-MOCVD). The carrier solvent then is removed under vacuum while traveling through the reactor, delivering an aerosol of $ZrNp_4$ to the substrate.[28]

High Brightness Electron Devices

Electron sources based on vacuum tubes have been around for many years, with the use of thermionic emission technology used for the last 30 years in high brightness electron sources. The Department of Defense currently operates over 170,000 of these tubes which are utilized in 272 applications in various fields. Devices such as the SPY-1 cross-field amplifier system, high speed data communications in submarines, radar, sonar, and other electronic warfare systems make use of these vacuum tubes. The devices operate by the electrical generation of heat reaching a threshold temperature at which the flow of electrons across the system is possible.

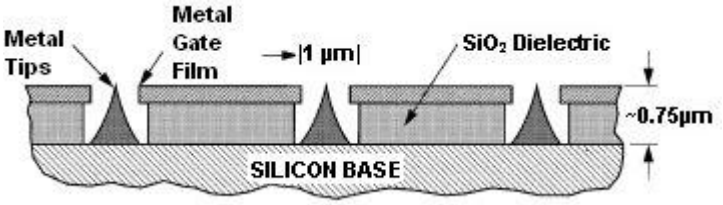

Figure 1-4. Spindt type field emitter cathode array.

Due to this parameter, the devices require high power consumption and have a long system response time in switching from “standby” to “on” modes. While thermionic emission technology is highly reliable, there exists a strong demand to decrease both

the size of the devices and their power consumption. One possible alternative to this technology is the use of gated field emission arrays (FEAs) (Figure 1-4).[29]

Gated FEAs provide a good alternative in that they have a near instant on capability and do not require time to heat prior to use. The units themselves operate cold and give off little heat of their own, consequently requiring much less heat dissipation equipment and lowering the overall size of the device. This results in space/weight savings over devices that employ vacuum tubes. Higher anode current is also possible from these devices while using less power overall. These reasons result in substantial savings over currently employed thermionic emission technology.

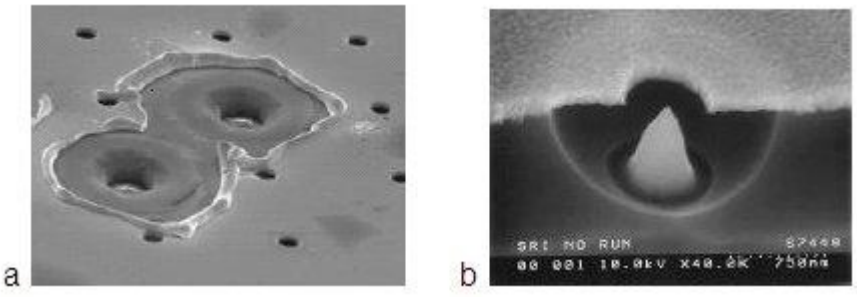

Figure 1-5. FEA device failure. a) Arcing damage to tips and gate electrode. b) Dulling of emitter tips due to ion bombardment.

The reliability of FEAs needs to be improved before the technology can be of general use. Some of the problems to be overcome are illustrated in Figure 1-5.[29] In the first the gate film has melted and vaporized, exposing the underlying SiO_2 film, thereby destroying the tips around the area. This cathode destruction can result in a partial or complete loss of system voltage from the array as a whole. Ion bombardment is also a problem attributed to ions being formed by electron beam ionization. These ions are accelerated and impact the field emitter surface, which can dull the emitter tip or lead to a nanoprotrusion on its surface. A nanoprotrusion is then capable of

generating a large local emission field, which if intense enough, can cause a vacuum arc to occur and damage the cathode.

Reliability of devices can be improved by lowering the operational voltage of the system, as this reduces the likelihood of the previously mentioned problems from occurring. This is done by either fabricating cathodes out of, or by coating conventional electrodes with a thin film of a low work function material. Certain carbides, borides, nitrides, and carbon based thin films have low work functions ranging from 2-3.5 eV.[30] When these materials are incorporated into a high brightness electron source, emission currents can be increased by a factor of 100, as shown in the use of conventional Si and Mo systems. This operational system was successfully able to have its work function lowered from 4 eV to 3 eV, resulting in an overall current density increase from the system.[30]

Of these low work function materials, ZrC is a promising candidate. Its bulk work function is between 2.0-2.2 eV and it has been demonstrated to lower the system's operational work function from 4.85 eV to 3.15 eV on a Si(100) tip array resulting in a voltage reduction of about 23% while maintaining the same current.[6] When a Mo(100) tip array was coated with ZrC, its work function was lowered from 4.60 eV to 3.58 eV, resulting in a voltage reduction of 44% while maintaining the same current. In addition to the power savings, ZrC is also much more durable than many substrates, like Si. The melting point of ZrC is more than twice that of Si.[20] Its durability and wear resistance are profound with hardness values as high as 30.2-35.6 GPa.[7,9] Lastly, the resistivity of ZrC is around 10^{-4} lower than that of Si making it a very good candidate for incorporation into high brightness electron sources.[20]

CHAPTER 2
SYNTHESIS, CHARACTERIZATION, AND COMPUTATIONAL ANALYSIS OF ALKYLZIRCONIUM COMPLEXES

Background

One of the most studied complexes for the MOCVD of ZrC is $ZrNp_4$. The molecule contains no β-hydrogens, is stable at temperatures reasonable for deposition, is reasonably volatile, and contains no heteroatoms which might contaminate the deposited film. It is a homoleptic compound, containing only one type of ligand, the neopentyl group. The inclusion of only one type of ligand makes its decomposition study easier as fragmentation has limited options. Due to this, its stability, and relative ease of synthesis, it has been the focus of decomposition studies conducted with the hope that knowledge of the decomposition mechanism can give insight into the MOCVD process. This may also lead to development of a new type of alkylzirconium compound as decomposition may lead to better understanding of ligand design. A particular issue that has been of interest is how the final film Zr/C ratio is not 1:1 as expected; rather ratios of 1:2 to 1:5 have been reported.[1,26-28,31]

Mechanistic Analysis of $ZrNp_4$ Decomposition

Early studies indicated that at a deposition temperature of 500 °C, ZrC could be deposited in stable crystalline thin films as confirmed by XRD and XPS data. However, AES data indicated that the Zr/C ratio was 1:2, despite efforts to lower it by controlling deposition parameters.[25] To help better understand this observed result, ZrC was deposited on Ni substrates and further studies conducted. The surface of these samples was then exposed to a set amount of $ZrNp_4$ below 125 K, to prevent premature $ZrNp_4$ decomposition. The films were then annealed at 275 K to remove the $ZrNp_4$ multilayers, achieving monolayer coverage.[1]

The films were then placed in an ultrahigh vacuum (UHV) chamber and heated to higher temperatures while monitoring the effluent gas by MS. Around 410 K a simultaneous mass loss of 29, 41, and 57 amu was observed with mass loss of 15 and 16 amu occurring near 500 K (Figure 2-1) as measured by mass spectrometry.[1]

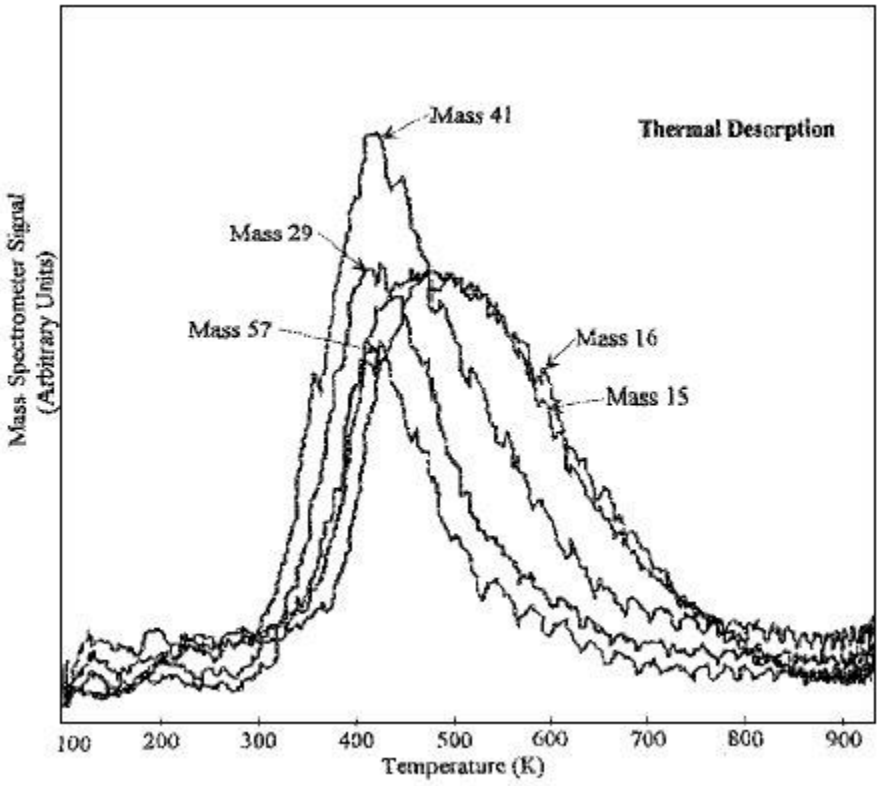

Figure 2-1. Thermal desorption following adsorption of $ZrNp_4$ on a nickel foil after annealing at 275 K prior to spectrum collection.[1]

As the films have already undergone desorption, this can only be attributed to hydrocarbon cracking in the mass spectrometer, most likely from a single desorbing hydrocarbon. No direct peak of m/z 56, corresponding to isobutylene, could be observed, making β-methyl elimination unlikely. Also, no Zr containing fragments were detectable. This makes the loss of fragments m/z 29, 41, and 57 likely to have come mostly from the loss of neopentane itself. This was very likely as surface IR confirmed

the presence of surface bound neopentane. Loss of fragments of 15 and 16 amu has previously been attributed to loss of adsorbed methyl groups as well as smaller fragments from previous hydrocarbon cracking.

One difficulty in using this UHV study as a direct correlation to the CVD of ZrC itself is that this study utilized a Ni substrate on to which a ZrC film was deposited with a Zr/C ratio of 4:1, while the samples obtained using a Si substrate had a ratio of 2:1.[1] It was shown that surface chemistry has at least some effect on the Zr/C surface stoichiometry. While not directly observing the loss of neopentane, the study indicated loss of neopentane appears to be necessary for further hydrocarbon cracking.

Similar studies using $TiNp_4$ did report direct loss of neopentane and the decomposition resulted in a Ti/C ratio of 1:0.93.[32-34] This raises the possibility that the decomposition of $ZrNp_4$ might undergo a different thermolysis mechanism than $TiNp_4$.[23] Of specific interest is the initial decomposition step of the two complexes, which could occur by either α- or γ-hydride abstraction. Computations conducted on $TiNp_4$ showed that α-hydrogen abstraction was favored over γ- by an E_a of 8 kcal/mol.[35] Experimental and further computational data were sought to identify the initial decomposition step.

To determine if the decomposition of $ZrNp_4$ proceeded by α- or γ-elimination, **2** and **3** were synthesized and used to deposit ZrC by CVD (Figure 2-2). Volatiles were collected by vacuum and analyzed by EI-MS, ^{1}H NMR, and ^{13}C NMR.[23] Complex **2** was determined to generate neopentane and isobutene in a 2.3:1 ratio per mol of starting material. The deuterated isotopologues of neopentane evolved from **3** were determined to be 15% d_0, 14% d_1, 59% d_2, and 12% d_3, giving a ratio of 4.9:1 between the d_2 and d_3 species. The two possible unimolecular pathways that can give rise to a d_2 product are

γ-hydride elimination or a radical process generating $Np_3Zr\cdot$ and $Np\cdot$. However, there was no evidence for Np-Np formation in the CVD of **3**. This does not rule out the possibility of radical formation, but simply makes it a less likely candidate. Computations showed that the Zr-C bond length is 0.15 Å longer than that of a Ti-C bond in MNp_4, where M is Zr and Ti respectively. The shorter bond length was expected when comparing a first row metal complex to a second row. In addition, it was determined that γ-hydrogen abstraction was 5.2 kcal/mol lower in activation energy than α-hydrogen abstraction computationally.[23]

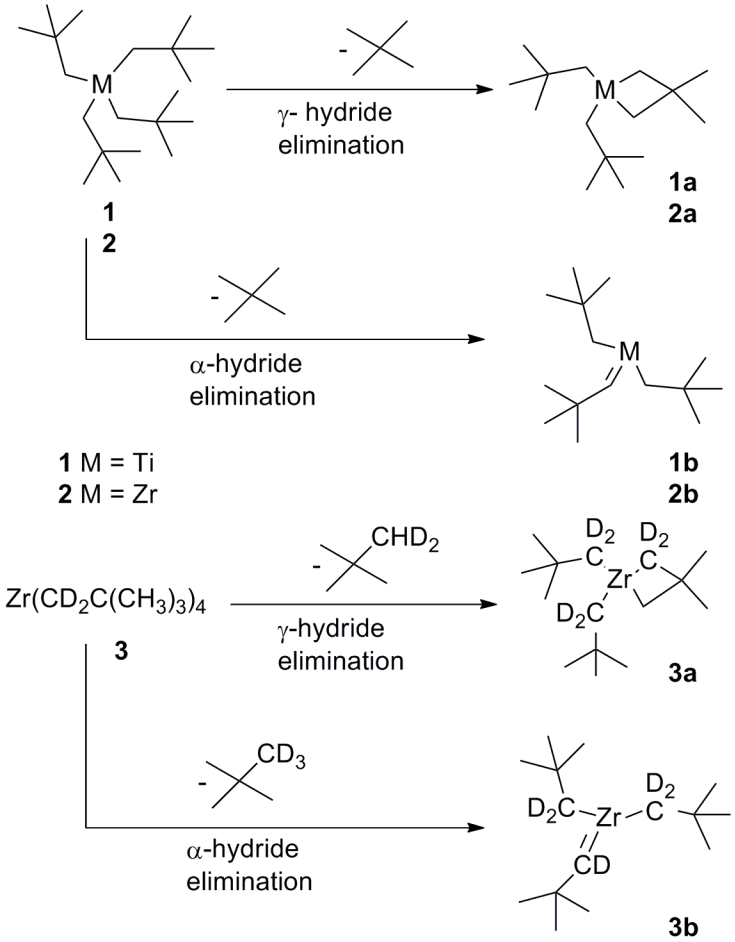

Figure 2-2. Initial decomposition pathways of MNp_4 and $ZrNp_4$-d_8.

The large amount of Np-d_2 present after deposition, absence of a Np-Np dimer, and computational evidence suggested that γ-hydrogen abstraction is the predominant pathway for initial decomposition of $ZrNp_4$. Lastly, overall 70.4% to 29.6% molar amounts of neopentane and isobutene were found for the decomposition of **2** and that the ratio holds within experimental error for **3**, suggesting that the two compounds undergo similar decomposition pathways.[23]

Both major studies on the deposition decomposition pathway have focused on following the deposition of ZrC from $ZrNp_4$ by experimentally examining the gases after deposition has occurred and with computational analysis reinforcing experimental results.

Propargyl/Allenyl Zirconium Complexes

The design and use of other alkylzirconium complexes that can potentially be used for MOCVD of ZrC has also been of interest. The inability to have ligands with a β-hydrogen or the presence of heteroatoms severely limits the functionality that can be incorporated into these molecules. One ligand group that had not received much examination is that of a propargyl group. Propargyl groups cannot undergo β-hydride elimination as they are completely unsaturated in the β-position. They also have unique structural and bonding characteristics that makes their potential usage chemically interesting.[36] A tautomerization exists between the allenyl and propargyl forms allowing for different modes of bonding to metals (Figure 2-3).[36]

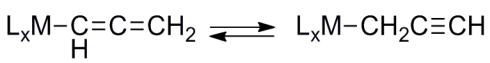

Figure 2-3. Tautomerization of a metal-allenyl and a metal-propargyl complex.

The ligands are capable of donating four electrons to the metal system through various σ and π interactions. Standard enthalpy of formation values of 42.2 kcal/mol for MeC≡CH and 45.5 kcal/mol for $H_2C=C=CH_2$ show that the free propargyl species is slightly more stable than the allenyl,[37] but studies have shown that the M-allenyl bonds are stronger than the corresponding propargyl-metal interaction. In general, the allenyl tautomer is favored when placed on a metal system.[38] Several synthetic strategies have been employed to generate η^3-allenyl/propargyl metal complexes.[36]

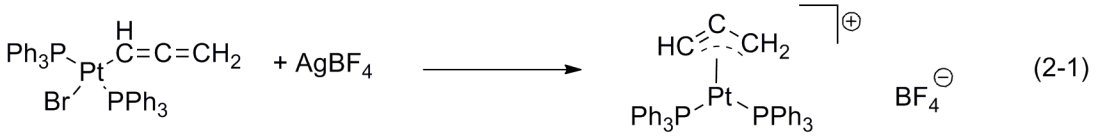

(2-1)

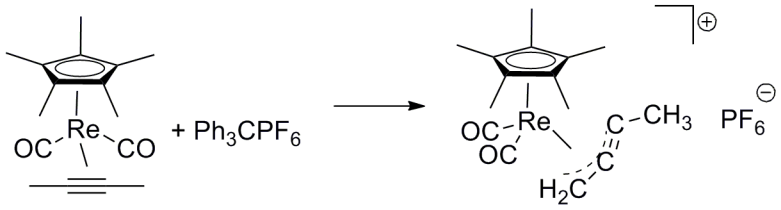

(2-2)

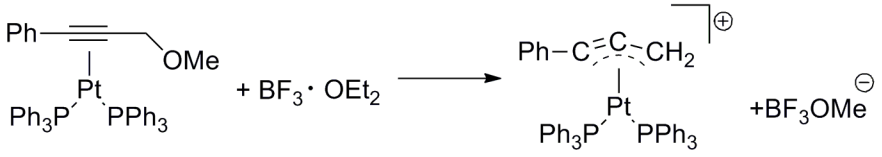

(2-3)

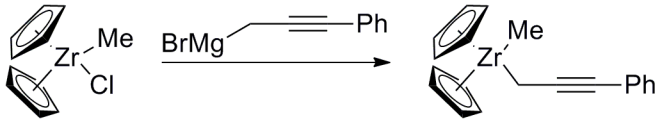

(2-4)

Figure 2-4. Synthetic routes to η^3-allenyl/propargyl metal complexes.

In Figure 2-4, (Eq. 2-1) shows the conversion of η^1-allenyl or η^1-propargyl to the η^3-allenyl/propargyl product via abstraction of a coordinated halide. This method has been applied to generate Pt(II) and Pd(II) complexes.[39] Equation 2-2 is a variant of this

by abstraction of a hydride from a coordinated η^2-acetylene ligand.[40] Another technique is to treat an η^2-propargyl alcohol or ether complex with a Lewis acid (Eq. 2-3).[39] Lastly, equation 2-4 shows how reactions of early transition metal halide complexes with Grignard or related reagents have proven useful to generate η^3-allenyl/propargyl complexes.

X-ray crystallography has been used to determine the structures of several η^3-allenyl/propargyl metal complexes and some significant features are associated with attachment to the metal center (Figure 2-5).[36] In general, metal complexes with an η^3-allenyl/propargyl ligand have a large distortion in the ligand with the C-C-C angle bent between 146-156°, as compared to a linear free alkyne moiety or an η^3-allenyl ligand angle of 120°.[36] This disparity is expected due to the electronic distortion at the central carbon. Another difference is shown in **4a** versus **4b**. In **4a**, the metal is virtually coplanar with the three carbon skeleton compared to the η^3-allenyl ligand being out of plane with the metal center in **4b**.

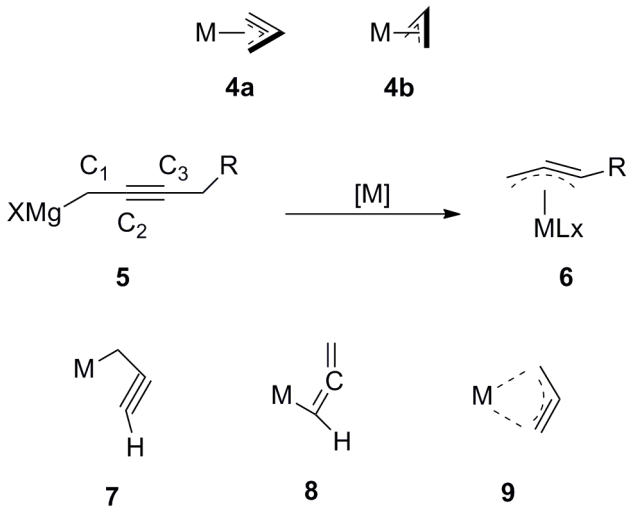

Figure 2-5. Bonding modes of η^3-allenyl/propargyl metal complexes.

The C_1-C_2 and C_2-C_3 bond lengths in ligands of the type in **6** are between 1.34-1.40 Å and 1.22-1.28 Å, respectively, different than that of the free alkyne in **5**, which has distances of 1.47 Å and 1.20 Å,[41] respectively. Complexes **7**, **8**, **9** illustrate the three possible η^1- and η^3-bondings of the allenyl/propargyl ligand itself. The bond lengths mentioned for **6** reduce the canonical structures to primarily those depicted in **7** and **9**.[36]

Synthesis of Alkylzirconium Complexes

The synthesis of alkyl substituted zirconium complexes was achieved using $ZrCl_4$ and the requisite Grignard or lithium reagents, resulting in a series of alkyl-halogen transmetalation reactions. Controlling stoichiometry of the alkylating reagent allows for the synthesis of mono through tetra-substituted complexes, depending on the desired molecule. The syntheses of the alkyl zirconium complexes utilized are outlined in Figure 2-6[42,43] and Figure 2-7.[44-46]

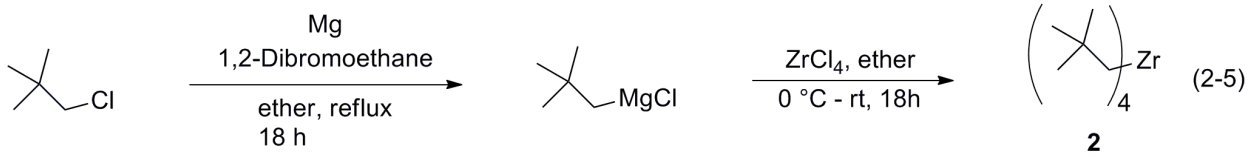

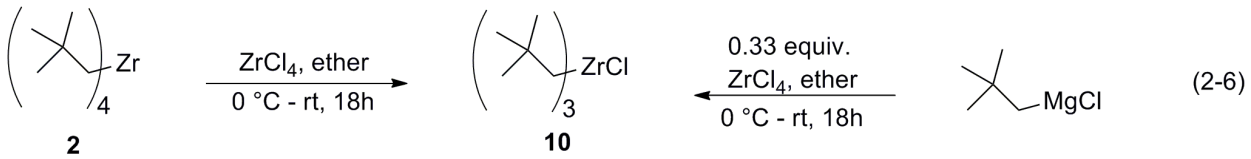

Figure 2-6. Synthesis of $ZrNp_4$ and $ZrNp_3Cl$.

Synthesis of **2** (Eq. 2-5) was achieved by literature procedures starting with the conversion of neopentyl chloride to the corresponding Grignard, which was then reacted with 0.25 equivalents of $ZrCl_4$ to afford the product in 70% yield.[42] The purified product

was a white to off-white air and moisture sensitive solid after sublimation. Complex **10** (Eq. 2-6) was synthesized by two methods. The literature method used neopentylmagnesium chloride in a 3:1 mixture with $ZrCl_4$.[43] The resulting yield was poor, due to the large amounts of impurities and separation was difficult. A second pathway used **2** as the starting material, which was reacted with 0.33 equivalents $ZrCl_4$ in ether overnight.[42] A bright yellow solid was obtained in 87% yield and was extremely sensitive to light, air, and moisture.

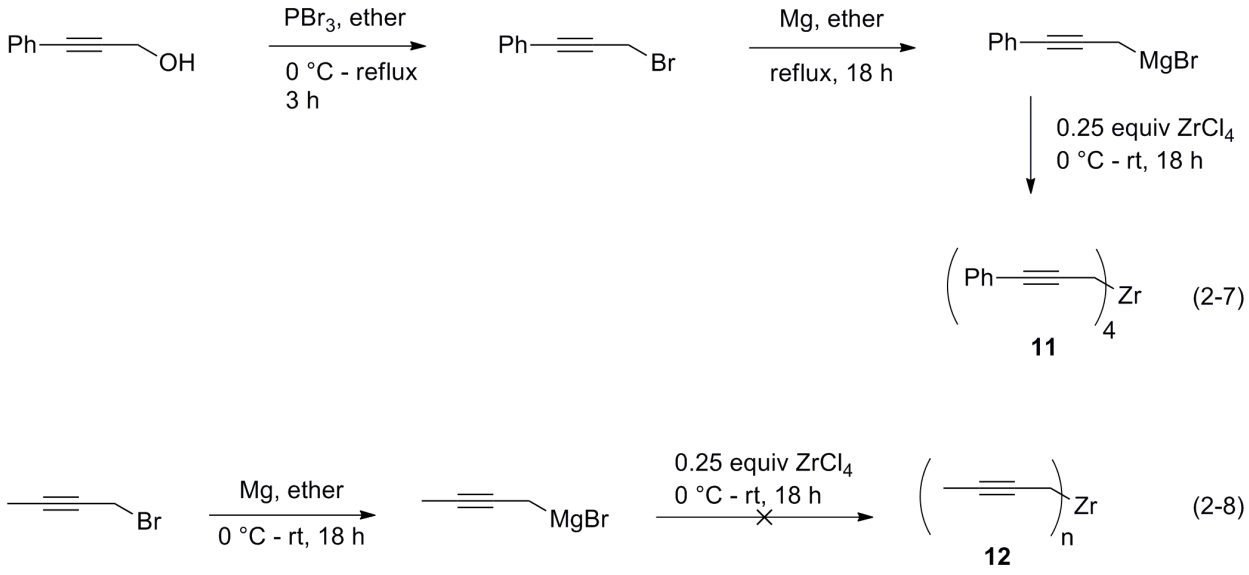

Figure 2-7. Synthesis of allenyl/propargyl zirconium complexes.

Complex **11** was obtained in 74% yield, based on $ZrCl_4$, from the synthesis, shown in Figure 2-7. Phenylpropargyl alcohol was treated with PBr_3 to phenylpropargyl bromide,[44] which was then converted to the corresponding Grignard[45] and reacted with 0.25 equivalents of $ZrCl_4$. The product was a crystalline white solid that proved to be air and moisture sensitive. Attempts to prepare compound **12** in similar fashion, (Eq. 2-8),[46] resulted only in a non-isolable, air and moisture sensitive compound.

Results and Discussion

Tetraneopentylzirconium ($ZrNp_4$) Studies

In order to generate alkylzirconium precursors that can successfully deposit ZrC by MOCVD, it is helpful to understand how the precursor decomposes under deposition conditions. The insight provided by the isotopologue analysis from Xue[23] is very helpful in examining the decomposition of **2** and **3** experimentally and comparing it with computational data. It suggested that the initial decomposition step of **2** was γ-hydrogen abstraction. However, the method employed collected and analyzed gasses from the entire deposition experiment, not just the initial decomposition. Another way to analyze these compounds is the use of mass spectrometry.[47-49] CVD is a thermal process whereas mass spectrometry is ionic, and care must be taken to not rely too heavily upon such data to predict CVD behavior, as smaller fragments are not necessarily derived from larger ones. Mass spectrometry can however provide good insight into the relative fragmentation patterns of various single-source organometallic precursors.[48,49]

A CI-MS of **2** was obtained and the spectrum indicated a complex mixture of peaks that could not be assigned to appropriate decomposition pathways. In addition, oxidized Zr-alkyl peaks were also visible in the spectrum preventing accurate assignment. Compound **10** was synthesized with the hope that a similar MS analysis could be conducted on the compound to yield insight into a similar decomposition pathway. However, **10** proved to be more sensitive than **2** as both light and the presence of solvents rapidly decomposed the complex, rendering analysis impossible.

Characterization of η³- Tetra(η³-phenylpropargyl)zirconium

The characterization of the phenylpropargyl compound **11** has yielded very interesting results. ^{1}H NMR data consisted of a single aliphatic methylene peak at δ 3.23 ppm. Comparisons can be made between **11** and **13** and **14** (Figure 2-8).[39,50]

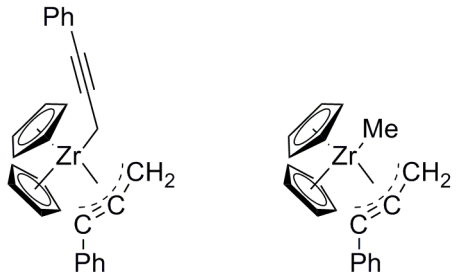

13 **14**

Figure 2-8. Other proparylzirconium complexes.

It was experimentally determined by variable temperature ^{1}H NMR that **13** contained two phenylpropargyl ligands on the zirconocene with one being coordinated in an η¹-fashion while the other exhibited an η³- mode of coordination. The ^{1}H NMR spectrum of **13** had one signal for the CH_2 group at δ 2.80 ppm from 223-303 K. At 180 K, the signal decoalesces into two equal intensity peaks at δ 3.3 and 1.9 ppm, which were assigned to η³- and η¹- coordination, respectively. Confirmation of this was subsequently obtained with **14** as it only has one resonance at δ 3.37 ppm, corresponding to an η³-propargyl ligand.

Based on these chemical shifts, it seemed probable that the lone resonance in the ^{1}H NMR spectrum of **11** corresponded to an η³-coordination of the phenylpropargyl ligand. While the reaction to synthesize **11** was conducted in a 4:1 ratio of Grignard reagent to $ZrCl_4$, the number of ligands on the zirconium center could theoretically be from four to six ($ZrR_{n=4-6}$). Any number *n* above four would result in an –ate complex,

with Mg^{2+} as the counterion. Also, formation of Zr dimers could have also been possible.

The structure of **11** was determined by X-ray crystallography to be a tetra(η^3-phenylpropargyl)zirconium complex (Figure 2-9). The structure itself contains high symmetry, belonging to the D_{2d} point group. All four ligands are bound in an η^3- fashion and are four electron donors, resulting in a 16 electron complex. Bond lengths for comparison to **14** are provided (Table 2-1, Table 2-2).

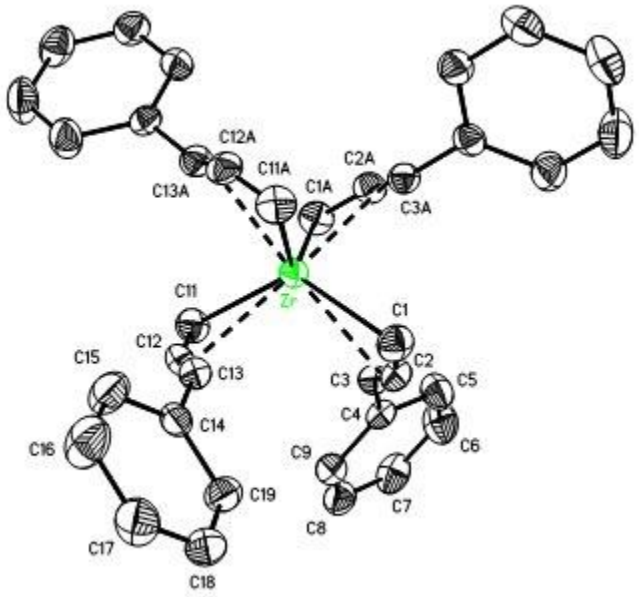

Figure 2-9. Thermal ellipsoid drawing of **11**. Hydrogen atoms are omitted for clarity.

Complexes **11** and **14** show structural similarities in that the C-C-C bond angles are 145.38(16)° and 155.4(3)°, respectively. The Zr-C1 bond length in **11** is shorter than that of **14** (Table 2-2) while the Zr-C2 is about the same in both structures and Zr-C3 is slightly longer in **14**. A point of interest is that all Zr-propargyl bond lengths in **11** are approximately the same length, differing by a net 0.09 Å overall, whereas those in **14** differ by a much larger value, 0.297 Å. This is possibly due to the large structural

differences between the two as **11** has an electron count of 16, while **14** has an electron count of 18 and the phenylpropargyl ligand is sterically encumbered by two cyclopentadiene rings. This could rationalize the shorter bond length along Zr-C1 in **11** as the metal must rely more on the σ-donation to gain electron density as it does not have the cyclopentadienyl π-system to draw upon.

Table 2-1. Selected bond angles and distances for **11**

Bond	**Angle (°)**
C2-C1-Zr	70.08(9)
C3-C2-C1	154.38(2)
C3-C2-Zr	77.01(1)
C4-C3-Zr	137.87(1)
Zr-C1-H1A	116.60(0)
C2-C1-H1A	116.60(0)
Bond	**Distance (Å)**
Zr-C1	2.4955(2)
Zr-C2	2.4043(1)
Zr-C3	2.4474(2)
C1-C2	1.3760(2)
C2-C3	1.2490(2)
C3-C4	1.4500(2)

.

Table 2-2. Bond distances* (Å) in crystal structure **14**

C1-C2	C2-C3	Zr-C1	Zr-C2	Zr-C3
1.344(5)	1.259(4)	2.658(4)	2.438(3)	2.361(3)

*Uses the numbering system as in compound **11**. Data are taken from ref.[50]

Complex **11** represents, to the best of the knowledge of the author, the first example of a homoleptic propargylzirconium complex and is also the first homoleptic propargyl metal complex synthesized to date. The interesting structural features

present in the X-ray structure needed further exploration to determine the full extent of the π-system interaction with the metal center.

Computational Analysis of η^3- Tetra(η^3-phenylpropargyl)zirconium

15

Figure 2-10. Ti pentalene complex **15**.

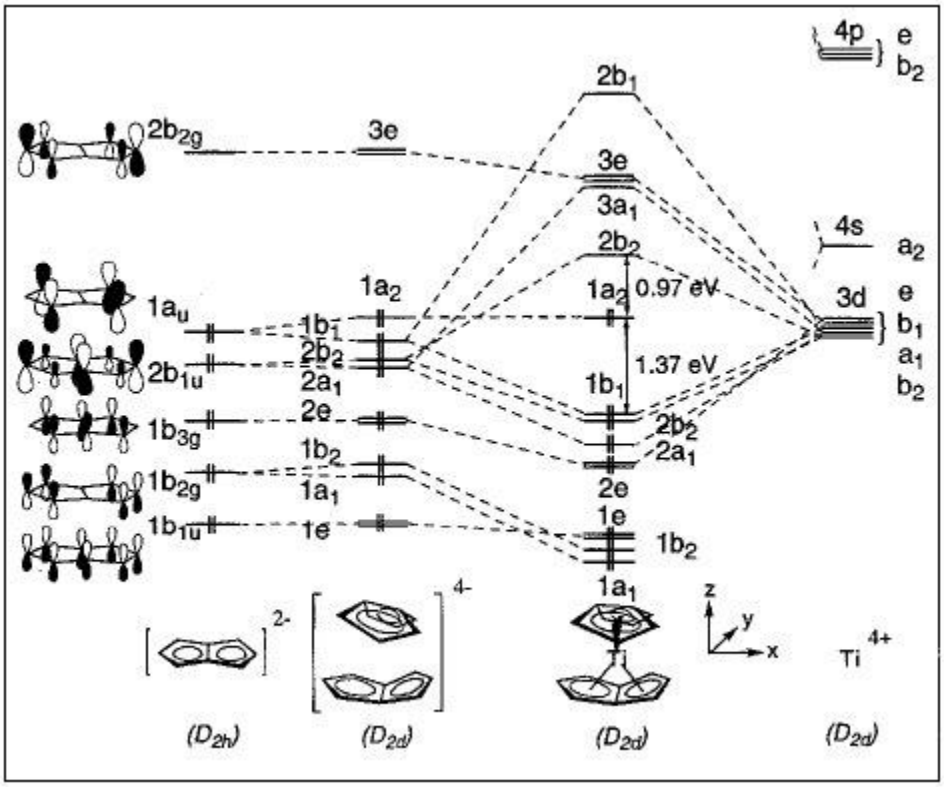

Figure 2-11. Molecular orbital diagram of **15**.[51]

Group IV D_{2d} metal complexes with conjugated π-systems are known in the literature.[51-53] The pentalene complex **15** (Figure 2-10) has a unique type of bonding that suggested an electron count of 20 for the metal.

Calculations showed that was not actually the case, due to a folding distortion of the pentalene ring that resulted in an overall electron count of 18.[51] A molecular orbital (MO) diagram was generated from the computational analysis (Figure 2-11[51]).

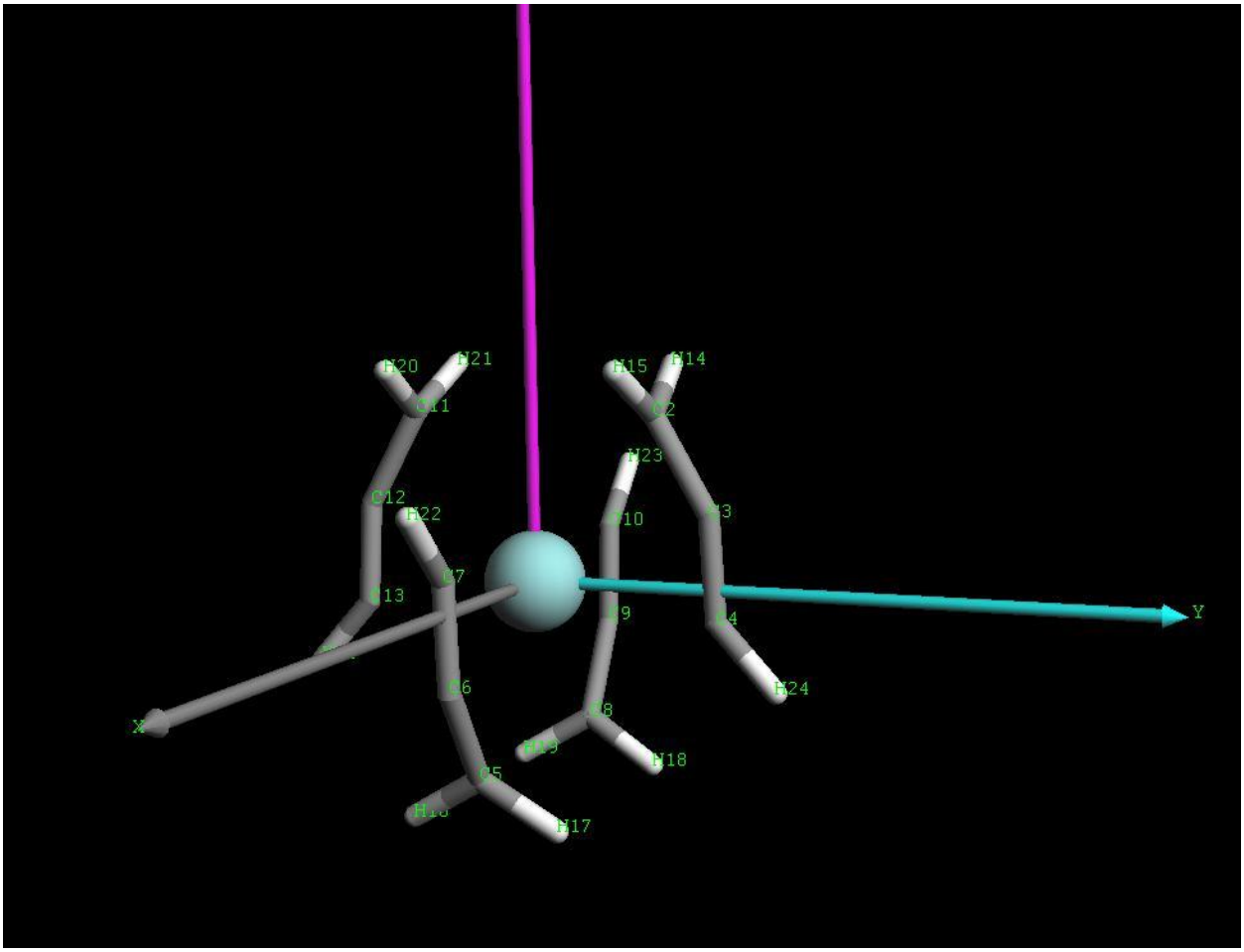

Figure 2-12. 3-Dimensional stick model of **16**.

This interest led to preparation of the Zr and Hf versions of the bispentalene sandwich complex.[52,54] Isolation of the $Zr(C_8H_6)_2$ complex was difficult as

decomposition readily occurred at room temperature. ^{13}C NMR suggested an overall staggered structure of the two rings, but this could not be confirmed by X-ray analysis.[52]

The complex π-system seen in **11** was analyzed by density functional theory (DFT) calculations (B3LYP/LANL2DZ), to better understand the bonding shown in the X-ray crystal structure.[55-58] Initial calculations were performed on **11**, but the contribution of the phenyl rings complicated the results by delocalizing the molecular orbitals to such an extent that visualization of them was difficult. To help simplify the visualization, the phenyl rings were replaced with hydrogen to give **16** which is also of D_{2d} symmetry (Figure 2-12).

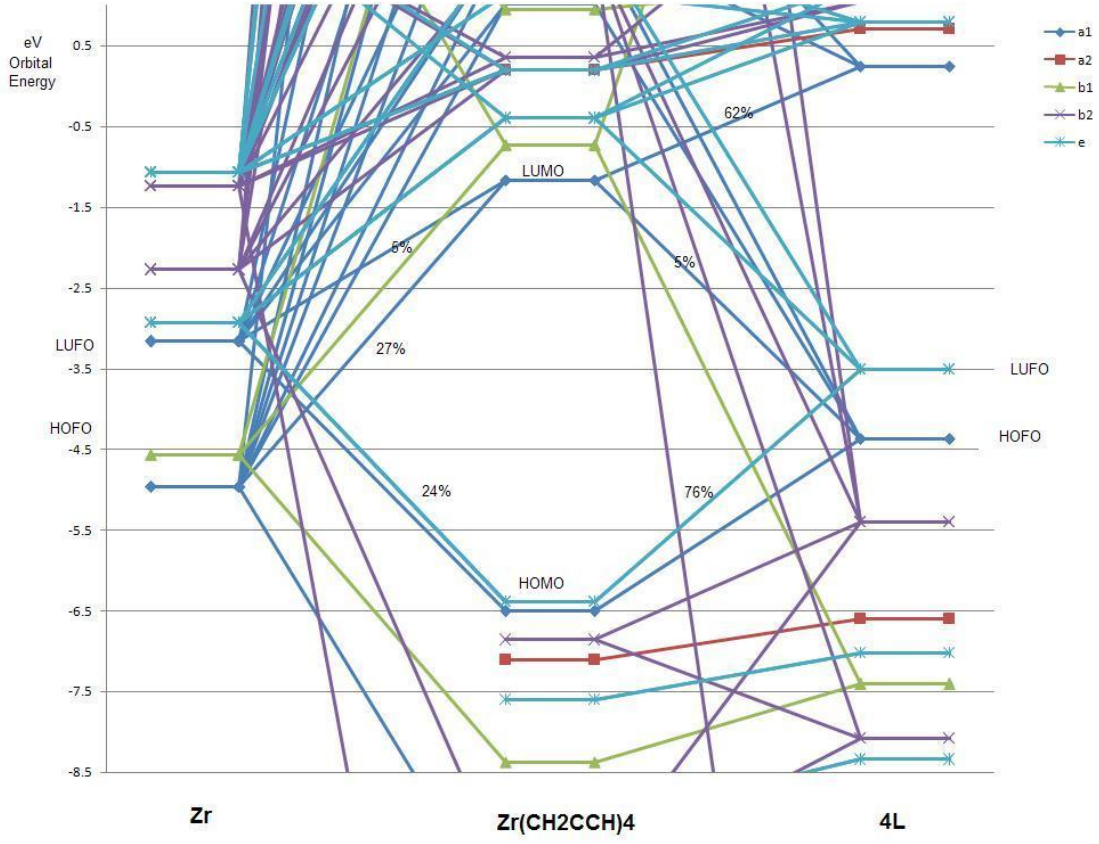

Figure 2-13. Molecular orbital diagram of **16**.

The molecular orbital diagram in Figure 2-13 was generated from the computational results. The calculated HOMO-LUMO gap was 5.2 eV. This was considerably larger than that obtained for D_{2d} symmetric **15**, which had a calculated band gap of 1.93 eV,[51] presumably due to the extensive conjugation in the molecule. Such a large HOMO-LUMO gap for **16** also helps explain the lack of color of the solid state in **11**, which is a transparent-to-translucent white depending on the degree of crystallinity in the solid.

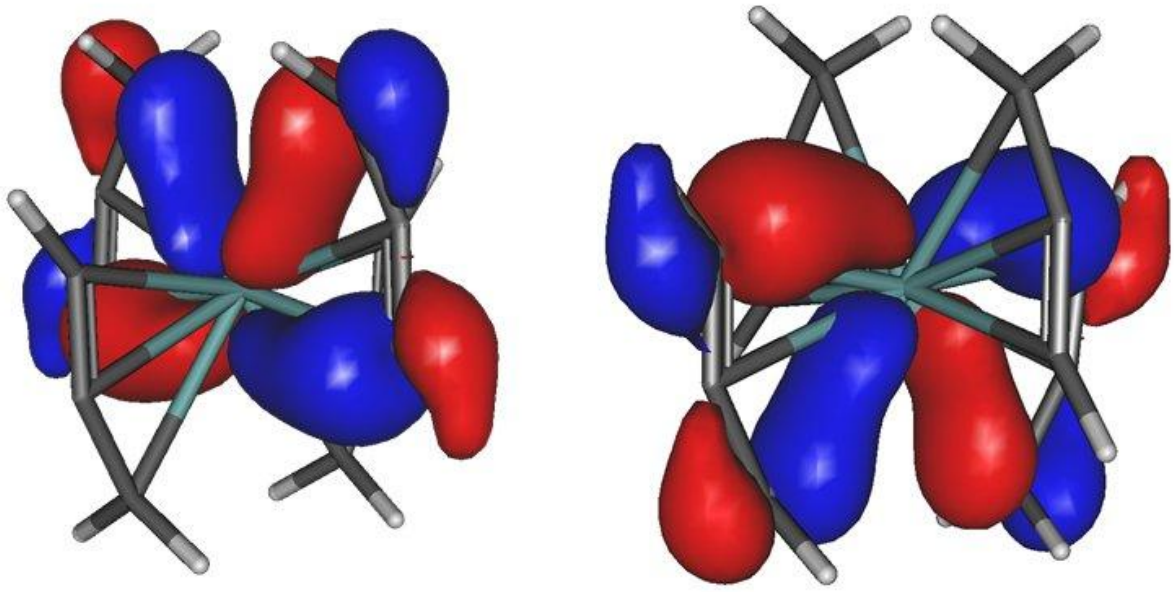

Figure 2-14. Degenerate HOMO orbitals of **16**.

The orbital contributions and images were also obtained. Select contributions are given below with the percent contribution listed in parentheses. The HOMO, comprised of two degenerate orbitals, contains the *p*-orbitals of the terminal carbons of the propargyl ligand that intersect the *yz* plane due to the interaction from the d_{zy} orbital on Zr (20.7%) (Figure 2-14). The other degenerate orbital uses d_{xz} of Zr (20.7%) instead. The HOMO-2 (not pictured) is mainly comprised of dz^2 on Zr (21.3%) and the *xy* plane of the *p* orbitals on the propargyl ligand.

The LUMO of **16** is mainly composed of many small interactions but has the strongest *p*-orbital contributions from the central carbon in the propargyl groups. The largest contributions of Zr are *s* (14.2%) and dz^2 (6.2%) (Figure 2-15). The LUMO+1 is mainly comprised of the d_{xy} orbital of Zr (76.1%). The LUMO+2 is comprised of two degenerate orbitals, one is composed primarily of d_{xz} (25.3%) and the other d_{yz} (25.3%), (Figure 2-16).

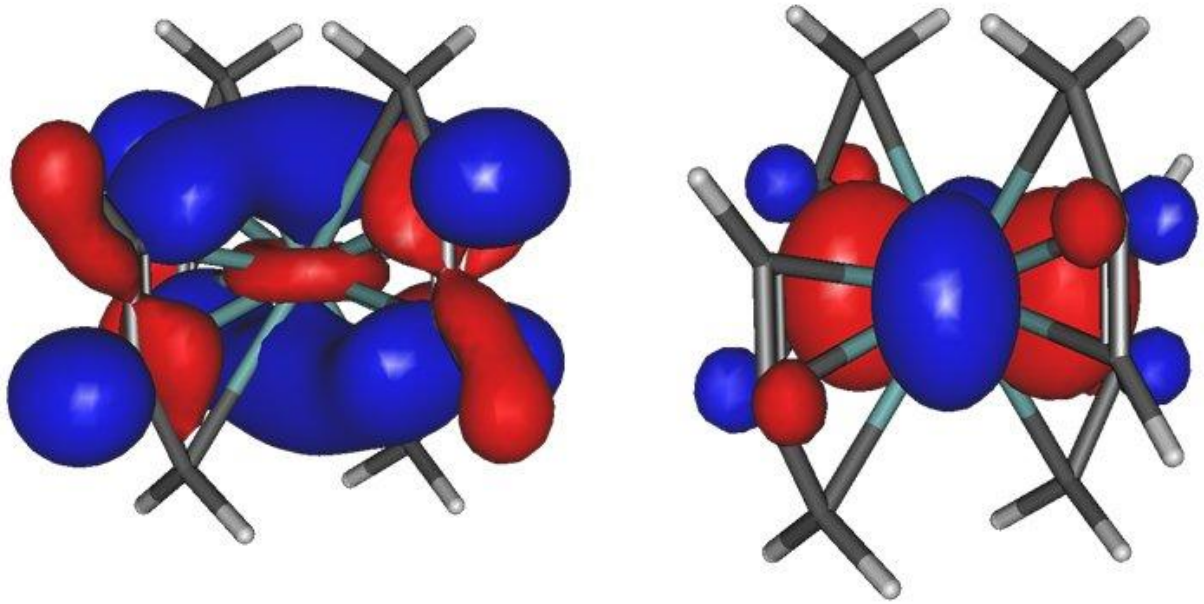

Figure 2-15. LUMO and LUMO+1 orbitals of **16**.
Left) LUMO. Right) LUMO+1.

The somewhat minor contributions from the orbitals are to be expected as this compound has a large π-system which disperses electron density. However, this does give excellent insight as to which orbitals are involved in the bonding and allows for an intellectual construct to help better understand the orbital interactions. It is interesting that this early transition metal 16-electron complex does not have an empty coordination site due to its symmetry. Complex **11** was also crystallized from THF with vapor diffusion of pentanes and did not show any coordinated THF in either the ^{1}H NMR or the

X-ray crystal structure. It is also possible that the large steric bulk afforded by the phenyl rings helps to exclude coordinating solvents.

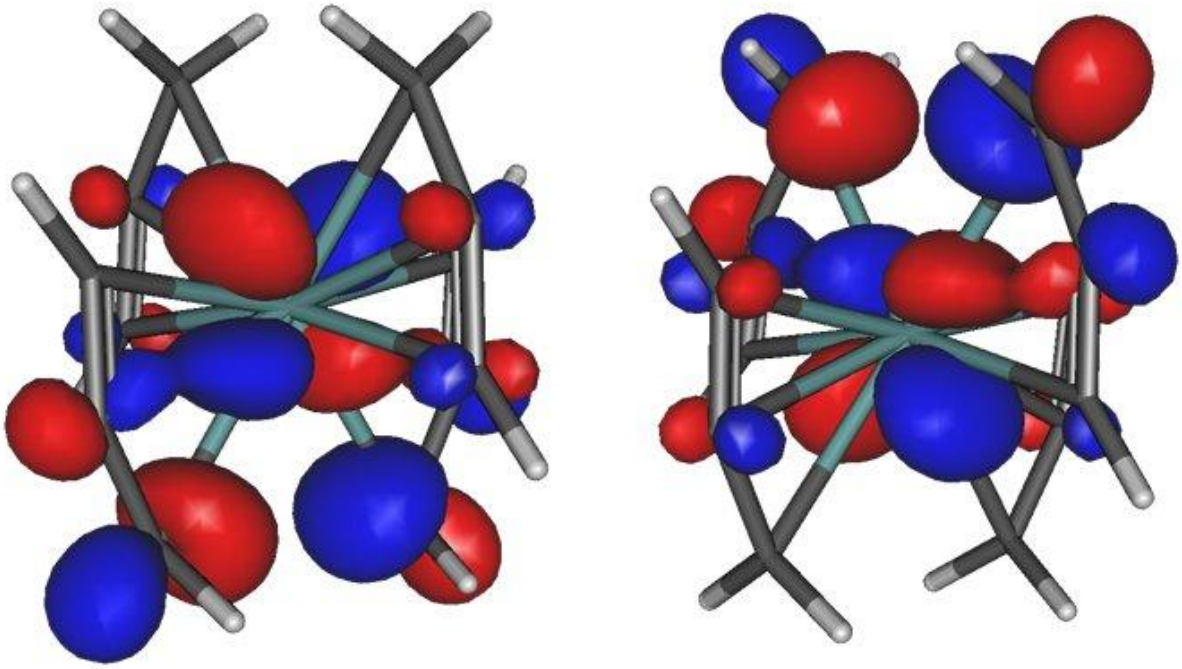

Figure 2-16. Degenerate LUMO+2 orbitals of **16**.

An electronically similar π-system is found in tetra-η^3-allylzirconium. Although the complex was first reported in 1966,[59] the complex is not well characterized owing to its ready decomposition at temperatures above -20 °C.

Spectroscopic ^{1}H NMR studies indicated that the allyl ligands do undergo internal rotation about the methylene carbon at temperatures above -70 °C. The material itself is a bright red solid, indicating that the HOMO-LUMO gap in the substance is low enough to allow LMCT. Compared with **11**, which is a white solid at room temperature, the HOMO-LUMO gap in tetra-η^3-allylzirconium must be considerably lower. A solid state comparison between the two is not possible as tetra-η^3-allylzirconium decomposes when placed on a microscope slide even when kept cool.[60]

Conclusions

Attempts at gaining insight in the decomposition mechanism of $ZrNp_4$ toward deposition of ZrC were undertaken with the synthesis of **2** and **10**, however a suitable mass spectral analysis was unable to be obtained due to the high sensitivity of the compounds to air and moisture.

The synthesis of **11** has yielded the first known example of a homoleptic propargylzirconium complex. The X-ray analysis has shown this complex to be structurally interesting with D_{2d} symmetry. The extent of the π-system in bonding was investigated by computational analysis and indicated that the molecule had an exceptionally large HOMO-LUMO gap of 5.3 eV. The high symmetry enabled wide dispersion of electron density greatly stabilizing the molecule. The HOMO was found to be comprised of two degenerate orbitals and the main orbital interactions with Zr are d_{yz} and d_{xz}, respectively. The LUMO was found to be mainly focused around the central carbons in the propargyl ligands and comprised of *s* and dz^2 interactions with Zr. The LUMO +1 was found to be comprised of and d_{xy} orbitals. The LUMO+2 was found to be degenerate and comprised of d_{xz} and d_{zy} orbitals.

CHAPTER 3
TRANSITION METAL-CATALYZED OXIDATIVE CARBONYLATION OF AMINES TO UREAS

Introduction and Background

The presence of urea moieties in molecules of interest in a wide range of fields and applications has stimulated interest in their synthesis. Much development into the synthesis of this particular functional group has occurred as it is seen in pharmaceuticals,[61-65] agrochemicals, precursors of resins, dyes, and additives to both petrochemicals and polymers.[66] Of particular interest has been their usage as non-protein based HIV protease inhibitors, CCK-B receptor antagonists, and endothelin antagonists.[63,67-70] Ureas themselves can also be synthons for other bulk chemicals by thermal cracking to yield isocyanates[71] or reacting with alcohols to yield carbamates.[72]

The traditional synthesis of ureas has been accomplished with the nucleophilic attack of amines on phosgene and its derivatives or isocyanates.[73,74] Phosgene is very reactive with both primary and secondary amines, and arrives at the product urea very well. However, phosgene is a highly toxic and corrosive gas that requires special handling and equipment. This has greatly discouraged its use in the laboratory setting. The production of phosgene on an industrial scale also includes serious risks to both safety of personnel and the environment in its usage, storage, and transportation.[75] Derivatives of phosgene are safer in all three of the above mentioned categories and include 1,1-carbonyldiimidazole, triphosgene, and many others. These are more common for use in laboratory scale synthesis than in industrial applications, as each equivalent of phosgene derivative used produces two equivalents of the leaving group. The generation of a large waste stream of byproducts is problematic with phosgene

derivatives on an industrial scale, but not with phosgene itself as only aqueous chloride is produced.

Other synthetic methods employed to convert amines to ureas include reaction with isocyanates and chloroformates. Isocyanates themselves are mainly derived from phosgene and are very toxic. Phenyl chloroformate has also been used, but has drawbacks as DMSO is the required solvent. In both laboratory and industrial scales, DMSO poses large risks to its potentially carcinogenic nature and because of its high boiling point making solvent removal very difficult.

Synthesis of ureas with phosgene also poses other synthetic problems due to its high reactivity. Unwanted side reactions involving nucleophilic functional groups, such as hydroxyl groups, can be a problem and require extensive protection/deprotection steps to avoid. Alternative routes have actively been sought that utilize either CO or CO_2 as the source of the carbonyl moiety.[75] These do not have the same problems of functional group compatibility and are generally safer to conduct, especially upon scale up.[76,77] The desire for catalytic systems as an alternative to stoichiometric reagents is evident and has been explored. Catalytic systems are also attractive from an atom economy[78] standpoint as catalytic oxidative carbonylation systems only employ amine, carbon monoxide, and some form of oxidant, which in turn only produces the reduced form of the oxidant and protons.[79,80]

With this in mind, the McElwee-White group reported the catalytic oxidative carbonylation of amines using a system comprised of $W(CO)_6$ as the catalyst, I_2, as the oxidant, and some form of base. This has been shown to convert primary amines,[81] secondary amines,[82] diamines,[83] and amino-alcohols to the corresponding ureas in the

presence of CO.[77] These reaction conditions tend to be relatively mild and have been shown to be highly tolerant of various functional groups.[84]

The use of the $W(CO)_6/I_2$ system is advantageous as the reagents are readily available commercially and are easy to handle. It provides an excellent laboratory scale alternative to urea synthesis from phosgene and its derivatives given its compatibility with functional groups. The remainder of this work will focus on the applications of the $W(CO)_6/I_2$ catalyzed carbonylation system to complex substrates.

Transition Metal Catalysts

New synthetic methods for preparing carbonyl-nitrogen bond moieties utilizing the metal-catalyzed carbonylation of amines are numerous and extensively studied. Mono- and dicarbonylation of amines have been reported as catalyzed by complexes of Mn,[85,86] Fe,[87] Co,[88-92] Ni,[93,94] Ru,[71,95-98] Rh,[89,98,99] Pd,[71,100-112] W,[76,77,81-84,113] Pt,[114] Ir,[114] and Au.[115,116] The products of these carbonylations include ureas,[71,86,89,90,93,98] urethanes,[92,117] oxamides,[118] formamides,[119-123] and oxazolidinones.[92,124] The conditions reported for these, in general, include elevated temperatures and moderate-to-high pressures of CO. Highlighted advances in transition metal catalyzed oxidative carbonylation of amines will be presented in this section.

Palladium-Catalyzed Oxidative Carbonylation of Amines

The Tsuji group first reported Pd-catalyzed carbonylation of amines in 1966.[109] Since then it has been extensively studied and recently reviewed.[71,80] Methods for oxidative carbonylation utilizing copper oxidants or O_2 as the terminal oxidant and CuX or CuX_2 mediating have been utilized effectively with $PdCl_2$ to form ureas,[125-127] carbamates,[100,128] and oxamides.[100,129-131] Non-metal oxidants have also been used effectively including desyl chloride to generate carbamates from In-based alkylating

reagents and $PdCl_2$ and phosphine ligands.[111] The use of 1,4-dichloro-2-butene (DCB) as oxidant with the catalyst $PdCl_2(PPh_3)_2$ has been found to afford oxamides while using the oxidant I_2 yielded ureas from primary and secondary amines.[118]

Heterogenous carbonylations of amines to ureas

The first oxidative carbonylations of alkylamines using Pd/C as a catalyst were reported by Fukuoka[132] and Chaudhari.[133] The reactions were successful in the presence of promoter iodide salts and O_2, to afford ureas and carbamates in good yields. Similarly, Gabriele reported the use of PdI_2 and O_2 for the formation of ureas and cyclic carbamates from amines,[134] high yields and turnover numbers over 4900 were obtained (Figure 3-1).[103,135]

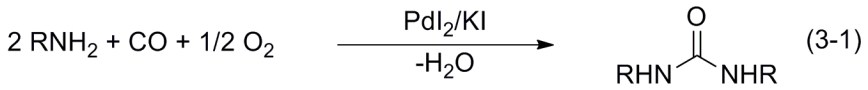

(3-1)

Figure 3-1. Oxidative carbonylation of alkylamines using a PdI_2 and KI system.[103]

Primary aliphatic amines (Eq. 3-1, R = alkyl) were carbonylated at 100 °C under elevated pressure with an atmosphere comprised of a 4:1:10 mixture of CO:air:CO_2 in the presence of a catalytic system comprised of PdI_2 utilizing KI as a promoter. The presence of CO_2 proved crucial to obtain higher yields. Solvent choice also dictated selectivity observed in the reaction. Urea formation was favored by using dioxane and glyme, while the oxamide predominated in much more polar solvents including N,N-dimethylacetamide (DMA) or N-methylpyrrolidinone (NMP).[135] It was postulated that the more polar solvents favored the formation of the intermediate $Pd(CONHBu)_2$, which then underwent reductive elimination to form the oxamide. Primary aromatic amines were also tested and found to be less reactive than their alkyl counterparts, unless

electron-donating groups were present on the aromatic ring, increasing their nucleophilicity.

When attempting to employ a similar system to the synthesis of carbonates from phenylacetylene and MeOH, Whiting found the system too difficult to effectively control (Figure 3-2).[112] While conditions were different than those for amines, they found that product distribution and yield could be affected by concentration, stirring speed, and grain size and loading of PdI_2. Combined product yields only approached 52% and ineffectively produced four different products. Overall, the method could not be adapted effectively to yield carbonates.

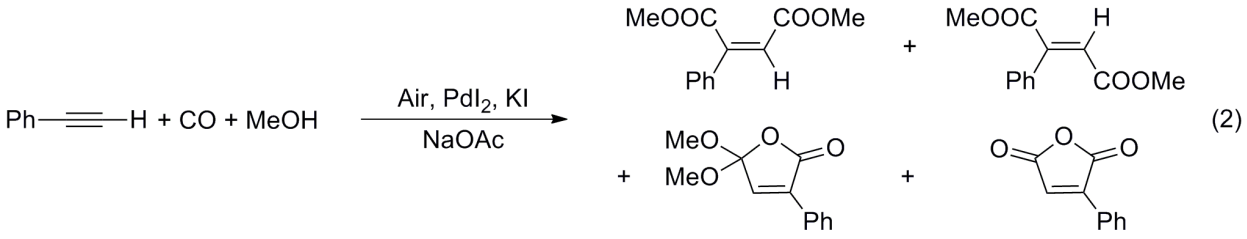

(2)

Figure 3-2. Oxidative carbonylation of phenylacetylene.

Mechanistic studies

The carbonylation of amines is generally thought to be carried out by a Pd(II) complex that is usually reduced to Pd(0) in the process.[71] Only a single case of the formation of a Pd(IV) complex has been reported.[136] It has been shown that direct oxidation of Pd(0) by O_2 is possible, but is too slow to prevent precipitation of metallic Pd under carbonylation conditions.[137] This necessitates that a co-catalyst be used to act as an oxidation catalyst for Pd. Shimizu and Yamamoto conducted a mechanistic study focusing on the role of reoxidation of the Pd(0) species formed in the principal catalytic cycle to electrophilic Pd(II) (**17**) during the selective carbonylation of amines to oxamides and ureas.[118] It was found that using DCB afforded oxamides and I_2 resulted

in the formation of ureas selectively. The independent generation of the carbamoyl palladium complex **18**, as a model species also generated further insight into the catalytic cycle (Figure 3-3).[135]

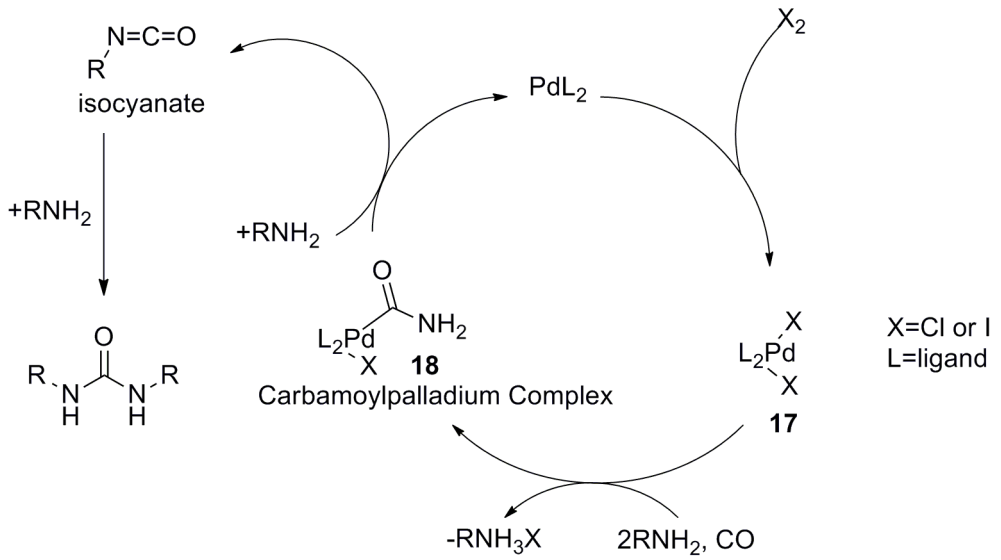

Figure 3-3. Postulated Pd catalytic cycle for Eq. 3-1.

The study discussed two possible mechanisms for the conversion of primary amines to ureas by Pd-catalyzed carbonylation. The first proposed mechanism involves the reductive elimination of a carbamoyl or amido ligand to generate the urea, in conjunction with work by Alper.[129] The second possible route is crucially dependant upon the formation of the alkyl isocyanate from the carbamoyl palladium species **18**. The urea is then generated through nucleophilic attack by either a primary or secondary amine on the intermediate isocyanate to generate either a symmetric or unsymmetrically substituted urea, as based on work by Gabriele on a similar system.[135]

It was found that diethylamine, dibutylamine, and morpholine, all secondary amines, were unreactive under the same conditions as their primary counterparts.[118] This supports the isocyanate pathway as secondary amines are unable to form tetra-

substituted ureas. Further support comes from tri-substituted ureas being synthesized upon carbonylation of mixtures of both primary and secondary amines. Lastly, trace isocyanates have been detected with GLC, TLC, and GLC/MS in the reaction mixtures of low-conversion experiments.[135]

Direct catalytic preparation of trisubstituted ureas in high selectivity is difficult, but made possible under these conditions by carbonylation of the primary amine in large excess of the less reactive secondary amine.[103] This proved effective for many urea type derivatives, especially cyclic ureas from primary diamines and *N*,*N*-bis(methoxycarbonylalkyl)ureas from primary α-amino esters. The synthesis of **19**, the neuropeptide Y5 receptor antagonist NPY5RA-972, was showcased utilizing this method (Figure 3-4).[103]

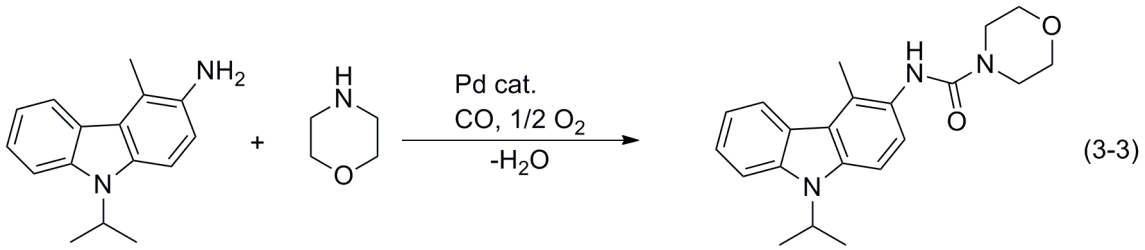

(3-3)

19

Figure 3-4. Synthesis of NPY5RA-972 using Pd catalyzed oxidative carbonylation.

Other Late Transition Metal Catalysts

Nickel-catalyzed oxidative carbonylation

Based on previous development of Pd-catalyzed oxidative carbonylations, efforts were made to use Ni as an inexpensive alternative. Nickel complexes have already been shown to yield stable carbamoyl derivatives upon carbonylation, suggesting that they could make potentially good candidates for oxidative carbonylation of amines.[93] Rather than the expected oxamides,[94] Giannoccaro obtained *N*,*N*′-dialkylureas from the

reaction of primary amines with the nickel amine complexes $NiX_2(RNH_2)_4$ (X = Cl, Br; R = alkyl). At temperatures above 50 °C side reactions became competitive.

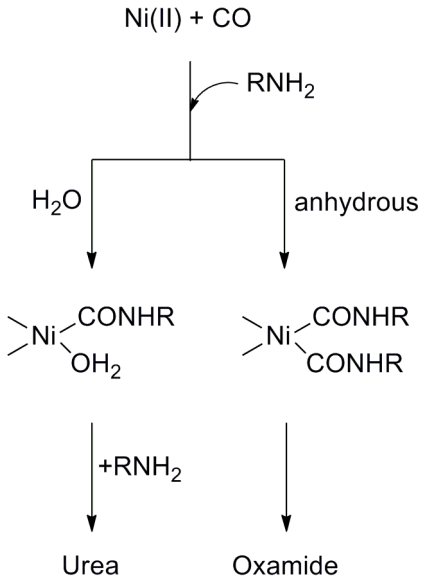

Figure 3-5. Nickel catalyzed oxidative carbonylation of amines.

At lower temperatures the reductive elimination of the oxamide did not occur. Selectivity between urea and oxamide was accomplished by controlling the amount of water present in the reaction. The presence of water afforded urea formation and anhydrous conditions yielded oxamide (Figure 3-5).[93] It was suggested that under aqueous conditions, water could coordinate to the Ni center and prevent more than one carbamoyl from forming. This intermediate would then be susceptible to nucleophilic attack from free amine, yielding the urea. Without the presence of water, two carbamoyls can form and reductively eliminate to form the oxamide.[93]

Ruthenium-catalyzed oxidative carbonylation

The oxidative carbonylation of aniline catalyzed by $[Ru(CO)_3I_3]NBu_4$ utilizing NiI as the promoter forms N,N′-diphenylurea (DPU) 99% selectively, as shown by Gupte.[98] The key step (Figure 3-6) is the formation of the carbamoylruthenium intermediate **24**.

Loss of CO from the catalyst precursor $[Ru(CO)_3I_3]^-$ **20** generates the ruthenium dicarbonyl intermediate **21** which then becomes susceptible to nucleophilic attack by aniline to form the aminoruthenium dicarbonyl species **22** and HI. Addition of CO to produce **23** is followed by insertion to afford the carbamoyl complex **24**. This then reacts with aniline to form both the product urea and the hydrido carbonyl species **25**. Addition of aniline yields **26**, which is oxidized by O_2 to regenerate the active species.[98] Similar results utilizing alkylamines have also been reported.[133,138]

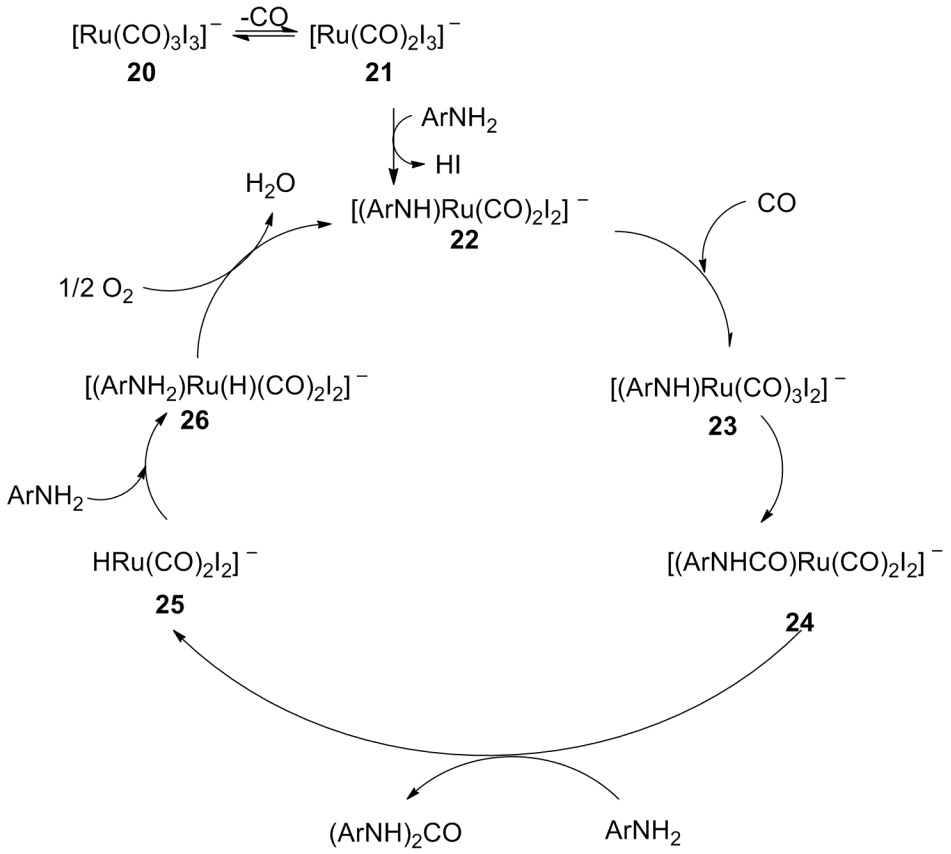

Figure 3-6. Oxidative carbonylation of arylamines using ruthenium catalysts.[97]

Cobalt- and rhodium-catalyzed oxidative carbonylation

The synthesis of acyclic and cyclic ureas from primary aromatic amines was accomplished by Rindone using *N*,*N*′-bis(salicylidene)ethylenediaminocobalt(II)

[Co(salen)] as catalyst.[90] No single set of reaction conditions could be obtained that was effective for multiple substrates. The pressure of O_2 affected the yield of urea as high pressures worked well for 4-methylaniline, but considerably lower pressures were more effective for 4-fluoroaniline. In general, electron-withdrawing groups in the *para* position lowered conversion of the starting amine. It was also found that electron-donating groups in the *ortho* position increased conversion as 2-aminophenol was more reactive than other amines.[139]

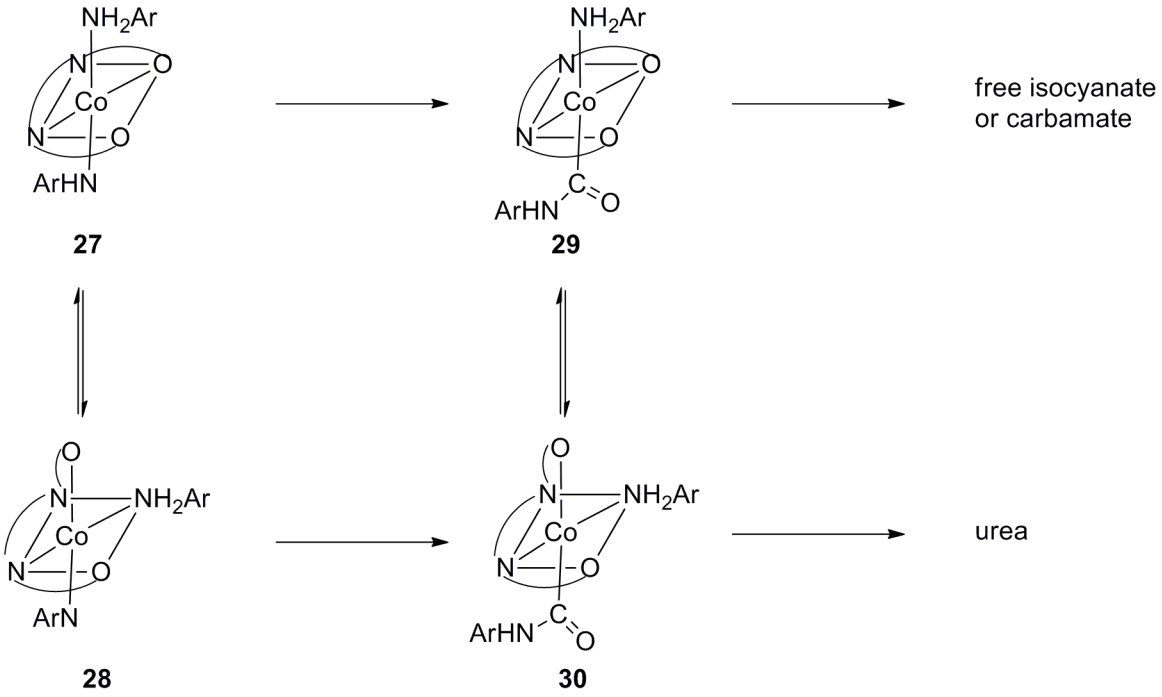

Figure 3-7. Cobalt (salen) catalyzed oxidative carbonylation of arylamines.

The proposed mechanism (Figure 3-7) involved the planar salen complex **27** being in equilibrium with the Co(III) amido complex **28**. Carbon monoxide can then insert into either complex generating another equilibrium mixture between **29** and **30**. The *trans*-geometry between the carbamoyl and the amine ligands could then lead to either free isocyanate or carbamates from **29**. The non-planar species **30** has a *cis* relationship between carbamoyl and amine ligands, which could then lead to urea formation.

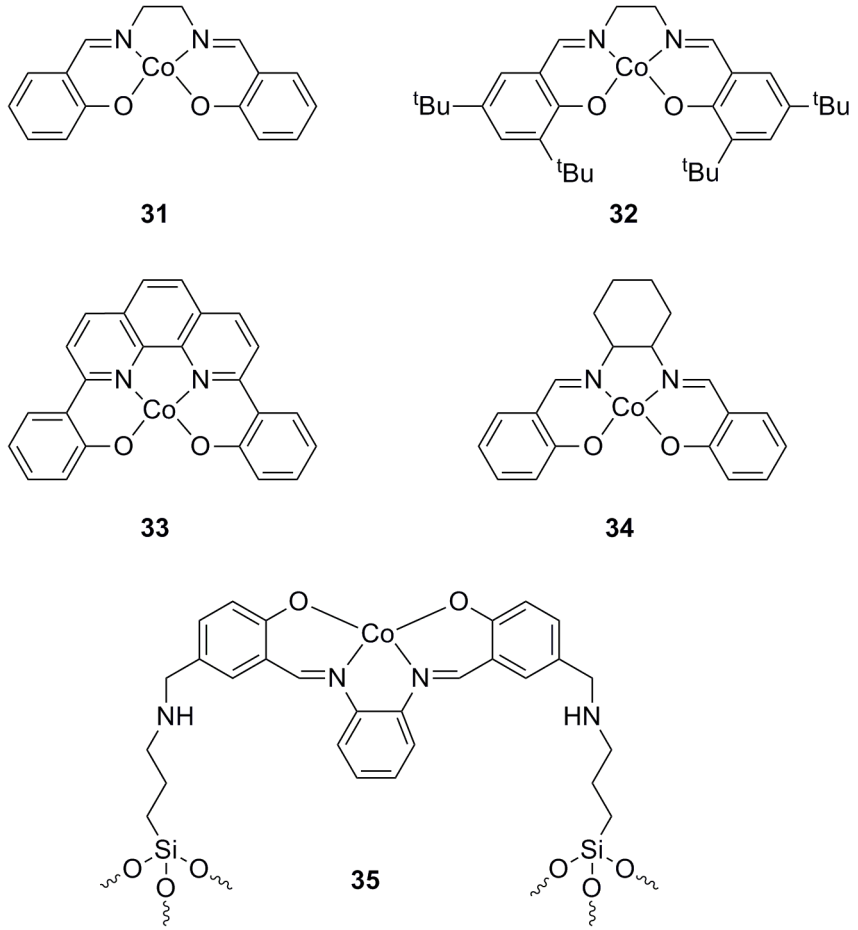

Figure 3-8. Co(salen) and modified Co(salen) complexes **31-35**.

Further studies on Co(salen) complexes led to the development of many new ligands to yield complexes capable of oxidative carbonylation. Compounds **31** and **32** were both found to yield diphenylurea, and **32** even does so 100% selectively in the presence of butanol.[140] The phenanthroline derivative **33** also was found to give 94% selectivity for the urea. Sun and Xia recently used **31** to produce cyclic carbamates in high yields from corresponding β-amino alcohols, but the substrates were limited to using aliphatic functionality only.[92] By using **34**, they were also successfully able to cyclize substrates containing isopropyl groups in 91% yield, which has been shown to be difficult under other circumstances.[83] Recently, in an effort to better increase catalyst

recovery, Co(salen) catalysts were covalently bonded to a silica matrix via a sol-gel process.[88] The heterogeneous catalyst **35** was used for the oxidative carbonylation of carbamates from aniline and methanol. While the reaction only produced a 60% yield of carbamate, it was able to be recovered five times with only a small drop in catalytic activity to still afford the product in 50% yield.

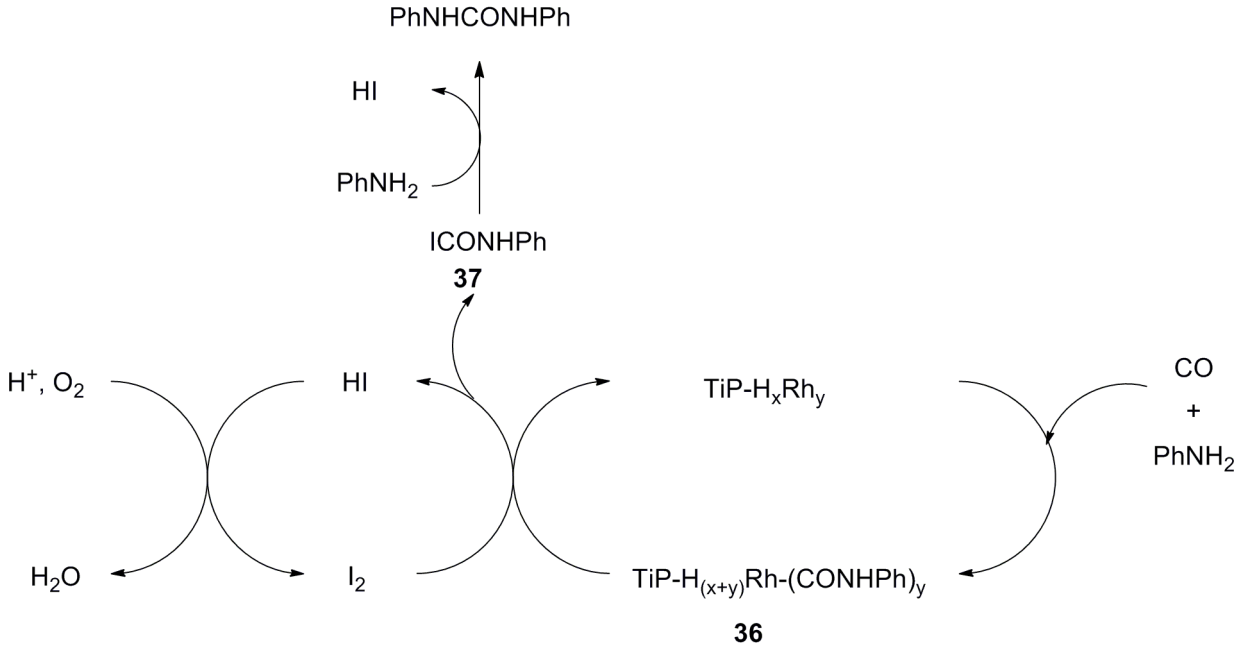

Figure 3-9. Rh-catalyzed oxidative carbonylation of aniline to DPU.[141]

Investigations of rhodium-catalyzed carbonylation of amines to ureas have been sparse recently. Chaudhari initially used Rh/C-NaI to make carbamates, but found some conditions that favored formation of ureas.[142] However, DMF was required as solvent to achieve urea synthesis, and all other solvents tested gave the carbamate product. Giannoccaro found that materials containing simple Rh^{3+} salts worked well for carbonylation of aniline to form DPU. The catalytic system worked better when intercalated with γ-titanium phosphate to make a heterogeneous system. A mechanism was postulated (Figure 3-9) and the key intermediate appears to be the Rh^{3+}-carbamoyl

complex **36** which reacts with I_2 to form the iodoformate intermediate **37**. Another molecule of aniline then reacts with **37** to form DPU.[141]

Attempts to further increase reactivity led to a bimetallic system. As heterogeneous catalysts with rhodium worked better than homogenous, a Co_2Rh_2/C complex was made. The strategy behind this was to immobilize nanoparticles of the metals in close proximity to one another for the oxidative carbonylation of amines using molecular oxygen as the oxidant.[89] This relied on the high surface-area-to-volume ratio that makes nanoparticles very reactive in these catalytic systems. The product ureas of aliphatic amines were obtained in good yields with butylamine giving 84% isolated urea and benzylamine generating 74%. Primary aromatic amines were also successful with aniline yielding 81% urea. *Para* substituted anilines were well tolerated, with *p-tert*-butyl giving 80% isolated product. Even allyl amine could be tolerated and was carbonylated in 44%. Recyclability of the heterogenous catalyst proved problematic as the yield of di-*n*-butylurea dropped to 31% after the fourth attempt. As less than 0.2% of the metals on a molar basis were found to have leached, the loss of activity could not be adequately explained.[89] A different mechanism also appears to be operative from traditional Co oxidative carbonylation but has not yet been determined.

Gold-catalyzed oxidative carbonylation

Gold catalysts for the oxidative carbonylation of amines have also been investigated and recently reviewed.[115,116,143] Simple Au^I salts formed carbamates from aniline, but aliphatic amines could be used to generate ureas.[115] Better results were obtained with polymer immobilized gold catalysts using arylamines to generate their methyl carbamates in the presences of methanol.[116] Ureas could be obtained only in the absence of methanol. The polymeric catalyst also showed enhanced activity and

ease of separation from the product compared to those gold catalysts previously reported. It was later shown that this reaction is capable of forming dialkylureas in high yield with high turnover frequencies, and worked in the presence of CO_2 as reactant, (Figure 3-10).[143] The exact mechanism for this reaction is still unknown.

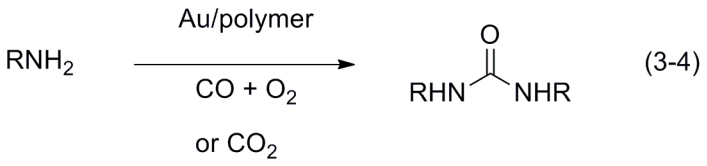

(3-4)

Figure 3-10. Polymer supported Au-catalyzed carbonylation of amines.

Tungsten-Catalyzed Oxidative Carbonylation of Amines

Carbonylation of primary amines

Examples of Group 6 metal complexes for the catalytic carbonylation of amines are rare. The initial report by McElwee-White utilized primary amines for catalytic oxidative carbonylation using the iodo-bridged tungsten dimer $[(CO)_2W(NPh)I_2]_2$ (**38**) as the precatalyst (Figure 3-11).[81] Those studies showed that primary aromatic and aliphatic amines could be carbonylated to the corresponding disubstituted urea, while secondary amines yielded modest amounts of formamides.

Mechanistic studies determined that primary amines reacted stoichiometrically with dimer **38** to yield the amine complexes $(CO)_2I_2W(NPh)(NH_2R)$, **39**. In the presence of an oxidant, these undergo nucleophilic attack by excess free amine to give the ureas.[81] The carbonyl ligand in **40** is susceptible to nucleophilic attack followed by proton abstraction from a second equivalent of amine to afford **41**. The reaction mixture was tested by FT-IR and indicated the presence of a carbamoyl species, as precedented from results from Angelici on the carbonylation of methylamine by $[(\eta^5\text{-}C_5H_5)W(CO)_4]PF_6$.[144] In that case, it was shown that the first step is conversion of $[(\eta^5\text{-}$

$C_5H_5)W(CO)_4]^+$ to the carbamoyl complex $(\eta^5\text{-}C_5H_5)W(CO)_3(CONHCH_3)$ after reaction with two equivalents of CH_3NH_2.

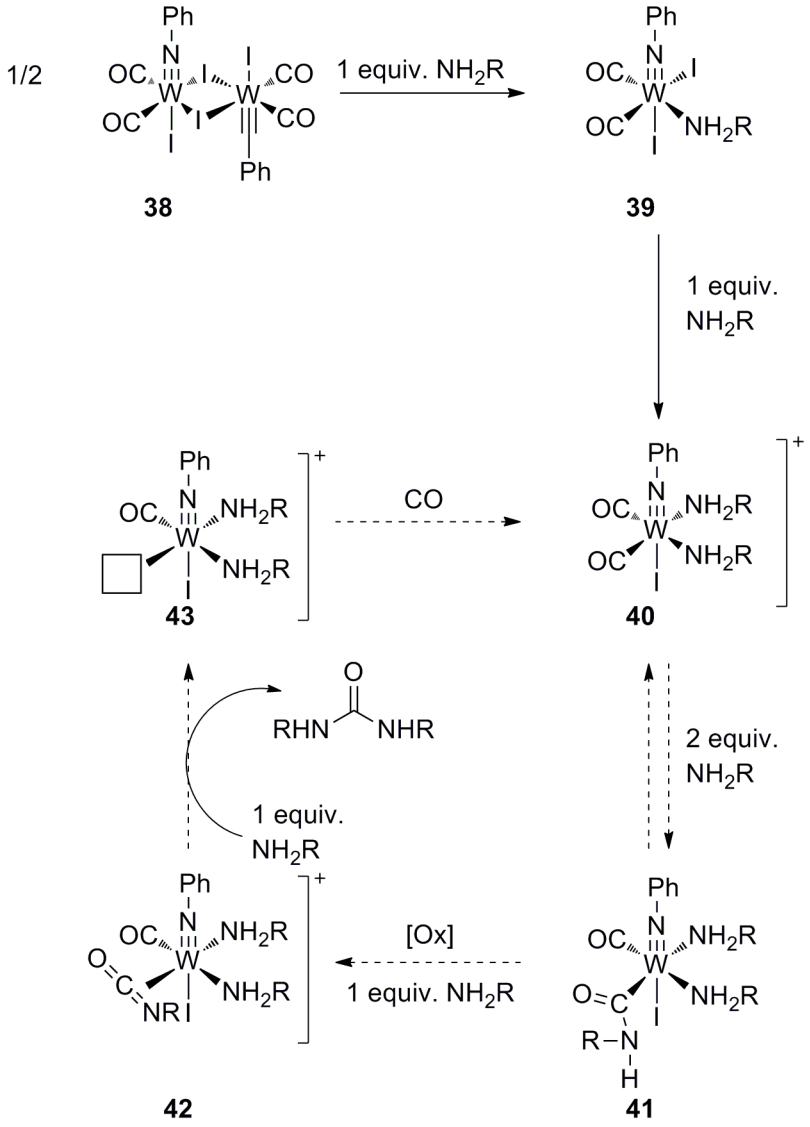

Figure 3-11. Mechanistic studies using **38**.

Assignment of the next step as oxidation was also supported by IR spectra showing the disappearance of the carbamoyl stretches upon exposure of the reaction mixture to air. Oxidation of **41** is expected to make the carbamoyl proton more acidic, thus enabling excess amine to deprotonate it to afford in the isocyanate complex **42**. Free amine would then be able to nucleophilically attack either coordinated or free

isocyanate to afford the disubstituted urea and also the coordinatively unsaturated complex **43**. Addition of CO would then regenerate the cationic species **40** and complete the catalytic cycle.

These results suggested that other tungsten carbonyl iodide complexes might also serve as catalysts. The choice to test $W(CO)_6$ as precatalyst was simple as it is commercially available, inexpensive, and air stable. Preliminary reactions using $W(CO)_6$, 100 equivalents of *n*-butylamine, 50 equivalents of iodine, and 100 equivalents of K_2CO_3 in a 125 mL Parr high-pressure autoclave pressurized with 100 atm CO produced di-*n*-butylurea in 80% yield with respect to amine, corresponding to 39 turnovers per equivalent of $W(CO)_6$.

Table 3-1. Oxidative carbonylation of primary amines to ureas under optimized conditions

Amine	Product	%Yield in CH_2Cl_2
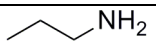	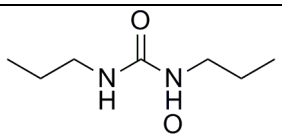	90
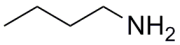	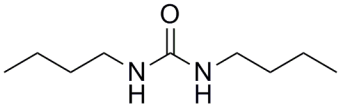	84
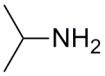	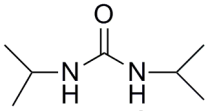	53
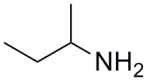	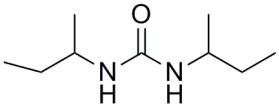	55
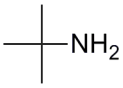	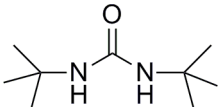	72
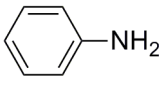	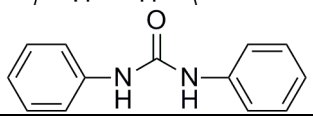	0

The $W(CO)_6/I_2$ system was subsequently optimized with *n*-propylamine and it was found that *N*,*N*′-disubstituted ureas could be obtained in good to excellent yields (Table

3-1).[70] After determining that a 2 mol% catalyst loading was ideal, other variables were examined. Overall optimal conditions were found to be 90 °C, 80 atm CO, 1.5 equivalents of K_2CO_3, and chlorinated solvents such as CH_2Cl_2 or $CHCl_3$. Aniline could not be successfully converted to DPU under any conditions tested, presumably due to its lower nucleophilicity as an aryl amine.

Carbonylation of primary and secondary diamines to cyclic ureas

Known methods for converting diamines to the corresponding cyclic ureas generally involve use of stoichiometric reagents based on nucleophilic attack of amines on phosgene and its derivatives.[73,74] The transition metal-catalyzed synthesis of cyclic ureas has not received much attention. The use of $Mn_2(CO)_{10}$ for the catalytic carbonylation of diamines to cyclic ureas from $H_2N(CH_2)_nNH_2$ was successful only when n = 3, to make the six membered ring, and in only 6% yield. This lack of success with other systems lead to the use of the $W(CO)_6/I_2$ system using high pressure CO as the carbonyl source as an alternative. Primary and secondary α,ω-diamines were both examined and found to yield the corresponding *N*,*N*′-disubstituted cyclic ureas.

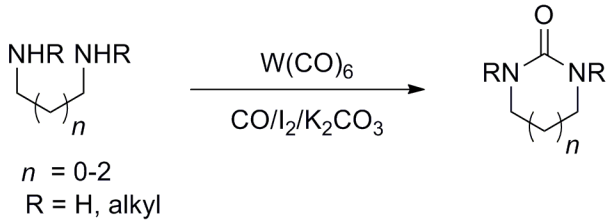

Figure 3-12. $W(CO)_6$-catalyzed oxidative carbonylation of diamines.

When using primary diamines, five-, six-, and seven-membered cyclic ureas could be formed in moderate to good yields (Figure 3-12).[83] The highest isolated yields were for six-membered cyclic ureas, with only trace amounts of the eight-membered ring compound being detected in the reaction mixture. This was not surprising as there are

no reports in the literature of the preparation of this compound from 1,5-pentanediamine. A 2-imidazolidinone derivative could be synthesized using this method from (+)-(1*R*,2*R*)-1,2-diphenyl-1,2-ethanediamine in 46% yield. Secondary diamines of the form $RNHCH_2CH_2NHR$ (Figure 3-12, R-Me, Et, ^{i}Pr, Bn) under similar conditions resulted in the formation of the corresponding *N*,*N*′-disubstituted cyclic ureas. The formation of oligomers upon carbonylation of both primary and secondary diamines was problematic, but could be overcome by employing high dilution. This strategy also been reported in the use of phosgene and its derivatives with diamines.[145]

An examination of steric effects on the ring closure was also undertaken using *N*,*N*′-dimethyl, diethyl, diisopropyl, and dibenzyl diamines under the standard conditions yielding both the dimethyl- and diethyl-cyclic ureas in nearly identical yields. The use of benzyl groups had only a minor lowering effect on the yield, but the use of isopropyl groups drastically lowered the yield of the imidazolidinone to only 10%. These steric effects could not be overcome by raising reaction temperatures. An interesting competition experiment yielded that when N-methylpropanediamine was reacted under the oxidative carbonylation conditions, the corresponding monosubstituted *N*-methyl cyclic urea was formed in preference to acyclic urea formation through the much more reactive primary amine.[83]

Further optimization of the carbonylation conditions for the conversion of α,ω-diamines to cyclic ureas used propane-1,3-diamine, $W(CO)_6$ as catalyst, and I_2 as the oxidant for tests of solvent effects and temperature variation.[70] Additional experiments on the effect of alkyl substituents in the linker of primary diamines were conducted (Table 3-2).[83]

Table 3-2. Tungsten-catalyzed oxidative carbonylation of substituted primary diamines

Amine	Product	% Yield
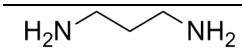	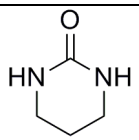	52
	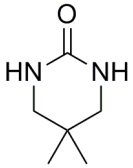	80
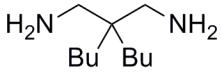	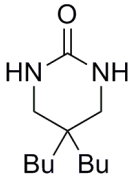	70
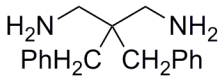	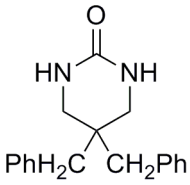	48
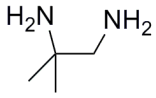	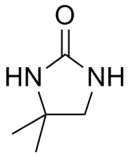	50
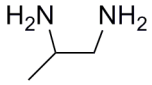	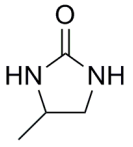	33
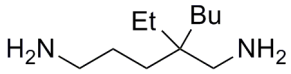	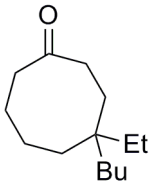	38

Simple *n*-alkyl substitution had dramatic effects on cyclic urea formation. 2,2-Dialkyl-1,3-propanediamines gave increased yields as compared to the parent propane-1,3-diamine as a result of the Thorpe-Ingold effect[146] and the enhanced solubility of the product resulting in simplification of the reaction workup.

The carbonylation of *N*,*N*′-dialkyl-2,2-dimethylpropane-1,3-diamines afforded tetrasubstituted ureas, but only in modest yields. Tetrahydropyrimidine byproducts were formed in significant amounts when the *N*-alkyl substituents were larger than methyl. When compared to the results obtained with carbonylations of secondary diamines to form five-membered cyclic ureas, the effects of the dimethyl substitution on ring size and those of the *N*-substituents are complex.

As cyclic ureas could be synthesized from the corresponding diamines, more complex synthetic targets were considered. However, no experiments on functional group tolerance had been conducted, and this tends to be an issue with early transition metals. Functional group compatibility was examined using a series of substituted benzylamines (Figure 3-13).[84]

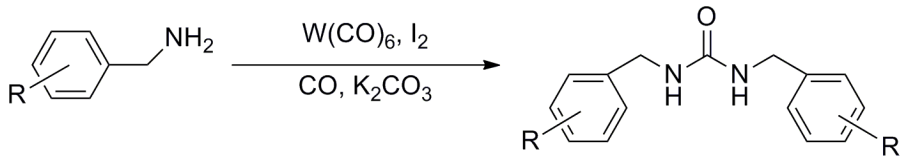

Figure 3-13. $W(CO)_6$-catalyzed carbonylation of substituted benzylamines.

The groups tested (Table 3-3[84]) demonstrated that the oxidative carbonylation of amines using the $W(CO)_6/I_2$ system was tolerant of a wide variety of functional groups. Amines containing substituents such as halides, esters, alkenes, and nitriles on the benzyl amine were successfully carbonylated to the corresponding ureas in moderate to good yields.

Table 3-3. Catalytic carbonylation of substituted benzylamines to ureas

Amine	% Yield[a]	Yield[b]	Amine	% Yield[a]	% Yield[b]
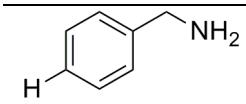	63	73	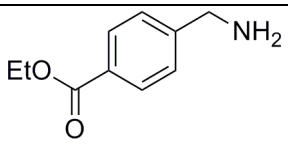	36	55
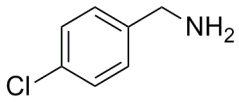	35	77	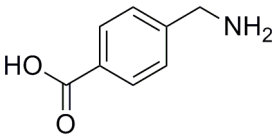	0	37
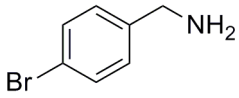	30	77	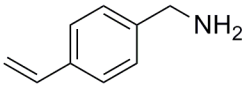	41	69
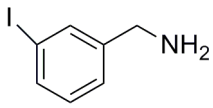	39	70	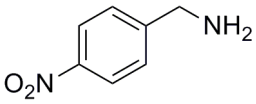	41	69
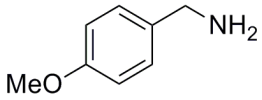	47	70	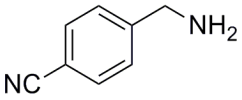	37	68
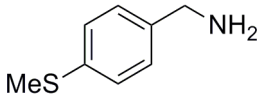	24	81	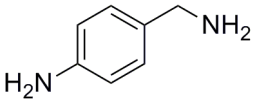	28	14
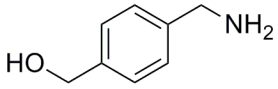	5	58	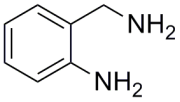	17	20
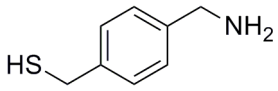	0	0			

[a] Reaction conditions: amine (7.1 mmol), $W(CO)_6$ (0.14 mmol), I_2 (3.5 mmol), K_2CO_3 (10.7 mmol), CH_2Cl_2 (20 mL), 70 °C, 80 atm CO, 24 h.
[b] The solvent was CH_2CH_2 (21 mL) plus H_2O (3 mL). Other conditions are as in footnote a.[84]

The presence of unprotected alcohols had been shown to be a problem using phosgene derivatives,[84] however, this was not the case in the tungsten system. Changing the reaction medium to using a biphasic solvent system produced a dramatic change in the yields of these functionalized ureas. This system provided solubility for

the starting amine, catalyst, the hydroiodide salt of the starting material formed from proton scavenging, and the K_2CO_3 base. Phase transfer conditions provided with this system then allowed for the amine salt to be deprotonated by aqueous carbonate, re-forming the free amine and allowing it to return to the organic phase for carbonylation.

After it was determined that the $W(CO)_6/I_2$-catalyzed system was tolerant of a broad range of functional groups in the conversion of amines to ureas,[84] use of this methodology to install the urea moiety into the core structure of the HIV protease inhibitors DMP 323 and DMP 450 was investigated (Figure 3-14).[147,148] Due to the large amount of literature present on the two synthetic targets, a direct comparison of the known routes using phosgene derivatives with the $W(CO)_6/I_2$-catalyzed system was possible.

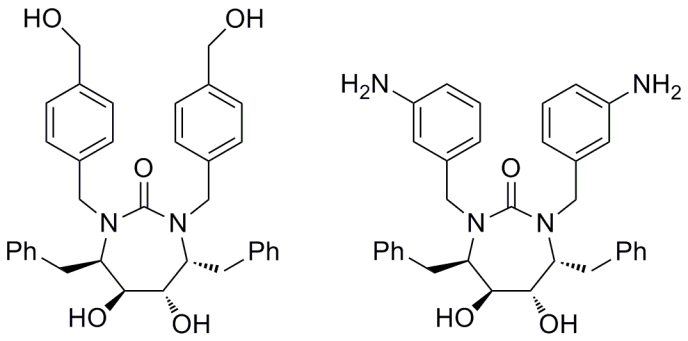

DMP 323 DMP 450

Figure 3-14. Structures of DMP 323 and DMP 450.

The use of an *O*-protected diamine diol to install the urea moiety of DMP 323 and DMP 450 by reaction with phosgene or its derivative had been reported. Small scale syntheses for initial testing were carried out using the phosgene derivative 1,1′-carbonyldiimidazole (CDI) followed by *N*-alkylation as appropriate.[148-151] On a practical scale, preparation of DMP 450 involves the reaction of a secondary diamine with phosgene to form the cyclic urea, as the use of stoichiometric CDI is cost prohibitive.

As using both phosgene and CDI required protection of the diol, much effort has been put into studying protecting groups in the stoichiometric reactions.[149,152] As a comparison, *O*-protecting groups acetonide, MEM ether, and SEM ether were tested in the catalytic carbonylation of diamine diols (Figure 3-15).[76]

The oxidative carbonylation of substrates **44-46** to cyclic ureas **47-49** by the $W(CO)_6$-catalyzed process allowed for a direct comparison to reactions conducted with the stoichiometric reagent CDI. Yields of the product were dependent on the identity of the protecting group in both the catalytic system and the stoichiometric one (Table 3-4).[76] These results show that the tungsten system can be used in preparation of complex targets.

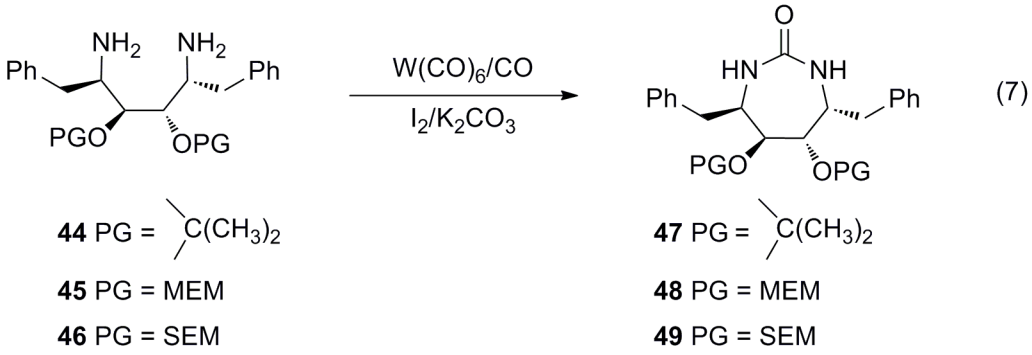

Figure 3-15. Carbonylation of **44-46**.

Table 3-4. Tungsten-catalyzed oxidative carbonylation of **44 – 46** to ureas **47 – 49**

Diamine	Reagent	Solvent	Urea % Yield	Ref.
44	CDI	CH_3CN	15	149
44	CDI	TCE	67	149
44	$W(CO)_6$/CO	CH_2Cl_2/H_2O	38	76
44	$W(CO)_6$/CO	CH_2Cl_2	23	76
45	CDI	CH_2Cl_2	62, 76	148,150,153
45	$W(CO)_6$/CO	CH_2Cl_2/H_2O	49	76
46	CDI	CH_2Cl_2	52, 93	148,150
46	$W(CO)_6$/CO	CH_2Cl_2/H_2O	75	76

The formation of oxazolidinones **51** and **52** resulted from the tungsten-catalyzed carbonylation of the unprotected diamine diol **50** (Figure 3-16).[77] While previous results on substituted benzyl amines had indicated the stability of unprotected –OH groups, this was not observed in the synthesis of DMP 323 or DMP 450. However, the formation of oxazolidinone as the major product was also reported in the reaction of **50** with both CDI and phosgene.[154] During the functional group tolerance experiments, the formation of carbamates was not possible due to geometric constraints owing to the 1,4-substitution pattern, thus favoring urea formation only.[84] With this constraint removed in **50**, oxazolidinone formation was preferred over that of the urea.

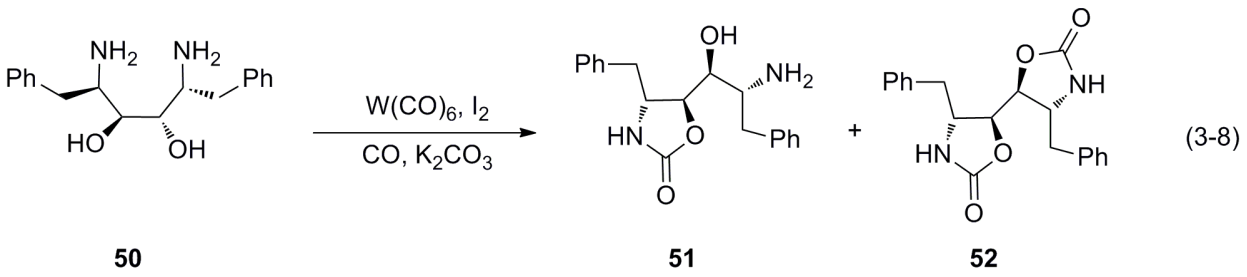

50 **51** **52**

Figure 3-16. Carbonylation of amino alcohols to form cyclic carbamates.

To further understand the limitations of the $W(CO)_6/I_2$-catalyzed system, 1,2-, 1,3-, 1,4-, and 1,5-amino alcohol substrates were subjected to $W(CO)_6$-catalyzed oxidative carbonylation to see if carbonate, carbamates, or urea formation was preferred (Table 3-5).[77] The varying substitution patterns and tether lengths also made it possible to probe whether formation of cyclic or acyclic ureas was preferred. A direct comparison to phosgene derivatives was sought with stoichiometric reagents CDI and dimethyl dithiocarbamate (DMDTC).[77]

The carbonylation of amino alcohols using the $W(CO)_6/I_2$-catalyzed system favored urea formation over that of the cyclic carbamates, even in the presence of

unprotected –OH groups, with respect to all tether sizes and substitution patterns tested. Neither acyclic carbonates or carbamates were detected as products. In comparison, carbonylation using the phosgene derivatives CDI and DMDTC resulted in variable selectivities between ureas and cyclic carbamates in the case of 1,2- and 1,3-amino alcohols. Optimized conditions for the $W(CO)_6/I_2$-catalyzed carbonylation of amino alcohols to ureas involved the use of pyridine as the base, removing the need for the biphasic solvent system originally utilized in the functional group compatibility experiments.[84]

Table 3-5. Carbonylation of amino alcohols to ureas and carbamates[77]

Substrate	Reagent	Urea (%)	Cyclic Carbamate (%)
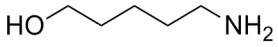	$W(CO)_6$/CO	64	2
	CDI	80	Trace
	DMDTC	45	0
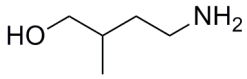	$W(CO)_6$/CO	93	0
	CDI	70	Trace
	DMDTC	93	0
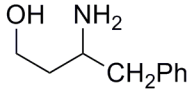	$W(CO)_6$/CO	95	Trace
	CDI	36	60
	DMDTC	30	8
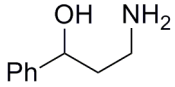	$W(CO)_6$/CO	72	14
	CDI	49	30
	DMDTC	34	47
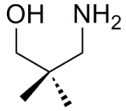	$W(CO)_6$/CO	60	5
	CDI	55	28
	DMDTC	32	29
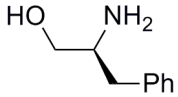	$W(CO)_6$/CO	78	10
	CDI	18	22
	DMDTC	72	Trace
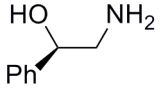	$W(CO)_6$/CO	79	14
	CDI	30	52
	DMDTC	73	Trace

Other synthetic targets that were prepared using the $W(CO)_6/I_2$-catalyzed carbonylation methodology included biotin and related heterocyclic ureas. More commonly known as Vitamin H, biotin is produced on an industrial scale as an additive

to the diet of poultry and swine. Synthesis of biotin has been extensively studied,[155] and the reports commonly employ the formation of the urea moiety by the reaction of phosgene with a diaminotetrahydrothiophene derivative. Biotin itself could not be obtained directly from the parent carboxylic acid, **53**, but the biotin methyl ester was obtained in 84% yield upon $W(CO)_6$-catalyzed oxidative carbonylation of substrate **54** (Figure 3-17).[156]

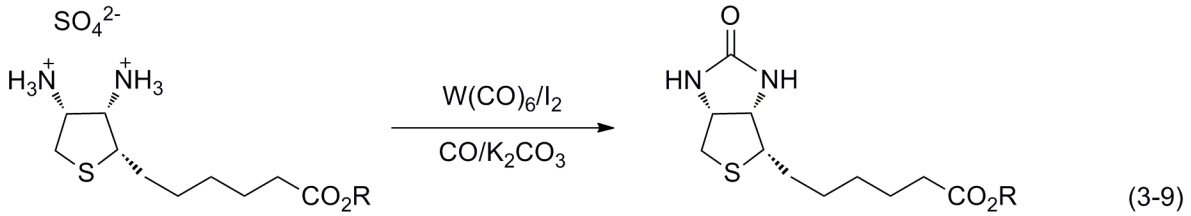

(3-9)

53 R=H
54 R=Me

55 R=H (0%)
56 R=Me (84%)

Figure 3-17. Synthesis of the biotin methylester **56**.

Heterocycles related to biotin, (**57-60**, Figure 3-18),[156] were also prepared via the $W(CO)_6$-catalyzed pathway and compared to reaction of the same substrates with CDI. Solubility of the diamine in dichloromethane appears to have a direct effect upon conversion of the diamine to the corresponding urea, resulting in moderate to good yields of the product (Table 3-6).[156]

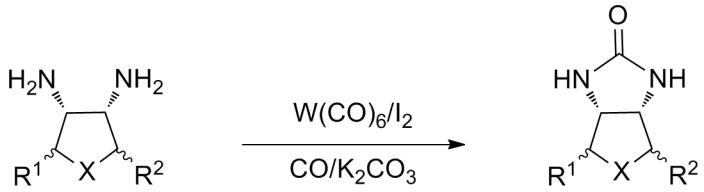

(3-10)

	X	R^1	R^2	Product
57	O	H	H	**61**
58	O	H	$(CH_2)_4CH_3$	**62**
59	N-Boc	CH_3	CH_3	**63**
60	CH_2CH_2	H	H	**64**

Figure 3-18. Carbonylation of heterocycles **57-60**.

Table 3-6. Yield of bicyclic ureas from diamines **57 – 60**

Amine	Urea	$W(CO)_6/I_2$ % Yield	CDI % Yield
57	**61**	Trace	20
58	**62**	47	67
59	**63**	46	37
60	**64**	57	56

Conclusions

The use of transition-metal-catalyzed carbonylation of amines offers efficient methodology to selectively synthesize ureas using mild reaction conditions. Being able to utilize CO as the carbonyl source directly, in the presence of both a catalyst and an oxidant, provides an effective alternative to traditional synthetic methods that employ stoichiometric reagents such as phosgene or phosgene derivatives, while maintaining selectivity, or even increasing it, for the formation of ureas from amines. The replacement of phosgene and the minimization of the waste streams associated with phosgene derivatives result in a greener alternative having less environmental impact.

Many transition metal complexes have successfully been employed in the carbonylation reactions, such as those of Pd, Ni, Co, Rh, and Au. These catalysts have been shown to afford ureas from amines, in both homogeneous, and more recently developed, heterogeneous processes. Tungsten-catalyzed oxidative carbonylation of functionalized amines has also been shown to be effective in the synthesis of complex targets such as the core structure of DMP 323 and DMP 450 and biotin.

CHAPTER 4
CATALYTIC OXIDATIVE CARBONYLATION OF α-AMINO AMIDES TO PRODUCE HYDANTOIN DERIVATIVES

Background

Considerable attention has been given to the synthesis of hydantoins and cyclic ureas, as they are frequently found as crucial moieties in many biologically active molecules with pharmaceutical relevance. Hydantoins substituted at the C-5 position (Figure 4-1) are important to medicinal chemistry as the heterocyclic derivatives are associated with a wide range of biological properties including anticonvulsant,[157] antidepressant,[158,159] antiviral,[158,159] and platelet inhibitory activities.[160]

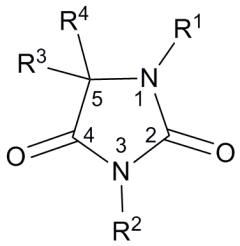

Figure 4-1. Numbering system for hydantoin rings.

Classic Ways to Synthesize Hydantoins

Various synthetic methods exist to prepare hydantoins from diverse starting materials. References to solution phase syntheses and polymer bound solid-phase organic synthesis can be found in the literature.[161-165] Different strategies have been employed to prepare the core structure including the use of ureas, cyanates, and phosgene reagents (Figure 4-2).[166]

Hydantoins can be prepared from ureas and carbonyl compounds as reported by Beller[167] utilizing methodology developed by Blitz (Figure 4-2a). The reaction of carbonyl compounds with inorganic cyanide incorporates the second nitrogen and carbonyl units to afford the hydantoin in the Bucherer-Bergs route (Figure 4-2b). The

Read-type reaction uses amino acid derivatives with inorganic isothiocyanate (Figure 4-2c) to yield hydantoins with hydrogen only at N-3. The use of alkyl or aryl iso(thio)cyanates (Figure 4-2d) allows for substituents at N-3. Amino amides can be used to introduce the last carbonyl, C-1, into a substrate already containing two carbons and two nitrogens (Figure 4-2e) with phosgene. Lastly, using α-halo amides and inorganic isothiocyanates can also afford a substituent at N-1 (Figure 4-2f).[166]

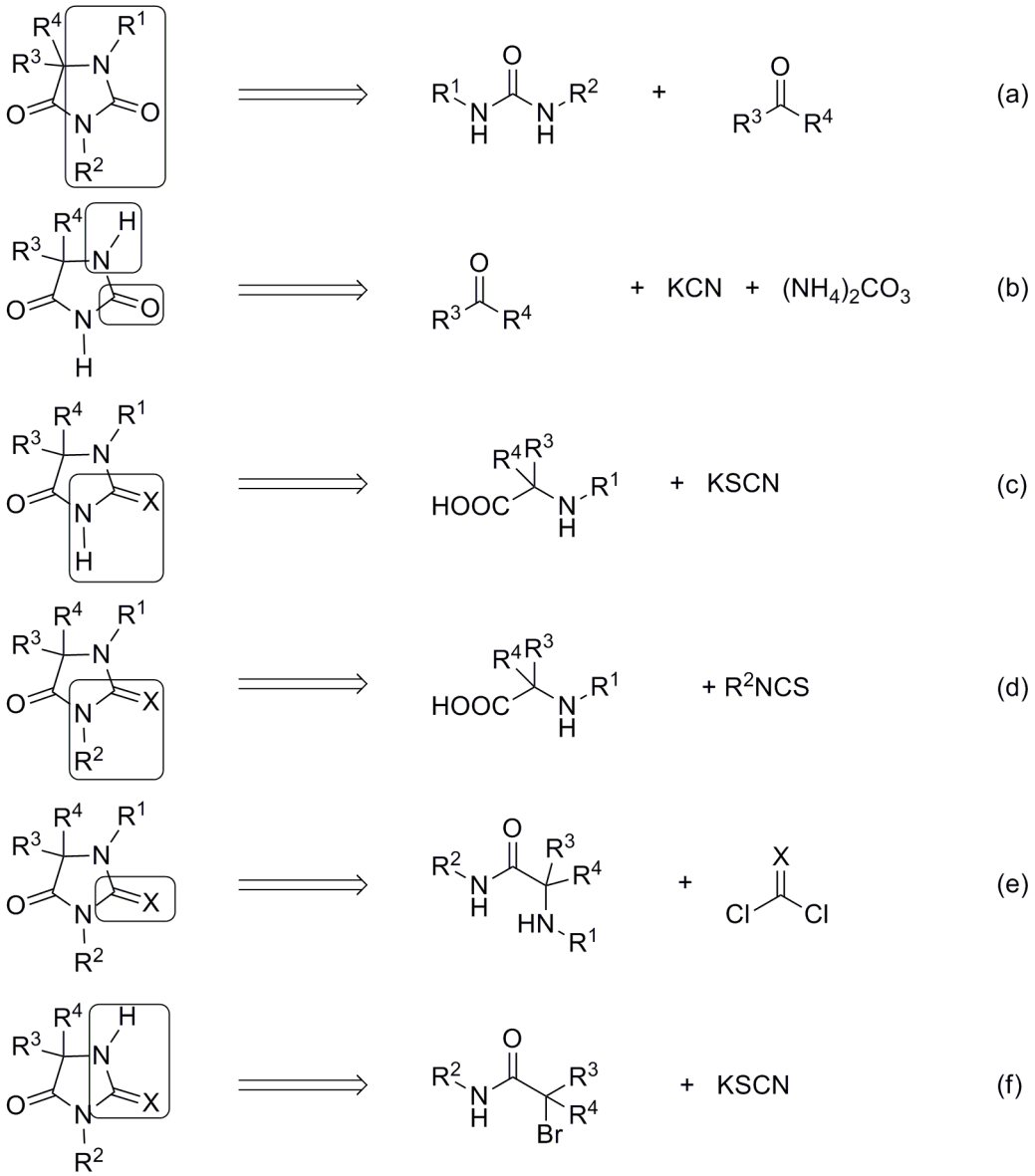

Figure 4-2. Synthetic approaches to hydantoins.

Solution Phase Syntheses

The Bucherer-Bergs synthetic method is commonly used in the synthesis of hydantoins to yield a 5-substituted ring employing aldehydes and ketones. This route uses potassium cyanide and ammonium carbonate with the requisite carbonyl compound as shown in the preparation of the aldose reductase inhibitor sorbinil (**67**), in which the absolute stereochemistry of the product is set using the alkaloid brucine (Figure 4-3).[161]

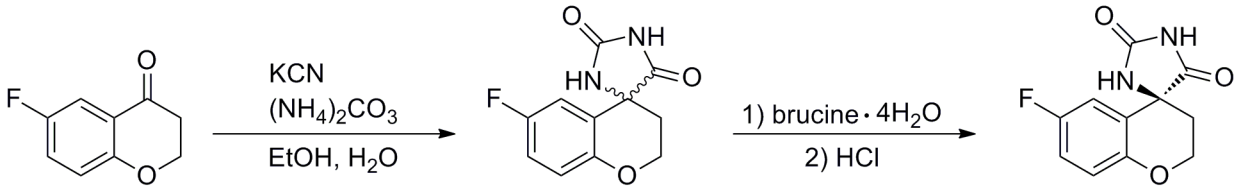

65 **66** **67**

Figure 4-3. Preparation of sorbinil (**67**).

For the synthesis of both hydantoins and thiohydantoins, the Read synthesis is also frequently used, as illustrated by Smith in the synthesis of a silicon-containing hydantoin starting from the silylated amino acid **68**. Treatment with potassium cyanate in pyridine followed by subsequent acid cyclization afforded hydantoin derivative **70** (Figure 4-4).[162]

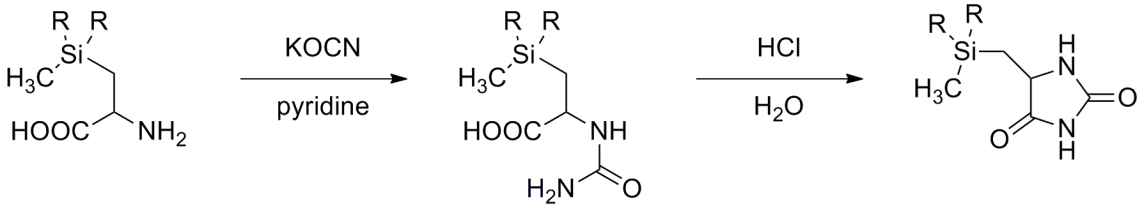

68 **69** **70**

Figure 4-4. Synthesis of hydantoin **70**.

Both the Bucherer-Bergs and Read-type methodologies have long been applied to the synthesis of hydantoins, but as more hydantoin derivatives have shown biological

activity, alternative methods have been of increasing interest. Among these is the synthesis of thiohydantoins.[163] The product thiohydantoin was afforded from an amino acid amide and reaction with a carbon sulfide. Amino amide **71** was treated with di-2-pyridylthiocarbonate (DPT) in THF at room temperature to yield the disubstituted hydantoin **72** (Figure 4-5).

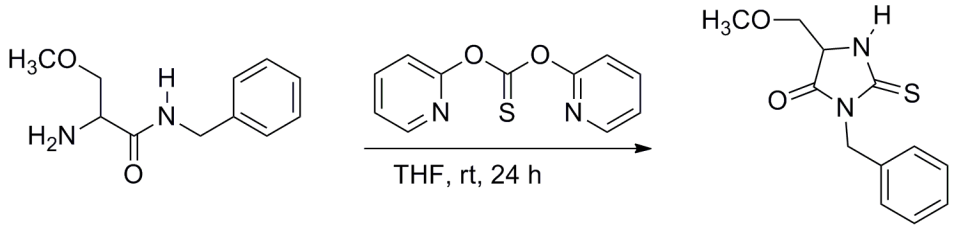

71 **72**

Figure 4-5. Synthesis of thiohydantoin **72**.

1,5-Disubstituted hydantoins can also be produced from other heterocyclic compounds. Aziridinone **73** can be used with cyanamide to yield the iminohydantoin intermediate **74** which is then treated with HNO_2 to afford the disubstituted product **75** (Figure 4-6).[168]

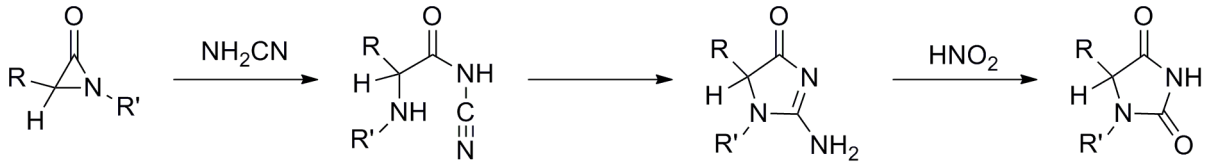

73 **74** **75**

Figure 4-6. Synthesis of hydantoin **75**.

Phosgene and its derivatives have also been employed in the synthesis of hydantoins as shown by Zhang's use of 1,1′-carbonyldiimidazole (CDI) to yield several enantiomerically pure hydantoins from α-amino amides derived from α-amino esters.[165]

Solid Phase Syntheses

The development of solid support systems capable of synthesizing structurally challenging heterocycles bearing one or more nitrogen atoms has received much attention in the last decade. A recent review by Gutschow addresses some of the more recent examples in this area that synthesize hydantoins via solid-phase organic synthesis (SPOS).[166]

A rather complex example of SPOS was shown in the assembly of trisubstituted hydantoins from multiple components as demonstrated utilizing Ugi/De-Boc/Cyclization methodology.[164] The five starting materials used in this reaction include aldehydes or ketones, amines, isonitriles, methanol, and CO_2 to yield hydantoins **76** (Figure 4-7).

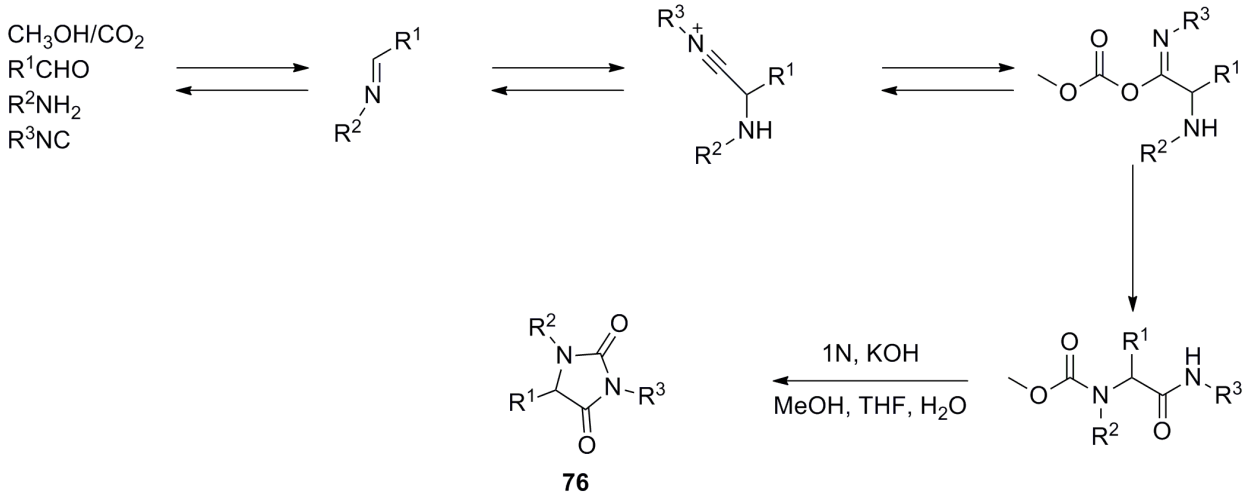

Figure 4-7. SPOS (solid phase organic synthesis) of **76**.

Based on success in utilizing $W(CO)_6/I_2$-catalytic oxidative carbonylation as an alternative to phosgene and phosgene derivatives, it was anticipated that this methodology could be extended to hydantoin targets. In theory, formation of the five membered ring from an α-amino amide should be kinetically favored over bimolecular

acyclic urea formation. Therefore, the synthesis of a series of hydantoins was undertaken to better understand the scope of the catalytic system.

A range of α-amino amides with differing substitution patterns was synthesized to determine the effect upon cyclization using the $W(CO)_6/I_2$ system (Figure 4-8).

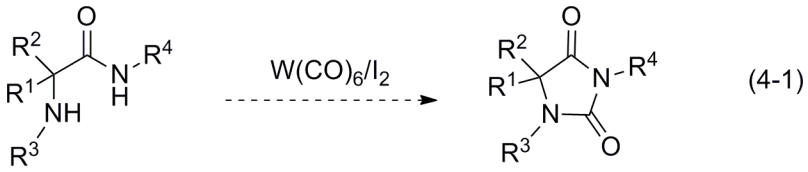

(4-1)

Figure 4-8. Proposed synthetic approach to using the $W(CO_6)/I_2$ system to yield hydantoins.

Synthesis of α-Amino Amides

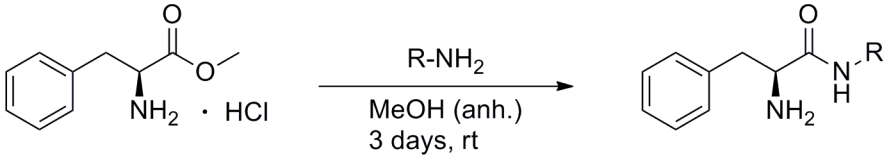

(4-2)

77

	R
78	Me
79	Et
80	$CH(CH_3)_2$
81	CH_2Ph

Figure 4-9. Synthesis of α-amino amides **78-81**.

Table 4-1. Synthesis of α-amino amides **78 – 81**

Entry	R	Product	Yield
1	CH_3	**78**	90
2	CH_2CH_3	**79**	82
3	$CH(CH_3)_2$	**80**	40
4	CH_2Ph	**81**	45

A series of seven disubstituted α-amino amides containing various aromatic and aliphatic side chains on either the amido or amino nitrogen was synthesized. Compounds **78-81** were synthesized by treatment of the corresponding amino acid

methyl ester hydrochloride with the requisite amine in anhydrous methanol (Figure 4-9, Table 4-1).[165]

An attempt at using a serine methyl ester (Figure 4-10) under similar circumstances using analogous methodology[169] as for **78** was conducted, but the product amide **82** could only be obtained in 35% yield. Thus an alternative approach was sought to obtain **82** using a mixed anhydride coupling procedure (MAC) followed by deprotection of the Cbz group by hydrogenation (Figure 4-11).[170]

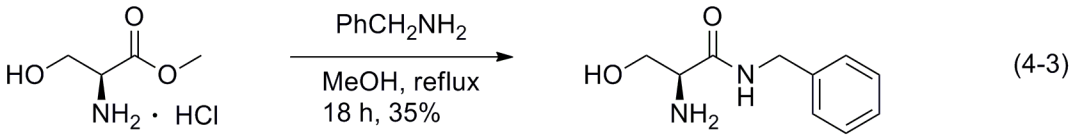

(4-3)

82

Figure 4-10. Synthesis of **82** from serine methyl ester.

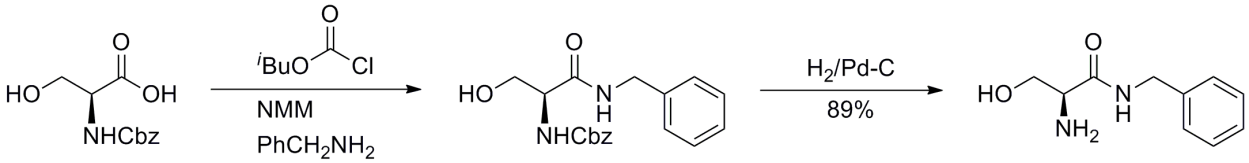

82

Figure 4-11. MAC synthesis of **82**.

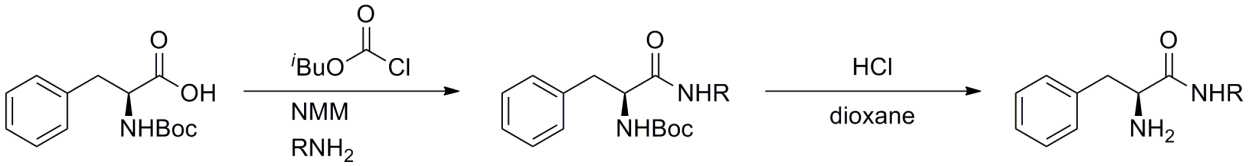

80 75%
81 84%

Figure 4-12. MAC synthesis of **80** and **81**.

The yields of both **80** and **81** using the procedure in Figure 4-9 were poor owing to difficulty in purification, presumably due to the 10 equivalents of amine used. The MAC

procedure was then extended to synthesize them from the commercially available *N*-Boc protected amino acid in overall yields of 75% and 84%, respectively (Figure 4-12).

The secondary amino amide **83** was obtained from the condensation of L-phenylalanamide with benzaldehyde followed by reduction with $NaBH_4$, in accordance with literature precedent (Figure 4-13).[171]

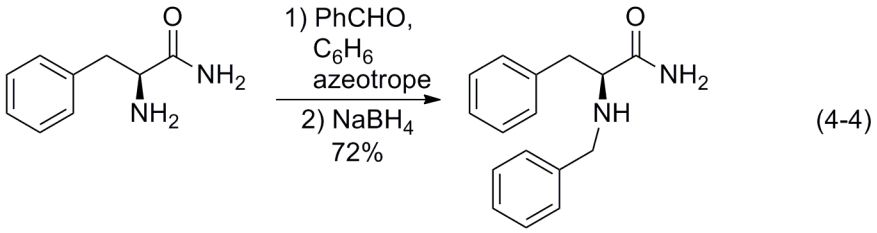

Figure 4-13. Synthesis of **83**.

The Boc-protection of commercially available α,α-diphenylglycine was carried out by adaptation of a literature procedure to give **84**.[172] The benzotriazole-mediated coupling of **84** with benzylamine gave **85** in overall 81% yield.[172]

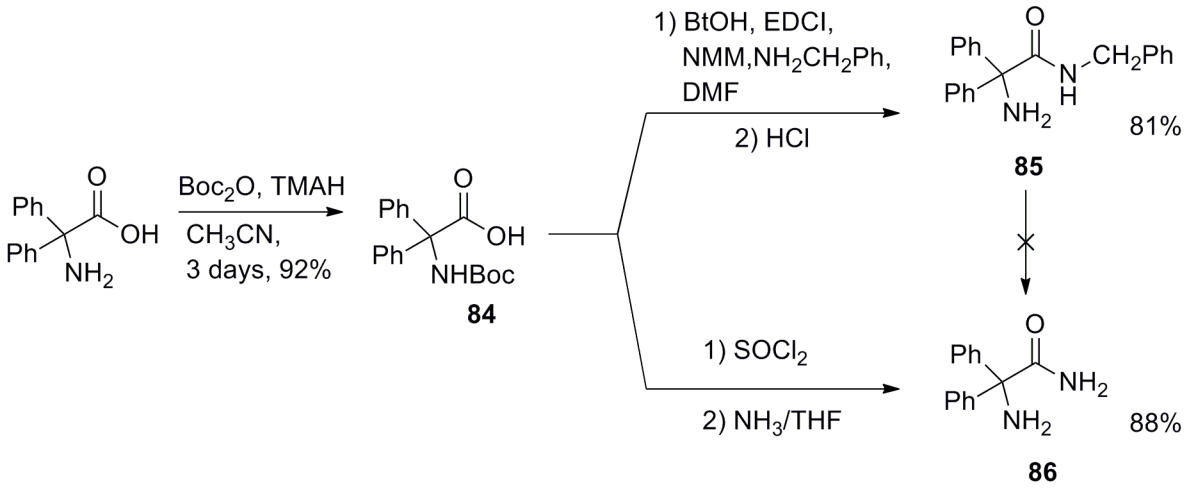

Figure 4-14. Synthetic scheme for **84-86**.

It was envisioned that **86** could be synthesized by the hydrogenation of **85**, but no conditions could be found for removing the benzyl unit from the amide, including 80

mol% Pd-catalyst, and 80 atm H_2 at 100 °C for 24 hours. Instead **86** was derived from treatment of **84** with $SOCl_2$ and saturated NH_3 in THF as adapted from the literature.[173] This proved fortuitous as it also resulted in the removal of the Boc group without needing a second deprotection step to afford the product in 88% yield.

Results and Discussion

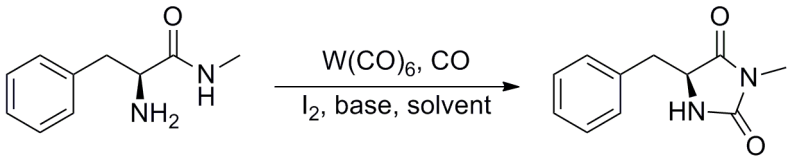

(4-5)

78 **78a**

Figure 4-15. $W(CO)_6$-catalyzed carbonylation of **78** to hydantoin **78a**.

Initial carbonylations of **78** were conducted under conditions optimized for the conversion of amino alcohols to ureas,[77] but the reaction did not produce the hydantoin and starting material was recovered.

Table 4-2. Carbonylation conditions for α-amino amide **78** to form **78a**

Entry	Time (h)	Pressure (atm)	Temp (°C)	Base/equiv.	Solvent	% Yield
1	18	80	40	Py/2	CH_2Cl_2*	0
2	24	80	45	Py/2	CH_2Cl_2	0
3	36	90	55	Py/2	CH_2Cl_2	40
4	45	80	25	Py/2	CH_2Cl_2	0
5	36	90	55	K_2CO_3	CH_2Cl_2/H_2O	20
6	42	90	45	DMAP/2	CH_2Cl_2	0
7	36	85	45	DMAP/3	Toluene	0
8	36	85	45	DMAP/3	CH_2Cl_2/H_2O	50
9	36	85	45	DMAP/4	CH_2Cl_2/H_2O	50
10	48	85	45	DMAP/4	CH_2Cl_2/H_2O	Trace
11	36	80	45	DBU/4	DCE	73

The solution concentration of Entry 1 was 4.0 M, (0.87 mL of solvent), all others were conducted at 0.031 M (35 mL of solvent).[174]

As the amide is considerable less nucleophilic than the amines present in the amino alcohol substrates, this was not surprising. A series of carbonylations testing different bases, higher temperatures, and longer reaction times was conducted using **78** (Figure 4-15, Table 4-2[174]).

The best conditions are described in Entry 11. The lower amide nucleophilicity is compensated by use of a stronger base. In addition, time was also a factor, as 36 hours was optimal for these conditions. At longer reaction times, the product began to decompose.

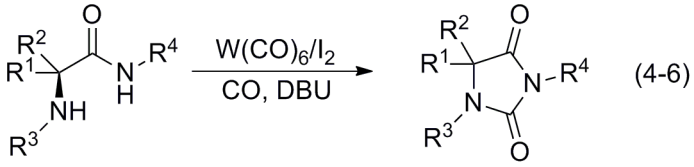

(4-6)

Figure 4-16. General carbonylation of amino amide substrates.

Table 4-3. Catalytic carbonylation of amino amide substrates

Entry	Cmpd	R^1	R^2	R^3	R^4	Product	Yield (%)
1	**78**	CH_2Ph	H	H	CH_3	**78a**	73
2	**79**	CH_2Ph	H	H	CH_2CH_3	**79a**	61
3	**80**	CH_2Ph	H	H	$CH(CH_3)_2$	**80a**	Trace
4	**81**	CH_2Ph	H	H	CH_2Ph	**81a**	75
5	**82**	CH_2OH	H	H	CH_2Ph	**82a**	50
6	**83**	CH_2Ph	H	CH_2Ph	H	**83a**	10
7	**85**	Ph	Ph	H	CH_2Ph	**85a**	Trace
8	**86**	Ph	Ph	H	H	**86a**	7

Starting with the conditions described in Table 4-2, Entry 11, the carbonylation of the other substrates was attempted (Figure 4-16, Table 4-3). Compounds **78-81** illustrate the effect of steric variation at the amide nitrogen on ring closure. The yields were highest for compounds **78**, **79**, and **81**, (R^4 = Me, Et, and Bn respectively), which

have no branching at the α-carbon of the substituent. The effect of the secondary alkyl substituent is seen in **80** ($R^4 = {}^{i}Pr$), where the hydantoin product **80a** was only observed in trace quantities. This is not surprising as similar effects have been found in the carbonylation of secondary diamines containing these *N*-alkyl substituents.[83,84] The substrate with the free –OH group, **82**, yielded the hydantoin product **82a** in 50% yield and no carbamate was observed. What was intriguing is that substrates **83**, **85**, and **86** yielded almost no product under these conditions. Since hydantoin **86a** is the anticonvulsant diphenylhydantoin (Dilantin™), and thus one of the more interesting targets, other conditions for successful carbonylation of **86** were sought.

The results of the reaction conditions tested in the carbonylation of **86** to form diphenylhydantoin **86a** (Table 4-4) show the complexity of this system. Lack of nucleophilicity rendered this substrate less reactive and stronger bases such as DABCO (entry 4) and DBU (entry 7) were required. However, the excess base also could have a deleterious effect upon the reaction as 1.1 equivalents of DBU (entry 8) gave 35% yield and 2.2 equivalents DBU (entry 13) lowered the yield to 12%. Utilizing either anhydrous solvent (entries 8 and 9) or high dilution (entry 12) also seemed to have no effect upon yield. Anhydrous solvents were examined because one of the major products was benzophenone, which presumably arises via hydrolysis, but the decomposition occurred regardless of the presence of adventitious water in the solvent or other reagents. Choice of solvent and temperature appeared to make the largest impact upon the system. When using 1,2-dichloroethane (DCE) the reaction mixture appeared often to undergo a coupling oligomerization as evidenced by a viscous dark orange solution following carbonylation. When dichloromethane was substituted, the

oligomerization was not observed. Although amines are known to react with chlorinated solvents,[175] no products of reaction with DCE were observed. Optimized results were obtained using DCM with 1.1 equivalents of DBU as base for 24 hours at 35 °C (entry 20). The higher yields of hydantoins in DCM, as compared to DCE, are attributed to the higher solubility of the substrate.

Table 4-4. Optimization of carbonylation of **86**

Entry	Base (equiv.)	Temp (°C)	Time (h)	Yield
1[a]	Py (1.1)	60	24	Trace
2	Py (2)	rt	48	Trace
3	Py (7)	60	48	0
4[a]	DABCO (1.1)	rt	24	5
5	DBU (1.1)	rt	24	9
6	DMAP (4)	60	24	0
7	DBU (1.1)	45	24	5
8	DBU (1.1)	60	24	35
9[a]	DBU (1.1)	60	24	31
10	DBU (1.1)	60	36	0
11	DBU (1.1)	70	24	Trace
12[a,b]	DBU (2.2)	60	24	11
13	DBU (2.2)	60	24	12
14	DBU (4)	60	24	Trace
15	DBU (4)	60	36	0
16[b]	DBU (4)	60	36	0
17	DBU (4)	60	48	0
18	DBU (4)	rt	60	0
19[c]	DBU (1.1)	35	12	51
20[c]	DBU (1.1)	35	24	64
21[c]	DBU (1.1)	35	36	12

[a] Anhydrous solvent and reagents. [b] Conducted at half concentration, 0.028 M, all others at 0.056 M. [c] Dichloromethane as solvent, all others are 1,2-dichloroethane. The CO pressure for all reactions was held constant at 80 atm.

Substrates **83** and **85** were then carbonylated using the optimized conditions for **86** (Eq. 4-6). The yields improved greatly over those obtained using the conditions optimized for the methyl amide **78**, but still are low to moderate (Table 4-5). Substrate **83**, the constitutional isomer of **81**, was only able to afford the hydantoin product in 41% yield whereas **81a** was obtained in 75%. This illustrates the effect that steric bulk on the amine nitrogen has on the system. Compound **85** underwent competitive decomposition to benzophenone during the formation of **85a**, as was observed in reactions of **86**. It appears in the case of **85**, the relative rate of decomposition into benzophenone is faster than that of the relative rate of carbonylation. One possible route to explain the low yields from **83a** and **86a** is that primary amides are less nucleophilic than their secondary counterparts, and as a result the rate of carbonylation is slower making decomposition pathways possible.

Table 4-5. Comparison of carbonylation conditions for **83**, **85**, **86**

Substrate	Hydantoin	%Yield[a]	%Yield[b]
83	**83a**	10	41
85	**85a**	Trace	11
86	**86a**	7	64

[a] Conditions optimized for **78a**. [b] Conditions optimized for **86a**.

When substrates **78-81** are carbonylated under the optimum conditions for phenytoin, the yield of the corresponding hydantoins drops to less than 15% for all amino amides. This could be due to differences in solubility of substrates in DCM versus DCE, the fewer equivalents of base present, or that both reaction times and temperatures were lower.

Conclusions

$W(CO)_6/I_2$ oxidative catalytic carbonylation of α-amino amides results in moderate-to-good yields of hydantoins. Steric hindrance at the nitrogen in the substrate has an effect on the yield and decomposition of the substrate is competitive with product formation in a few cases. The use of this methodology provides an alternative to previous existing synthetic pathways to hydantoins.

CHAPTER 5
CATALYTIC OXIDATIVE CARBONYLATION OF β-AMINO AMIDES TO PRODUCE 5,6-DIHYDROURACIL DERIVATIVES

Background

The synthesis of 5,6-dihydrouracils has been of interest in organic chemistry due to their importance in the biochemistry of cells and their potential as biologically active molecules.[176] Long known to be intermediates in the catabolism of uracils, 5,6-dihydrouracils have been studied for their biological significance.[177,178] The applications of this class of molecules are anticancer,[179,180] antifungal agents[181] and herbicides,[182] and inhibitors of HIV-1 integrase.[183] 5,6-Dihydro-5-fluorouracil is a potential pro-drug form of 5-fluorouracil, which is a widely prescribed antineoplastic drug used in the treatment of breast and colorectal cancers.[184]

Synthetic Routes to Form Dihydrouracils

While 5,6-dihyrouracils (Figure 5-1) have been heavily investigated for their biological effects and have been of spectroscopic interest for their conformational characteristics,[185-187] the synthetic methods to yield these compounds have not been heavily investigated. Since the early 1950's only a few solution phase methods have been explored, mainly utilizing isocyanates or hydrogenations of parent uracils to their 5,6-dihydrouracil products. There has also been recent interest in the application of solid phase organic chemistry (SPOC) to synthesize these compounds.

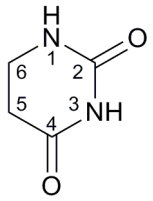

87

Figure 5-1. 5,6-Dihydrouracil.

Solution Phase Methods

The condensation of α,β-unsaturated carboxylic acids with ureas has been an effective way to synthesize 5,6-dihydrouracils (Figure 5-2).[187,188] Initially, this synthesis was applicable only on large, multi-molar scales and tended to only give moderate yields of products, around 45%.[188]

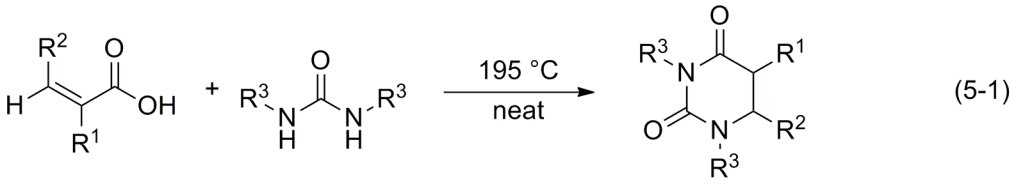

(5-1)

Figure 5-2. Synthesis of 5,6-dihydrouracils using α,β-unsaturated carboxylic acids.

Scaling the method down proved problematic as urea decomposition occurred readily at the reaction temperature in the presence of air. To overcome this limitation, a millimolar amount of reactant could be sealed in a 40 mL steel tube and heated to the appropriate temperature for 1-2 hours.[187] The reaction is still limited in that it could only use matched alkyl groups on the ureas (Eq. 5-1, R^3=H, Me) to yield symmetrically substituted N's. Yields obtained varied between 10-80% depending on the substituents present on the alkene.

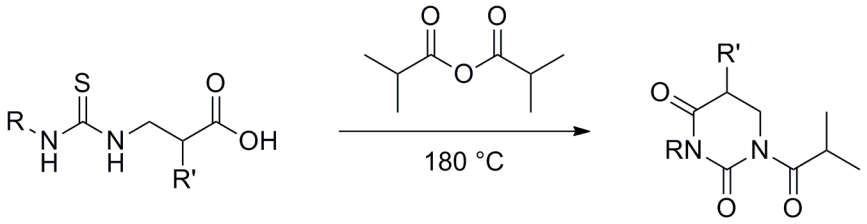

(5-2)

Figure 5-3. Synthesis of 5,6-dihydrouracils using isobutyric anhydride.

More recently, a variant of this reaction using *N*-3-substituted 3-thioureidopropanoic acids combined with isobutyric anhydride resulted in the formation of 5,6-dihydrouracils (Figure 5-3).[189] This was a serendipitous discovery in an attempt

to generate 2-amino-4,5-dihydro-1,3-thiazin-6-ones. Instead of the intended compound a dihydrouracil was obtained. Upon further exploration of the reaction it was determined that the ureido-*N*-substituent generally could only be an activated benzene. Deactivated aryl rings were found to give poor yields and the presence of aryl halogens resulted in inseparable mixtures. When the reaction was conducted at 80 °C, samples analyzed by HPLC after 15 minutes indicated that characterizable quantities of products and other intermediates were present in the reaction mixture (Figure 5-4).[189] Compounds **89-91** were all discrete compounds, each identified by NMR and/or LCMS. Only 5% of the dihydrouracil had been formed at this point and the mixture was comprised of 9% **89**, 52% **90**, and 10% **91**. The remainder of the mixture was unidentifiable. The identity of the compounds led them to postulate a mechanism that rationalized the products formed.

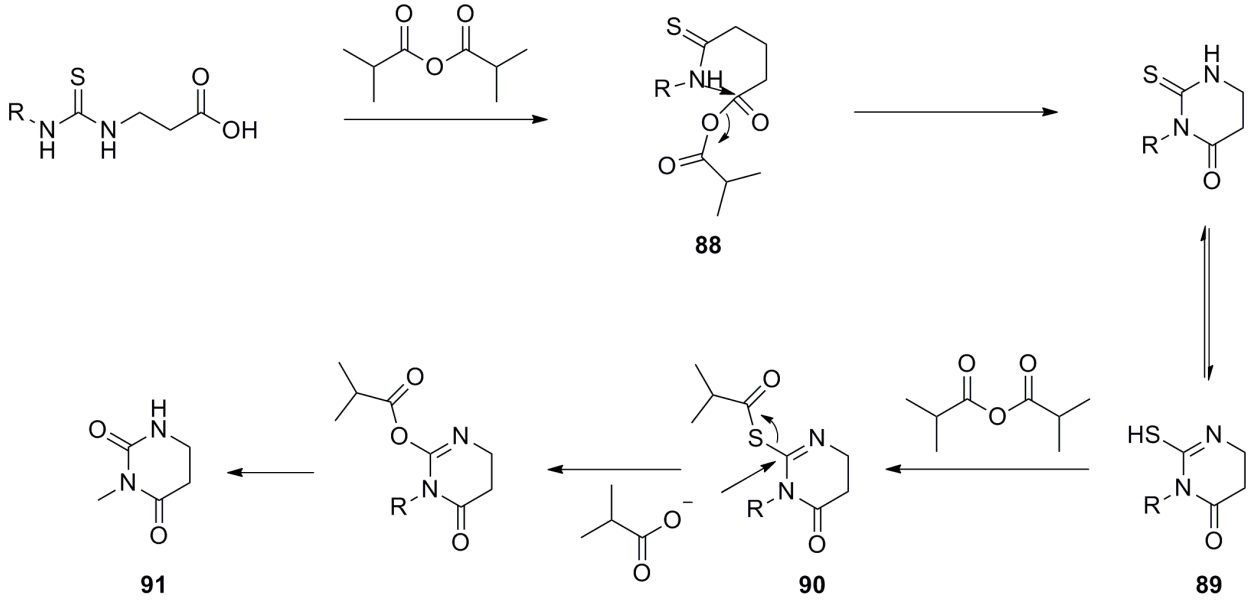

Figure 5-4. Proposed mechanism of 5,6-dihydrouracil formation.

Using lead tetraacetate to oxidize substituted succinamides has also been successful in regioselectively furnishing dihydrouracils (Figure 5-5).[190] The yields of **92**

and **93** approach 90%. However, if the acetoxy group is placed in the 3-position as opposed to the 4-position, the molecule loses AcOH upon reaction with $Pb(OAc)_4$ to produce the uracil derivative in 70% yield. The reaction has limited scope, as lead tetraacetate is not compatible with most functional groups.

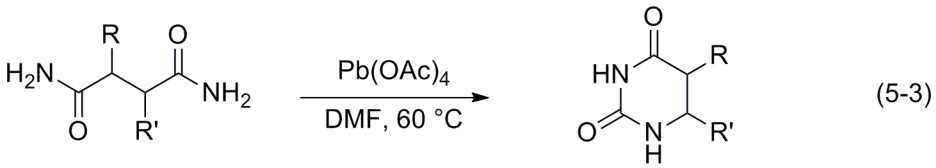

(5-3)

92 R = Me, R' = H
93 R = Me, R' = OAc

Figure 5-5. Conversion of diamides to 5,6-dihydrouracils by reaction with $Pb(OAc)_4$.

The hydrogenation of uracil derivatives (Figure 5-6) has also been demonstrated to yield 5,6-dihydrouracils, but has proven problematic in some regards. Established methodology includes use of hydrogen with a Rh-Al amalgam, Pd/C, or $NaBH_4$.[191] Problems often encountered with these methods are low yields, epimerization at C5, or complete removal of the N1 alkyl group.[192] Newer techniques using ammonium formate as an H_2 source in methanol do not epimerize C5, although yields still are moderate (39-50% depending on water content of the solvent).[193]

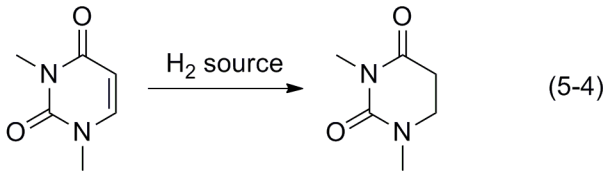

(5-4)

Figure 5-6. Hydrogenation of uracil to 5,6-dihydrouracil.

A milder reduction pathway utilizing lithium tri-*sec*-butyl borohydride (L-selectride) was found by Kundu to reduce substituted uracils to their 5,6-dihydrouracil adducts in yields of 72-94% (Figure 5-7).[176] The reaction tolerates a range of alkyl groups (H, propargyl, methyl, and benzyl). The propargyl group is not reduced under these

conditions, showing chemoselectivity. The limitation to the reaction is that N-H bonds are incompatible with L-selectride, and the reaction was successful only where R = Me and aryl. [194] The requirement for matched alkyl substituents on the nitrogens limits applicability of the reaction to varied substrates.

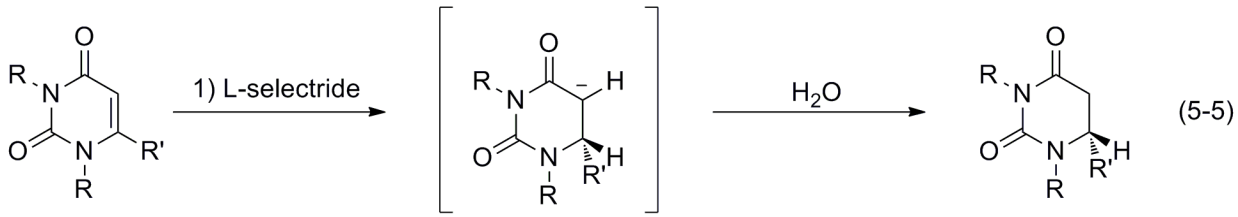

(5-5)

Figure 5-7. L-selectride reduction of uracils to form 5,6-dihydrouracils.

The most common pathway seen in solution phase organic chemistry is the combination of a β-amino acid derivative with an alkyl isocyanate or alkyl isothiocyanate to afford the 5,6-dihydrouracil or 5,6-dihydro-thione adduct (Figure 5-8).

The reaction of an amino nitrile with an isothiocyanate was shown to yield the thione derivative after treatment with acid (Eq. 5-6).[195] Similarly, the reaction of an alkyl isocyanate with an amino nitrile afforded the 5,6-dihydrouracil after cyclization of an isolable urea intermediate (Eq. 5-7).[196] While not a 5,6-dihydrouracil, the product in Eq. 5-8 comes from the condensation of an amino ester and either an alkyl isocyanate or isothiocyanate, but this time from a base induced cyclization.[197] These reactions give between 50-86% yield and are compatible with R = alkyl, aryl, and substituted aryl groups. These reactions do not have wide applicability as the isocyanates used are very reactive with some functional groups and do not work well with a primary amino nitrogen.[196] Also the starting material in Eq. 5-8 is not commercially available.

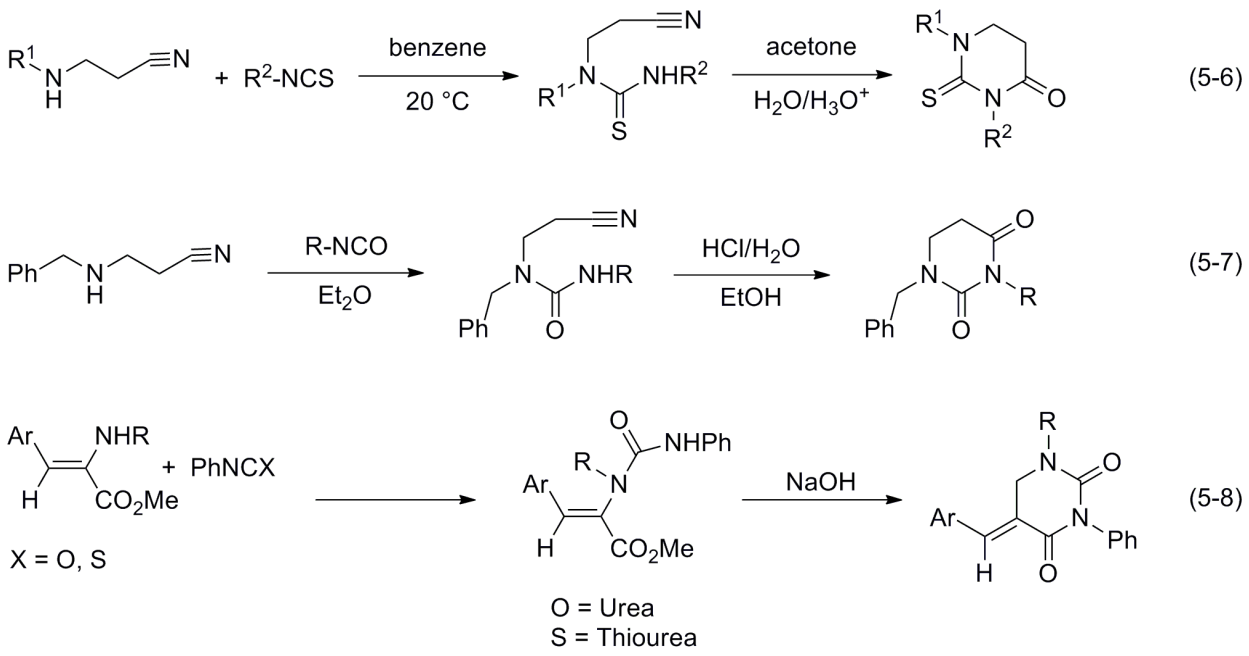

Figure 5-8. Synthesis of dihydrouracils from β-amino acid derivatives.

Solid Phase Organic Chemistry (SPOC)

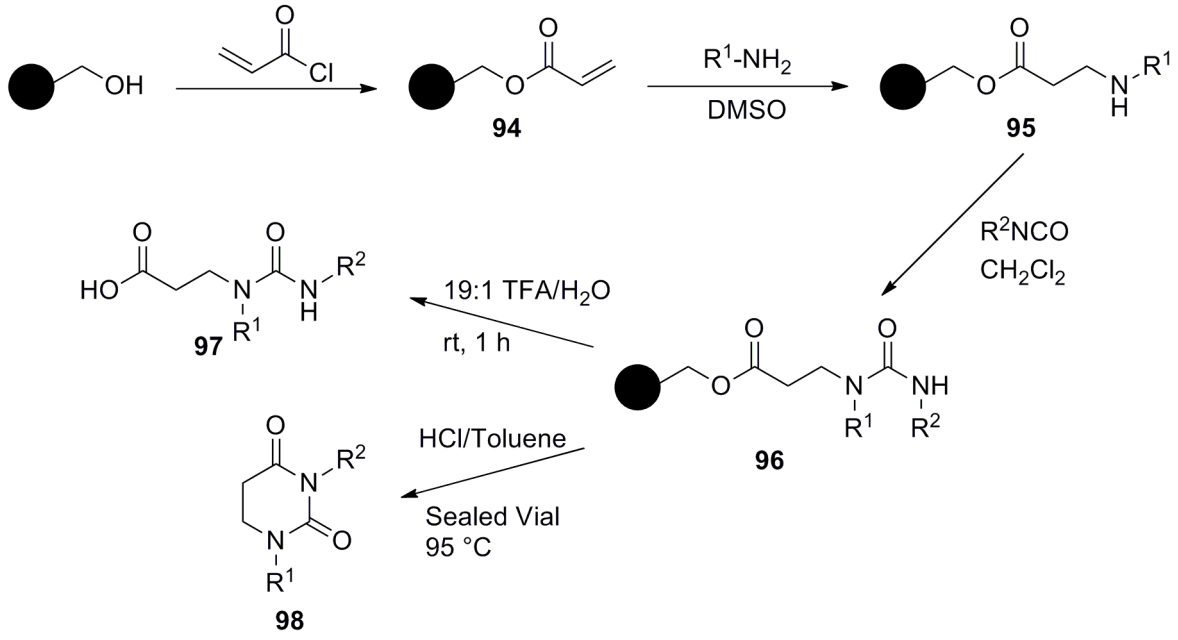

Figure 5-9. SPOC synthesis of 5,6-dihydrouracils.

The use of combinatorial chemistry to prepare nitrogen-containing heterocyclic compounds by SPOC has seen tremendous growth in the last decade.[181] Synthesis of

ring systems including imidazoles,[198] pyrazoles,[199] isoxazoles,[199] pyridines,[200] and isoquinlines[201] are all well described. Pyrimidinone derivatives have also been formed using solid phase three component process,[202] but are rarer. Hamper reported a successful system that was capable of generating 5,6-dihydrouracil systems in moderate to good yields (Figure 5-9).[181] The reaction employed a Wang resin which is initially reacted with acryloyl chloride in the presence of triethyl amine to afford the acrylate resin **94**. Michael addition of a substituted amine yielded **95**, a β-aminoester, which when combined with a 2:1 molar excess of an alkyl isocyanate afforded the urea moiety, **96**. Initial attempts at using TFA to cyclize the ureido ester **96** to form the desired 5,6-dihydrouracil **98** instead formed a mixture of β-ureido acid **97** and **98**. More consistent results were obtained using HCl as the acid source in toluene to afford **98** in a hydrolysis yield of 95-99%. When either aqueous 6 N HCl or HCl in dry ethanol were employed the yields obtained were only 10% and 60%, respectively. Overall yields for the four step synthesis were 13-76% and tended to be lower when resonance delocalizing groups like phenyl and allyl were employed. This system was expanded later by Janusz to include thio-derivatives of the uracil product.[203]

Current methodologies for preparation of 5,6-dihydrouracils have much room for improvement on both yields and tolerance to alkyl/aryl substituents. In addition, synthetic strategies of using condensation of ureas with α,β-unsaturated carboxylic acids are difficult to scale down to a laboratory level, and systems using SPOC are difficult to scale up to an industrial level. Hydrogenation methods suffer from inability to obtain good yields, scrambling of stereochemistry, and non-compatibility with acidic

hydrogens. Use of isocyanates has a negative environmental impact, which makes their reaction with β-amino acids difficult on a large scale.

As we were able to employ the $W(CO)_6/I_2$ system in the synthesis of hydantoins, it was a natural extension to attempt the synthesis of dihydrouracils. While not as kinetically favored as formation of a 5-membered ring in the hydantoin case, it was theorized that these products could be formed in good yields as we had shown with the carbonylation of 1,4-diaminobutanes.

Synthesis of β-Amino Amides

A series of five β-amino amides with various alkyl and aryl substituents β- to the carbonyl was synthesized to explore the effect of the β-substituent on cyclization. Previous results with hydantoins suggested the use of a benzyl group on the amide moiety as they tended to afford higher yields. β-Alkyl substitution specifically was examined due to the difficulty in incorporating it after cyclization has occurred, giving rise to products that would not have been readily available through other synthetic methods.

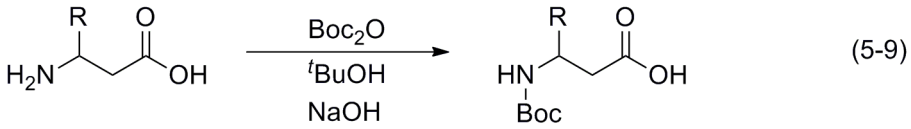

(5-9)

	R	% Yield
99	H	N/A
100	CH_3	88
101	Ph	75
102	CH_2Ph	79
103	^{i}Pr	81

Figure 5-10. *N*-Boc protection of amino acids to generate **100-103**.

Different synthetic methodology to afford β-amino amides was required compared to the synthesis of the α-amino amides used in the preparation of hydantoins.

Commercially available β-alkyl substituted β-amino acids were employed. As most were not available in *N*-protected form, protection was required initially. The *N*-Boc protected amino acid was then subjected to a mixed anhydride coupling (MAC) reaction to afford the protected amino amide. Deprotection with HCl afforded the final β-amino amide.

Compound **99** was commercially available as the *N*-Boc derivative. Initially the amino acid to afford **101** was protected through a protocol developed for the synthesis of **84** using acetonitrile and tetrabutylammonium hydroxide with Boc_2O. However, this gave yields of only 56% so a new method[204] was sought and proved to be more successful (Figure 5-10).

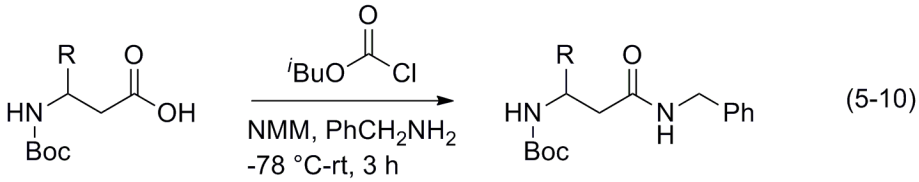

(5-10)

	R	% Yield
104	H	93
105	CH_3	88
106	Ph	85
107	CH_2Ph	79
108	^{i}Pr	80

Figure 5-11. MAC reaction to yield **104-108**.

Once the *N*-Boc protected amino acid was synthesized, it was converted to the *N*-Boc-protected amino amide through a previously employed MAC reaction (Figure 5-11).[170] Even though the literature procedure employed utilized Cbz-protected amino acids, it was found that the Cbz-protected form of **101** gave less than 10% yield of the resulting amide due to poor solubility of the starting amino acid when the MAC reaction

was attempted using the same methodology. Boc-protected substrates proved to be more successful and were then exclusively utilized for further reactions.

Deprotection using 4.0 M HCl in dioxane proved to be slightly problematic as widely different times were needed to complete the reaction (Figure 5-12). Constant monitoring by TLC was needed to determine deprotection reaction time as the material would decompose into an intractable yellow oil if left for times over two hours.

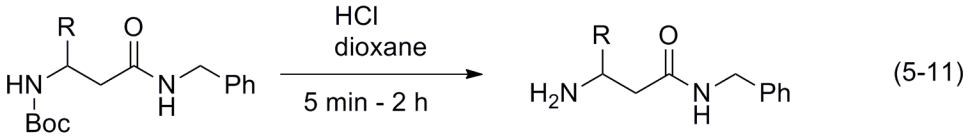

(5-11)

	R	% Yield
109	H	95
110	CH_3	96
111	Ph	85
112	CH_2Ph	90
113	^{i}Pr	90

Figure 5-12. Deprotection of *N*-Boc amino amides to afford **109-113**.

Results and Discussion

Initially chosen for carbonylation was substrate **109** as it was the simplest amino amide (Figure 5-13). Optimized conditions for the carbonylation of **86** to hydantoin **86a**, 35 °C, 1.1 equivalents of DBU, and 24 hours with dichloromethane (DCM) as solvent, were tested as a starting point, however, no dihydrouracil was formed. Even when the temperature was increased to 60 °C, no product could be found. Carbonylation conditions were then more extensively examined and the base concentration, identity, temperature, and time were optimized (Table 5-1).

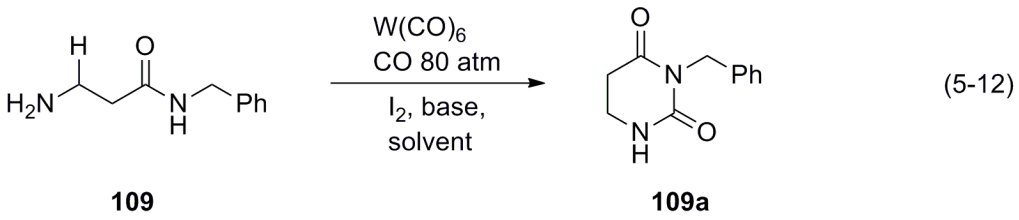

(5-12)

109 **109a**

Figure 5-13. $W(CO)_6$-catalyzed carbonylation of **109**.

Table 5-1. Optimization of carbonylation conditions for **109** to form **109a**

Entry	Time (h)	Temperature (°C)	Base (Equiv.)	Solvent	%Yield **109a**
1	24	35	DBU (1.1)	DCM	0
2	24	60	DBU (1.1)	DCM	0
3	24	35	DBU (1.1)	DCE	48
4	24	30	DBU (2.5)	DCE	27
5	24	30	DBU (4.0)	DCE	8
6	24	30	Pyridine (1.1)	DCE	13
7	8	30	DBU (1.1)	DCE	5
8	12	30	DBU (1.1)	DCE	45
9	36	30	DBU (1.1)	DCE	7
10	24	45	DBU (1.1)	DCE	88
11	24	60	DBU (1.1)	DCE	13

It is important to note that the molar amounts of **109**, $W(CO)_6$, I_2, and solvent volume were held constant for the optimization experiments. The best system was found in Entry 10 with 45 °C, 24 hours, and 1.1 equivalents of DBU using 1,2-dichloroethane (DCE) as solvent. The choice of solvent proved critical again for the carbonylation system, as was seen with the formation of hydantoins. When using DCM, starting material decomposed forming no product (Entry 1), but upon switching to DCE (Entry 3) the 5,6-dihydrouracil was isolated in 48% yield. Not as much effort was placed into analyzing base identity as the β-amino amides should have very similar pKa's when compared to the α-amino amides used to form hydantoins. DBU was found to be

necessary for high yields, as when pyridine was used (Entry 6), the yield dropped significantly. Longer reaction times were also found to decompose the product and the optimum reaction time was determined to be 24 hours.

Product identification was based preliminarily on ^{1}H and ^{13}C NMR along with IR data indicating a new carbonyl peak at 1726 cm^{-1}. The new CO stretch is within the range of reported values for 5,6-dihydrouracil compounds[205] and the structure of **109a** was confirmed by comparison to literature data.[206]

Using the optimized conditions for **109** to form dihydrouracil **109a**, the remaining β-amino amides were carbonylated (Figure 5-14, Table 5-2). While **109** formed the corresponding dihydrouracil in good yield, the β-alkyl substituted substrates resulted in acyclic urea formation. New CO stretches were found around 1640 cm^{-1} in the IR data to corroborate this conclusion. These new CO stretches are sharply lower than reported values for 5,6-dihydrouracil by 80 cm^{-1} and are consistent with those reported for acyclic ureas.[70,205] Structure confirmation was obtained from MS data (vide infra).

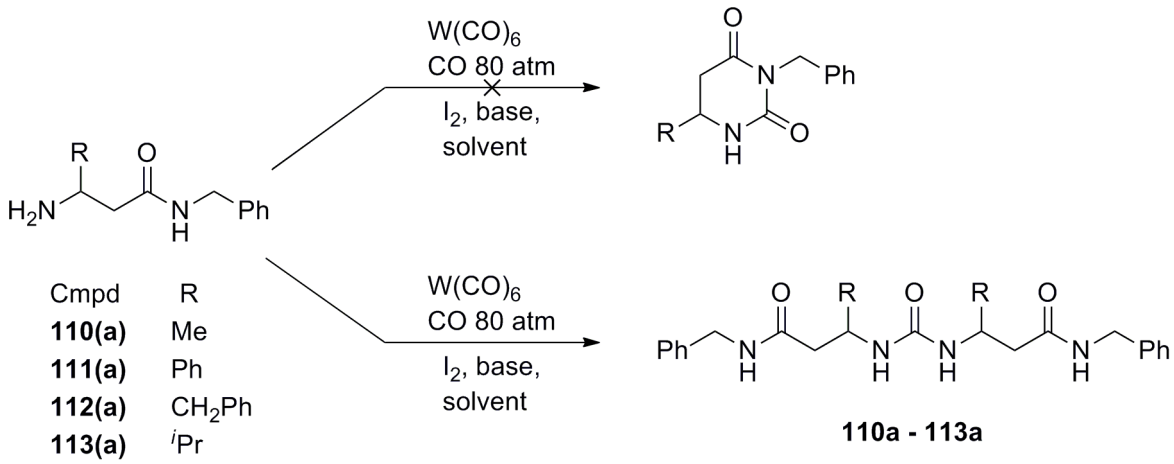

Cmpd	R
110(a)	Me
111(a)	Ph
112(a)	CH_2Ph
113(a)	^{i}Pr

Figure 5-14. Carbonylation of substrates **110-113** to form **110a – 113a** using optimized conditions from **109a**.

Table 5-2. Carbonylation of β-amino amides to acyclic ureas **110a – 113a**

β-Amino Amide	β-R Group	% Yield of Acyclic Urea
110	CH_3	86
111	Ph	7
112	CH_2Ph	29
113	^{i}Pr	0

The highest yield of acyclic urea formed was obtained with the β-substituent being methyl, affording 86% yield of **110**. As the size of the β-substituent increases, the yield drops significantly. The substrate tested with the most steric hindrance was the β-^{i}Pr amino amide **113**, from which no carbonylated products could be detected and complete decomposition of starting material was observed. When the β-substituent was phenyl (**111**), the reaction produced very low yield, presumably due to oxidation of the amino nitrogen. Similar degradation pathways may also exist for the ^{i}Pr variant **113**, which would explain both the lack of products and observed degradation of the starting material. When the phenyl group is shifted a CH_2 unit further from the amino nitrogen (**112**), the carbonylation yielded significantly higher amounts of the acyclic urea product, compared to that seen from β-phenyl substrate **111**.

Understanding the effect of sterics on the formation of acyclic ureas is difficult with this system as seen in the formation of **110a** and **112a**. The benzyl group in **112** is not much sterically larger than the methyl group in **110**, but the yield is significantly less. The A-value for CH_2Ph is 1.68 kcal/mol while that for CH_3 is 1.74 kcal/mol,[207] predicting that sterically, the benzyl substituted **112** would be the easier substrate to carbonylate, while the opposite trend is observed. The σ-electron withdrawing effect of the phenyl group in **112** is now two carbons removed from the amino nitrogen, which should make

the nucleophilicity of the amino nitrogens approximately the same in **112** and **100**. The interplay between sterics and electronics of this system is very complex.

An attempt to carbonylate substrate **110** under high dilution conditions was also examined with a substrate concentration of 0.0028 M (compared to 0.028 M for optimized conversion of **109** to **109a** and 0.055 M used in the formation of **86a**) in DCE. After the 24 hour reaction time, only complete degradation of the starting material was observed. Neither acyclic urea nor 5,6-dihydrouracil formation was detected in the reaction mixture.

A direct comparison of product ratios is available between substrates **81** and **111** as they are constitutional isomers. Hydantoin **81a** forms in 75% yield from the carbonylation of **81**, whereas **111** forms the acyclic urea in only 7%. It appears that the relative rate of cyclization is significantly faster for the formation of the five-membered hydantoin ring over the relative rate of formation for the acyclic urea. In the case of formation of 5,6-dihydrouracils, the opposite trend is seen. While not surprising that the relative rate of five-membered ring formation is faster than that of the six-, it is interesting that even a small β-alkyl substituent, like a methyl group, can slow down the relative rate of cyclization enough to favor acyclic urea formation over cyclization of the dihydrouracil. This was demonstrated in the ability of **109** to carbonylate to form 5,6-dihydrouracil **109a** in 88% yield, while as β-methyl substituted **110** only forms the acyclic urea.

Conclusions

The oxidative carbonylation of β-amino amides using the $W(CO)_6/I_2$ system has only proven effective to form 5,6-dihydrouracil **109a**, which has no β-alkyl substituent. When alkyl substituents are added in the β-position, the carbonylation of the amino

amide affords acyclic urea preferentially over formation of the 5,6-dihydrouracil. The interplay between sterics and electronics brought about by the β-alkyl substituent is not fully understood, but has a large effect upon the yields of acyclic ureas. This methodology provides a synthetic route to form 5,6-dihydrouracils, although it is limited in scope.

CHAPTER 6
EXPERIMENTAL SECTION

Synthesis of Alkylzirconium Complexes

General

All manipulations were carried out using standard Schlenk and glove box techniques under an inert atmosphere of argon or nitrogen. All solvents, unless otherwise noted, were purchased from Fisher and passed through an M. Braun MB-SP solvent purification system or were distilled from sodium/benzophenone prior to use.

All ^{1}H and ^{13}C NMR spectra were obtained on a VXR 300 MHz spectrometer. Mass spectrometry services were provided by the University of Florida analytical service.

Synthesis of $ZrNp_xCl_y$ Complexes

Neopentylmagnesium chloride

A mixture of 9.00 mL (73.0 mmol) freshly distilled neopentyl chloride and 1.21 mL (14.0 mmol) 1,2-dibromoethane were placed in an addition funnel and added dropwise to a three-neck Schlenk flask containing 3.65 g (151 mmol) activated Mg turnings and 50 mL ether over a 1 hour period, in accordance with literature procedure.[42] The resulting mixture was refluxed overnight and filtered through a 1 cm pad of Celite (previously dried and evacuated) to afford a pale yellow product. Yield: 57 mL of 1.0 M solution, 78%. ^{1}H NMR (C_6D_6) δ 0.890 (s, 9 H), 1.18 (s, 2H).[42]

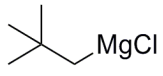

Tetraneopentylzirconium (2)

Neopentylmagnesium chloride concentration was determined[208] and 8.1 mL of 1.0 M (8.1 mmol) of the Grignard reagent in ether was measured into an addition funnel

and added dropwise to a three-neck Schlenk flask containing 0.629 g (2.70 mmol) $ZrCl_4$ slurried in 60 mL ether at 0 °C over a 1 hour period. The mixture was then allowed to warm to room temperature and stirred vigorously overnight. Volatiles were then removed via reduced pressure and the resulting brown solid was extracted with hexanes and filtered through a 1 cm Celite pad (previously dried and evacuated). Volatiles were removed again to leave a pale-brown solid which was sublimed (75 °C, 0.02 mmHg) to produce $ZrNp_4$ as a white solid. Yield 0.523 g, 70%. The product was identified based on literature values.[42] ^{1}H NMR (C_6D_6) δ 1.15 (s, 9H), 1.55 (s, 2H)

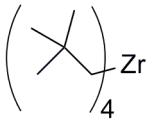

2

Trisneopentyl zirconium monochloride (10)

A three-neck Schlenk flask with 0.721 g (1.92 mmol) of **2** was dissolved in 40 mL ether and added at 0 °C to 0.149 g (0.640 mmol) $ZrCl_4$ dropwise over a one hour period. The reaction temperature was maintained at 0 °C overnight and resulted in a bright yellow solution. Volatiles were then removed leaving a bright yellow solid. The solid was then stored at -30 °C in the dark. Yield 0.755 g, 87%. Decomposition can be seen at room temperature by darkening of the product. The product was identified based on literature values.[43] ^{1}H NMR (C_6D_6) δ 1.15 (s, 9H), 1.55 (s, 2H).

10

Synthesis of Propargylzirconium Complexes

Phenylpropargyl bromide

A 50-mL Schlenk flask containing 5 mL ether and 4.78 g (0.0370 mol) phenylpropargyl alcohol and 1 g pyridine was cooled to 0 °C and 5.0 g (0.18 mol) to which phosphorus tribromide was added dropwise over a 45 minute period with strong stirring under nitrogen in accordance with literature procedure.[44] The resulting mixture was added to 25 mL of ice to deactivate the excess PBr_3 and extracted three times with 25 mL ether. The ether was then washed with sodium bicarbonate and dried over $MgSO_4$. Ether was removed by reduced pressure. Yield 6.0 g, 83%. ^{1}H NMR (C_6D_6) δ 4.1 (s, 2H), 7.4 (m, 5H). ^{13}C NMR ($CDCl_3$) δ 15.3, 84.2, 86.6, 121.9, 128.1, 128.7, 131.7.

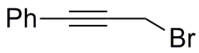

Phenylpropargylmagnesium bromide

An addition funnel was charged with 12.0 g (61.6 mmol) phenylpropargyl bromide and 30 mL ether and the mixture was added dropwise to a three-neck flask cooled to 0 °C containing 1.80 g (75.0 mmol) activated Mg turnings with a few crystals of $HgCl_2$ in ether over a four hour period in accordance with literature preparation.[45] After the addition, the reaction was refluxed for 1 hour. The resulting mixture was filtered through a 1 cm pad of Celite (previously dried and evacuated) and yielded a dark yellow solution. Yield 30 mL of 1.85 M product, 90.1%. ^{1}H NMR (C_6D_6) δ 2.11 (s, 2H), 6.8 (m, 5H).

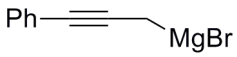

Tetra-η^3(phenylpropargyl) zirconium (11)

An addition funnel was charged with 20.0 mL of 1.85 M phenylpropargylmagnesium bromide (37.0 mmol) and added dropwise to a three-neck flask containing 2.16 g (9.25 mmol) $ZrCl_4$ slurried in 100 mL ether over a one hour period and stirred overnight at room temperature. Volatiles were removed via reduced pressure and a brown solid remained. The solid was extracted with 150 mL toluene and filtered through a fine glass frit. The filtrate was then condensed and crystallized with hexanes. The recrystallized product was tan in color and was subjected to repeated vapor diffusion recrystallization using THF and pentanes until a colorless-to-white solid remained. Yield 3.77 g, 74%. ^{1}H NMR ($C_6D_5CD_3$) δ 3.22 (s, 2H), 6.95 (m, 5H).

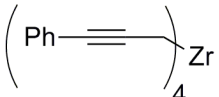

11

Structure determination for 11

X-ray experimental data for **11** were collected at 173 K on a Siemens SMART PLATFORM equipped with A CCD area detector and a graphite monochromator utilizing MoK radiation (λ = 0.71073 Å). Cell parameters were refined using up to 8192 reflections. A full sphere of data (1850 frames) was collected using the ω-scan method (0.3° frame width). The first 50 frames were re-measured at the end of data collection to monitor instrument and crystal stability (maximum correction on I was < 1 %). Absorption corrections by integration were applied based on measured indexed crystal faces.

The structure was solved by the Direct Methods in SHELXTL6,[209] and refined using full-matrix least squares. The non-H atoms were treated anisotropically, whereas

the hydrogen atoms were calculated in ideal positions and were riding on their respective carbon atoms. The complexes are located on 2-fold rotation axes; thus a half complex occupies the asymmetric unit. A total of 168 parameters were refined in the final cycle of refinement using 2730 reflections with I > 2σ(I) to yield R1 and wR2 of 2.44% and 6.76%, respectively. Refinement was done using F2.

Computational Analysis of 11

Geometry optimizations and single-point calculations were performed using the DFT B3LYP functional and the LANL2DZ basis set utilized in the Gaussian 03[210] program package.[55-58] Compositions of molecular orbitals were calculated using the AOMix program.[211,212] Molecular orbital pictures were generated from Gabedit. Computational resources and support were provided by the University of Florida High-Performance Computing Center.

Methylpropargylmagnesium bromide

An addition funnel was charged with 6.61 mL (75.5 mmol) freshly distilled 1-bromo-2-butyne was diluted with 20 mL ether and added dropwise to a three-neck flask containing a 20 mL ether suspension of 2.02 g (83.1 mmol) activated Mg turnings and a few crystals of $HgCl_2$ cooled to 0 °C over a 1 hour period. After addition, the reaction was allowed to warm to room temperature and stirred overnight. The resulting cloudy green-yellow solution was filtered through a 1 cm pad of Celite (previously dried and evacuated) and yielded a bright yellow solution. Yielded 50 mL of a 0.792 M solution, overall 83.6%. ^{1}H NMR (C_6D_6) δ 1.68 (t, 3H) 1.8 (q, 2H)

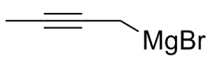

(Methylpropargyl)$_n$zirconium (12)

An addition funnel was charged with 20.0 mL of 0.792 (15.8 mmol) methylpropargylmagnesium bromide was added dropwise to a flask containing 0.923 g (3.95 mmol) $ZrCl_4$ slurried in 100 mL ether over a 1 hour period. The mixture was then stirred overnight at room temperature. Volatiles were removed by reduced pressure and the resulting brown solid was extracted with 150 mL toluene. The extract was then filtered through a fine glass frit and condensed and recrystallized with hexanes. The resulting air and moisture sensitive brown solid showed a myriad of peaks in the ^{1}H-NMR spectrum and was unable to be further purified.

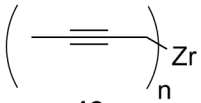

12

Synthesis of α- and β-Amino Amides for Oxidative Carbonylation

General Procedures

All experiments, unless otherwise noted, were carried out under an inert argon atmosphere with oven dried glassware. Solvents for carbonylation reactions were passed through a solvent purification system (vide supra) prior to use or were distilled from CaH_2. Commercially available substrates were used without further purification. All column chromatography was conducted with 270-400 mesh silica. All ^{1}H and ^{13}C NMR spectra were obtained on a Varian Gemini 300 MHz, VXR 300 MHz, or Mercury 300 MHz spectrometer. Infrared spectra were recorded on a Perkin-Elmer 1600 FT-IR. High-resolution mass spectrometry was performed by the University of Florida analytical service.

General Procedure for the Synthesis of α-Amino Amides 78-82

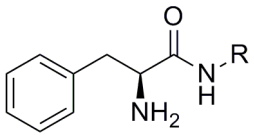

	R
78	Me
79	Et
80	$CH(CH_3)_2$
81	CH_2Ph

The amino acid methyl ester hydrochloride (4.0 mmol) and the alkylamine (40 mmol) were dissolved in anhydrous methanol (20 mL) and stirred at room temperature for 3 days, in accordance with literature protocol.[165] The reaction mixture was concentrated, and the residue was purified by column chromatography using EtOAc/MeOH (96:4) as eluant affording the α-amino amides **78-82** in yields reported in Table 4-1. Product identification was made from literature comparison.[165,170]

(*S*)-2-Amino-*N*-methyl-3-phenylpropionamide (78)

^{1}H NMR ($CDCl_3$) δ 1.35 (broad s, 2H, NH_2), 2.67 (dd, 1H, CH_2CHCO), 2.84 (d, 3H, $NHCH_3$), 3.48 (d, 2H, $PhCH_2$), 7.22-7.30 (m, 5H, C_6H_5).

(*S*)-2-Amino-*N*-ethyl-3-phenylpropionamide (79)

^{1}H NMR ($CDCl_3$) δ 1.56 (broad s, 2H, NH_2), 2.65 (t, 3H, $NHCH_2CH_3$), 2.71 (dd, 1H, CH_2CHCO), 3.31 (m, 2H, NCH_2CH_3), 3.64 (d, 2H, $PhCH_2CH$), 7.25-7.34 (m, 5H, C_6H_5).

(*S*)-2-Amino-*N*-isopropyl-3-phenylpropionamide (80)

^{1}H NMR ($CDCl_3$) δ 1.52 (broad s, 2H, NH_2), 2.43 (d, 6H, $NHCH(CH_3)_2$), 2.59 (dd, 1H, CH_2CHCO), 3.17 (m, 1H, $NCH(CH_3)_2$), 3.46 (d, 2H, $PhCH_2CH$), 7.21-7.30 (m, 5H, C_6H_5).

(*S*)-2-Amino-*N*-benzyl-3-phenylpropionamide (81)

^{1}H NMR ($CDCl_3$) δ 1.46 (broad s, 2H, NH_2), 2.72 (dd, 1H, CH_2CHCO), 3.37 (d, 2H, $PhCH_2CH$), 3.51 (d, 2H, $NHCH_2Ph$), 7.25-7.38 (m, 10H, aromatics).

General Preparation of α-Amino Amide 82 by MAC

A two step procedure, as described in the literature,[170] was followed starting with commercially available Cbz-serine. A 25 mL solution of dry THF containing carbobenzyloxy-DL-serine (2.00 g, 8.40 mmol) was cooled to -78 °C and then 4-methylmorpholine (1.29 g, 10.5 mmol) was added and stirred for 5 minutes. Isobutyl chloroformate (1.46 g, 10.5 mmol) was then added and the reaction mixture was strirred for 15 minutes after which benzylamine (1.08 g, 10.5 mmol) was added. The reaction was then stirred for 15 minutes at -78 °C, before allowing to warm to room temperature where it continued to stir for one hour. The reaction mixture was filtered and the filtrate evaporated by reduced pressure. The concentrated residue was suspended in ether (75 mL) and filtered again. The crude product was purified by column chromatography with 5% MeOH/DCM eluent. A 1.95 g amount of product was isolated, a 74% yield.

The hydrogenation of the Cbz-protecting group was then accomplished. A flask containing 1.71 g (5.44 mmol) amount of the purified benzamide (vide supra) was combined with 0.286 g of Pd/C (10% w/w) and slurried in 50 mL anhydrous MeOH. The reaction was stirred under an atmosphere of H_2 for 3 hours after which the mixture was filtered through a 2 cm pad of Celite. The filtrate was condensed by reduced pressure. The crude residue was purified by column chromatography using 7.5% MeOH/DCM as eluent affording 0.951 g of **82** in a yield of 90%. The product was identified by comparison to literature values.[170] ^{1}H NMR (DMSO) δ 1.90 (broad s, 2H, N*H*$_2$), 3.23 (t, 1H, CH_2C*H*CO), 3.41 (m, 2H, C*H*$_2$OH), 4.25 (d, 2H, NHC*H*$_2$Ph), 4.76 (broad s, 1H, O*H*),

7.18-7.31(m, 5H, C_6H_5), 8.36 (broad s, 1H, N*H*). Substrates **80** and **81** were also alternatively made using this synthetic protocol.

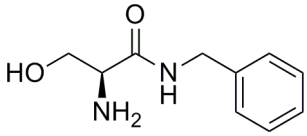

82

Synthesis of α-Amino Amide 83

According to the literature[171] L-Phenylalanamide (3.05 mmol) and benzaldehyde (3.05 mmol) were dissolved in 40 mL anhydrous benzene in a round bottom flask equipped with a Dean-Stark trap and condenser. The mixture was then refluxed for 3 hours and the benzene/water azeotrope was removed as needed. Solvent was then removed via reduced pressure and replaced with 20 mL MeOH to which 1.10 mmol of $NaBH_4$ was added and stirred for 1 hour. Solvent was removed and the resulting solid was triturated in hexanes to afford an oily solid. Column chromatography with 95/5 (DCM:MeOH) was then used to complete the purification. The product was obtained in 72% yield and was identified by comparison to literature values.[171] ^{1}H NMR ($CDCl_3$) δ 1.77 (broad s, 1H, N*H*), 2.78 (t, 1H, CH_2CHCO), 3.34 (dd, 2H, $PhCH_2CH$), 3.65 (dd, 2H, $PhCH_2NH$), 5.83 (broad s, 2H, $CONH_2$), 7.10-7.31 (m, 10H, aromatics).

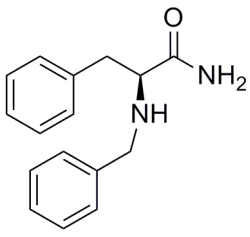

83

Boc-Protection of α,α-Diphenylglycine to 84

The commercially available α,α-diphenylglycine (2.26 g, 10.0 mmol) was slurried in 80 mL acetonitrile and dissolved using a minimum amount of 25% (w/w) tetramethylammonium hydroxide in H_2O. Di-*tert*-butyldicarbonate (5.00 g, 25.0 mmol) was added over a three day period and allowed to stir for a total of four days until TLC indicated that the reaction was complete. The reaction mixture was then concentrated under reduced pressure and dissolved in 150 mL EtOAc and acidified to pH 3-4 using 1.0 N HCl. The organics were then separated and the aqueous material extracted twice with EtOAc. The organics were then combined and washed with brine, then dried over $MgSO_4$. The product was obtained in 92% yield following flash column chromatography using 97/3 (DCM:MeOH). The product was identified by comparison to literature data.[172] ^{1}H NMR ($CDCl_3$) δ 1.49 (s, 9H, $C(CH_3)_3$, 5.1 (broad s, 1H, NH), 7.2-7.35 (m, 10 H, C_6H_5). ^{13}C NMR ($CDCl_3$) δ 28.0, 58.4, 81.7, 127.1, 127.3, 128.5, 148.2, 155.2, 172.9.

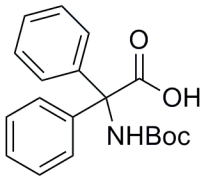

84

***N*-Benzyl-α,α-Diphenylglycamide (85)**

The *N*-Boc protected amino acid **84** was converted to the amino amide via benzotriazole-mediated coupling.[172] After workup, the mixture was taken without purification and deprotected using 5 molar equivalents of 4.0 M HCl in dioxane and stirred overnight. The resulting mixture was purified by flash column chromatography with a solvent gradient shift from DCM to 90/10 (DCM:MeOH). Yield 72% The product

was identified by comparison to literature data.[172] ^{1}H NMR ($CDCl_3$) δ 4.31 (d, 2H, $NHCH_2Ph$), 4.36 (broad s, 1H, NHCO), 4.82 (broad s, 2H, NH_2), 7.25-7.35 (m, 15H, C_6H_5). ^{13}C NMR ($CDCl_3$) δ 43.6, 68.0, 127.3, 127.4, 127.5, 127.5, 128.3, 128.6, 138.3, 145.1, 173.4.

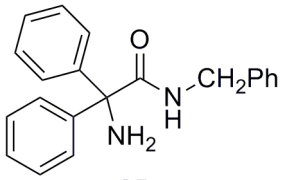

85

α,α-Diphenylglycamide (86)

The *N*-Boc protected amino acid **84** (1.00 g, 3.18 mmol) was dissolved in 20 mL anhydrous DCM and brought to reflux, according to literature procedure.[173] Then $SOCl_2$ (1.13 g, 9.54 mmol) was added, and the mixture continued to reflux for 3 hours. After cooling, the acid chloride solution was evaporated *in vacuo* and 50 mL of THF saturated in ammonia was slowly added and the mixture was stirred overnight. The excess ammonia was removed by sparging with N_2 and the concentrate dissolved in DCM and washed once with water. The organics were separated and dried over $MgSO_4$. The resulting residue was purified by flash column chromatography with 95/5 (DCM:MeOH) to afford **86** in 95% yield. The compound was identified by comparison to literature data.[213] ^{1}H NMR ($CDCl_3$) δ 2.14 (broad s, 2H, NH_2), 6.05 (broad s, 1H, $CONH_2$), 7.02 (broad s, 1H, $CONH_2$), 7.25-7.43 (m, 10H, C_6H_5). ^{13}C NMR ($CDCl_3$) δ 68.0, 127.4, 127.4, 128.3, 144.7, 176.8.

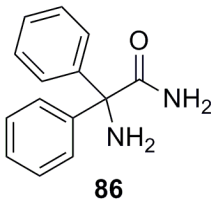

86

Procedure A for Carbonylation of α-Amino Amide 78

To a 300 mL glass lined Parr high pressure vessel containing 35 mL of 1,2-dichloroethane were added α-amino amide **78** (400 mg, 2.20 mmol), $W(CO)_6$ (56 mg, 0.16 mmol), I_2 (396 mg, 1.56 mmol), and DBU (1.36 mL, 8.96 mmol). The vessel was then charged with 80 atm CO and heated to 60 °C for 36 hours with constant stirring. After cooling, the pressure was released and 15 mL water was added. The organics were then separated and washed successively with Na_2SO_3 and 0.1 M HCl. The aqueous layer was then extracted with EtOAc (20 mL x 4). The combined organic layers were then dried over $MgSO_4$, filtered and concentrated. The resulting residue was purified via flash column chromatography using DCM/EtOAc (80:20) to afford hydantoin **78a**. The same procedure was applied to prepare hydantoins **79a**-**82a**. The products were identified by comparison to literature data.[165,214,215]

(S)-5-Benzyl-3-methylimidazolidine-2,4-dione (78a)

The hydantoin was synthesized through carbonylation procedure A. ^{1}H NMR ($CDCl_3$) δ 2.80 (t, 1H, CH_2CH), 3.0 (s, 3H,NCH_3), 3.32 (dd, 1H, $PhCH_2$), 4.25 (dd, 1H, $PhCH_2$), 5.19 (broad s, 1H, NH), 7.21-7.40 (m, 5H, C_6H_5); ^{13}C NMR ($CDCl_3$) δ 25.8, 41.0, 56.4, 126.7, 128.6, 129.2, 174,4; IR (neat) ν_{CO} 1772, 1709 cm^{-1}.

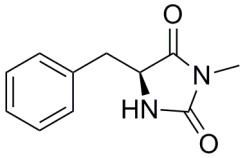

78a

(S)-5-Benzyl-3-ethylimidazolidine-2,4-dione (79a)

The hydantoin was synthesized through carbonylation procedure A. ^{1}H NMR ($CDCl_3$) δ 1.19 (t, 3H, CH_2CH_3), 2.82 (dd, 1H, CH_2CH_3), 3.24 (dd, 1H, CH_2CH_3), 3.43-

3.60 (m, 2H, C*H*$_2$Ph), 4.21 (dd, 1H, CH$_2$C*H*CO), 7.19-7.39 (m, 5H, C$_6$*H*$_5$); ^{13}C NMR ($CDCl_3$) δ 12.0, 33.9, 38.1, 58.1, 127.0, 130.0, 131.2, 134.5, 157.5, 172.4. IR (neat) v_{CO} 1770, 1714 cm^{-1}.

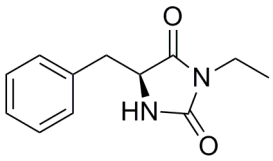

79a

(S)-5-Benzyl-3-benzylimidazolidine-2,4-dione (81a)

The hydantoin was synthesized through carbonylation procedure A. ^{1}H NMR ($CDCl_3$) δ 2.82 (dd, 1H, C*H*$_2$Ph), 3.24 (dd, 1H, C*H*$_2$Ph), 4.22 (s, 2H, C*H*$_2$Ph), 4.60 (t, 1H, CH$_2$C*H*CO), 5.38 (broad s, 1H, N*H*), 7.23-7.42 (m, 10H, C$_6$H$_5$); ^{13}C NMR ($CDCl_3$) δ 38.4, 43.9, 61.7, 125.8, 126.7, 126.9, 127.7, 128.9, 135.5, 135.7, 158.5, 169.5. IR (neat) v_{CO} 1775, 1716 cm^{-1}.

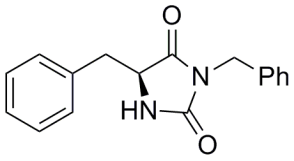

81a

(S)-3-Benzyl-5-(hydroxymethyl)imidazolidine-2,4-dione (82a)

The hydantoin was synthesized through carbonylation procedure A. ^{1}H NMR (DMSO) δ 3.46 (dd, 1H, C*H*$_2$Ph), 3.53 (dd, 1H, C*H*$_2$Ph), 4.26 (t, 1H, CH$_2$C*H*CO), 4.48 (d, 2H, C*H*$_2$OH), 4.77 (broad s, 1H, O*H*), 7.21-7.30, (m, 5H, C$_6$*H*$_5$). IR v_{CO} 1765, 1708 cm^{-1}.

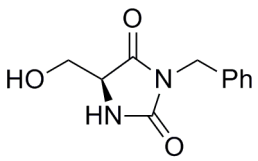

82a

Procedure B for Carbonylation of α-Amino Amide 86

To a 300 mL glass lined Parr high pressure vessel containing 20 mL of dichloromethane were added α-amino amide **86** (250 mg, 1.1 mmol), $W(CO)_6$ (29 mg, 0.081 mmol), I_2 (195 mg, 0.770 mmol), and DBU (187 mg, 1.22 mmol). The vessel was then charged with 80 atm CO and heated to 35 °C for 24 hours with constant stirring. After cooling, the pressure was released and 20 mL of 95/5 (DCM:MeOH) was added. The organics were then washed immediately with Na_2SO_3 and separated. The aqueous layer was then extracted with ethyl acetate (2 x 20 mL). The combined organic layers were then dried with $MgSO_4$, filtered, and concentrated. The resulting residue was then purified via flash column chromatography using DCM/EtOAc (80:20) to afford hydantoin **86a**, also known as phenytoin. The same procedure was applied to prepare hydantoins **83a** and **85a**. Phenytoin was identified by comparison to a commercially available sample. Other products were identified by comparison to literature data.[216,217]

Hydantoin 83a

The hydantoin was synthesized through carbonylation procedure B. ^{1}H NMR ($CDCl_3/CD_3OD$) δ 3.35 (dd, 1H, BnC*H*CO), 4.33 (d 2H, PhCH_2CH), 6.78 (d, 2H, PhCH_2N), 7.21-7.47(m, 10H, C_6H_5), 8.98 (broad s, 1H, N*H*) 7.24-7.45 (m, 10H, C_6H_5). ^{13}C NMR ($CDCl_3/CD_3OD$) δ 37.2, 49.8, 69.5, 122.1, 122.7, 123.1, 125.1, 128.3, 129.0, 140.8, 144.2, 165.6, 175.6. IR (solid) ν_{CO} 1738, 1651 cm^{-1}.

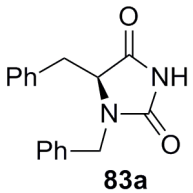

83a

3-Benzyl-5,5-diphenylimidazoidine-2,4-dione 85a

The hydantoin was synthesized through carbonylation procedure B. ^{1}H NMR ($CDCl_3$/CD_3OD) δ 4.26 (s, 2H, PhC*H*$_2$N), 7.15-7.60 (m, 15 H, C_6H_5), 7.88 (broad s, 1H, N*H*). IR (solid) v_{CO} 1734, 1650 cm^{-1}.

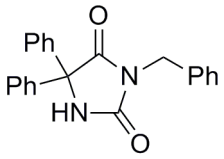

85a

Phenytoin, 86a

The hydantoin was synthesized through carbonylation procedure B. ^{1}H NMR (DMSO) δ 7.15-7.60 (m, 10 H, C_6H_5), 9.30 (broad s, 1H, N*H*), 10.54. IR (solid) v_{CO} 1729, 1660 cm^{-1}. ^{13}C NMR (DMSO) δ 68.4, 122.3, 123.5, 124.3, 137.5, 164.1, 172.6. IR (solid) $_{CO}$ 1732, 1654 cm^{-1}.

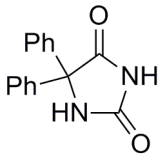

86a

General Procedure C for *N*-Boc Protection of β-Amino Acids to Form 100

In a 100 mL round bottom flask, 10.0 mmol of (±)-3-aminobutanoic acid (1.03 g) was slurried in 10 mL *tert*-butanol and 10 mL 1.0 N NaOH then cooled to 0 °C in accordance with literature procedure.[204] Then 11.0 mmol Boc_2O (2.40 g) was added in one portion, strired at 0 °C for 10 minutes, then allowed to warm to room temperature. The pH of the reaction mixture was adjusted continuously to pH 9-10 by adding 4.0 N NaOH. The reaction stirred for a total of 3 hours, after which the mixture was concentrated to approximately 15 mL by reduced pressure. The remaining aqueous

layer was covered with EtOAc and cooled to 0 °C where it was then acidified to pH 1-2 using 5.0 N HCl. The organics were separated and the aqueous layer extracted with EtOAc three times with 25 mL. The organics were combined and dried over $MgSO_4$, filtered and volatiles were then removed by reduced pressure. The resulting oil was purified by column chromatography starting with 3% MeOH/DCM and gradient shifting to 5% MeOH/DCM after 500 mL, resulting in 1.78 g of amino acid **100**. Yield 88%. Product identification was made by comparison to literature data.[204] ^{1}H NMR ($CDCl_3$) δ 1.21 (d, 3H, C*H*$_3$), 1.40 (s, 9H, C(C*H*$_3$)$_3$), 2.42 (d, 2H, C*H*$_2$), 3.96 (m, 1H, C*H*CH$_3$), 5.2 (broad s, 1H, BocN*H*). ^{13}C NMR ($CDCl_3$) δ 20.9, 28.6, 43.0, 43.8, 70.6, 155.7, 170.9.

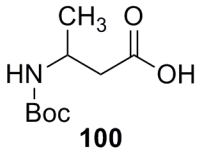

100

3-((*tert*-butoxycarbonyl)amino)-3-phenylpropanoic acid 101

The procedure followed was the same as described in general procedure C to afford compound **100**. ^{1}H NMR ($CDCl_3$) δ 1.40 (broad s, 9H, C(C*H*$_3$)$_3$), 2.84 (broad s, 2H, C*H*$_2$), 5.09 (broad s, 1H, C*H*Ph), 5.54 (broad s, 1H, N*H*Boc), 7.25-7.36 (m, 5H, C$_6$*H*$_5$), 9.90 (broad s, 1H, COO*H*). ^{13}C NMR ($CDCl_3$) δ 21.1, 28.5, 31.8, 71.2, 126.4, 127.7, 128.8, 155.2, 164.8, 181.8. HRMS $[M+Na]^+$ calcd 288.1206, found 288.1193.

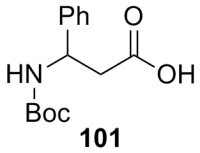

101

3-((*tert*-butoxycarbonyl)amino)-4-phenylbutanoic acid 102

The procedure followed was the same as described in general procedure C to afford compound **100**. ^{1}H NMR ($CDCl_3$) δ 1.41 (s, 9H, C(C*H*$_3$)$_3$), 2.53 (d, 2H,

CHCH_2COOH), 2.86 (m, 1H, NHCHCH$_2$), 4.18 (d, 2H, PhCH_2), 7.20-7.32 (m, 5H, C$_6H_5$). ^{13}C NMR ($CDCl_3$) δ 21.5, 28.4, 39.3, 43.8, 72.4, 126.7, 128.0, 129.5, 138.3, 155.2, 170.9.

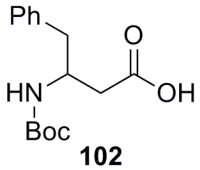

102

3-((*tert*-butoxycarbonyl)amino)-4-methylpentanoic acid 103

The procedure followed was the same as described in general procedure C to afford compound **100**. ^{1}H NMR ($CDCl_3$) δ 0.92 (d, 6H, CH(CH_3)$_2$), 1.44 (s, 9H, C(CH_3)$_3$), 1.86 (m, 1H, CH(CH$_3$)$_2$), 2.55 (d, 2H, CH$_2$COOH), 3.76 (m, 1H, CHNHCHCH$_2$). ^{13}C NMR ($CDCl_3$) δ 18.7, 19.6, 28.6, 31.9, 37.4, 63.1, 155.9, 177.3.

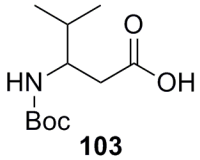

103

General Procedure D for Mixed Anhydride Coupling of β-Amino Acid 99 to Form 104

Into a 100 mL round bottom flask were placed 5.29 mmol of *N*-Boc-β-alanine (1.00 g) and 6.6 mmol *N*-methylmorpholine (0.66 g). The flask was cooled to -78 °C and 6.61 mmol isobutylchloroformate (0.88 g) was added and stirred for 5 minutes. Then 6.61 mmol benzylamine (0.71 mL) was added and stirred for 10 minutes before allowing the flask to warm to room temperature. The reaction then stirred for one and a half hours after which solid was removed and washed with hexanes. The filtrate was concentrated by reduced pressure then re-suspended in hexanes and filtered again. The solids were combined and purified by column chromatography 95/5 (DCM:MeOH). Isolated 1.37 g,

93% yield of **104**. ^{1}H NMR ($CDCl_3$) δ 1.42 (s, 9H, C(C*H*$_3$)$_3$), 2.45 (t, 2H, C*H*$_2$CONHBn) 3.42 (t, 2H, C*H*$_2$NHBoc), 5.21 (broad s, 1H, N*H*), 6.15 (broad s, 1H, N*H*), 7.24-7.33 (m, 5H, C$_6$*H*$_5$). ^{13}C NMR ($CDCl_3$) 20.5, 31.3, 36.1, 44.1, 63.7, 126.7, 127.1, 128.2, 137.4, 155.4, 173.9. HRMS $[M+Na]^+$ calcd 301.1523, found 301.1515.

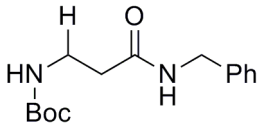

104

3-((*tert*-butoxycarbonyl)amino)-*N*-benzyl-butanamide 105

The procedure followed was the same as described in general procedure D to afford compound **104**. ^{1}H NMR ($CDCl_3$) δ 1.23 (d, 3H, CHC*H*$_3$), 2.42 (t, 2H, CHC*H*$_2$CO), 3.97 (sextet, 1H, NHBocC*H*), 4.42 (d, 2H, NHC*H*$_2$Ph), 5.21 (broad s, 1H, N*H*), 6.25 (broad s, 1H, N*H*), 7.26-7.34 (m, 5H, C$_6$*H*$_5$). ^{13}C NMR ($CDCl_3$) δ 20.7, 26.8, 28.4, 33.7, 43.5, 79.4, 127.5, 127.7, 128.7, 138.1, 155.4, 170.6. HRMS $[2M+Na]^+$ calcd 607.3466, found 607.3454.

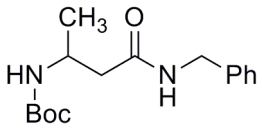

105

3-((*tert*-butoxycarbonyl)amino)-*N*-benzyl-3-phenyl-propanamide 106

The procedure followed was the same as described in general procedure D to afford compound **104**. Compound **106** was unable to be purified so the crude product was carried to the deprotection step and used without purification .

3-((*tert*-butoxycarbonyl)amino)-*N*-benzyl-4-phenyl-butanamide 107

The procedure followed was the same as described in general procedure D to afford compound **104**. ^{1}H NMR ($CDCl_3$) δ 1.39 (s, 9H, C(C*H*$_3$)$_3$), 2.46 (d, 2H,

CHCH_2CO), 4.12 (m, 1H, C*H*NHBoc), 4.40 (d, 2H, NHCH_2Ph), 4.47 (d, 2H, PhCH_2CH), 5.42 (broad s, 1H, *N*H), 5.94 (broad s, 1H, *N*H), 7.15-7.34 (m, 10H, aromatics). ^{13}C NMR ($CDCl_3$) δ 20.1, 28.6, 33.7, 43.8, 49.8, 59.6, 126.7, 127.7, 128.0, 128.7, 129.0, 129.5, 138.2, 138.6, 155.7, 170.9.

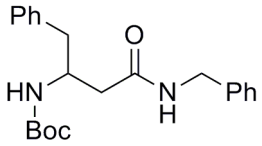

107

3-((*tert*-butoxycarbonyl)amino)-*N*-benzyl-4-methyl-pentanamide 108

The procedure followed was the same as described in general procedure D to afford compound **104**. ^{1}H NMR ($CDCl_3$) δ 0.91 (d, 6H, CH(CH_3)$_2$), 1.39 (s, 9H, C(CH_3)$_3$), 1.83 (m, 1H, C*H*(CH$_3$)$_2$), 2.46 (d, 2H, NHCHCH_2), 3.67 (m, 1H, NHC*H*CH$_2$), 4.41 (d, 2H, NHCH_2Ph), 5.07 (broad s, 1H, NH), 6.47 (broad s, 1H, NH). ^{13}C NMR ($CDCl_3$) δ 19.4, 28.3, 32.1, 39.5, 43.6, 53.4, 63.1, 127.4, 127.7, 128.6, 138.2, 163.4, 166.7.

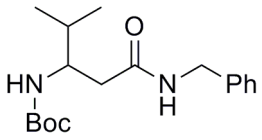

108

General Procedure E for Deprotection of *N*-Boc β-Amino Amide 104 to Form 109

Compound **104**, 4.91 mmol (1.36 g), was placed in a round bottom flask and dissolved in 10 mL DCM. Then 24.6 mmol (6.13 mL) of 4.0 M HCl in dioxane was added and stirred for 18 hours. After reaction time, the excess HCl was removed by sparging with N_2. The resulting solid was purified via column chromatography using 5% MeOH in DCM and gradient shifting 2.5% MeOH increases per 400 mL eluent used until a final percentage of 15% MeOH/DCM was achieved. Isolated **109**, 0.832 g, 95% yield

^{1}H NMR ($CDCl_3/CD_3OD$) δ 2.55 (t, 2H, CH_2CH_2CO), 3.04 (t, 2H, $NH_2CH_2CH_2$), 4.22 (s, 2H, $NHCH_2Ph$) 7.08-7.20 (m, 5H, C_6H_5). ^{13}C NMR ($CDCl_3/CD_3OD$) δ 31.0, 35.8, 42.9, 126.8, 127.0, 128.0, 137.4, 170.2. HRMS $[M+H]^+$ calcd 179.1179, found 179.1175.

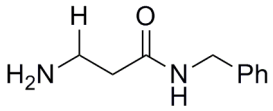

109

3-amino-*N*-benzyl-butanamide 110

The procedure followed was the same as described in general procedure E to afford compound **109**. ^{1}H NMR ($CDCl_3/CD_3OD$) δ 1.24 (d, 3H, $CHCH_3$), 2.50 (d, 2H, $CHCH_2CO$), 3.51 (m, 1H, CH_3CHCH_2), 4.25 (s, 2H, $NHCH_2Ph$), 7.13-7.20 (m, 5H, C_6H_5). ^{13}C NMR ($CDCl_3/CD_3OD$) δ 17.7, 38.2, 43.1, 45.2, 127.2, 127.4, 128.3, 137.5, 164.7.

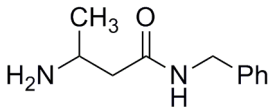

110

3-amino-*N*-benzyl-3-phenyl-propanamide 111

The procedure followed was the same as described in general procedure E to afford compound **109**. ^{1}H NMR ($CDCl_3/CD_3OD$) δ 3.10 (d, 2H, $CHCH_2CO$), 4.10 (d, 2H, $NHCH_2Ph$), 4.81 (t, 1H,$PhCHCH_2$), 7.15-7.35 (m, 10H, aromatics). ^{13}C NMR ($CDCl_3/CD_3OD$) δ 39.3, 44.2, 48.4, 127.1, 127.6, 127.9, 128.2, 128.7, 129.1, 135.4, 137.2, 171.9.

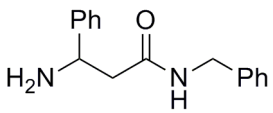

111

3-amino-*N*-benzyl-4-phenyl-butanamide 112

The procedure followed was the same as described in the general procedure to afford compound **109**. ^{1}H NMR ($CDCl_3/CD_3OD$) δ 2.70 (d, 2H, CHC*H*$_2$CO), 2.99 (dd, 1H, PhC*H*$_2$CH), 3.29 (dd, 1H, PhC*H*$_2$CH), 3.88 (m, 1H, PhCH$_2$C*H*CH$_2$), 7.10-7.525 (m, 10H, aromatics). ^{13}C NMR ($CDCl_3/CD_3OD$) δ 37.2, 38.9, 41.4, 46.7, 127.2, 127.4, 127.7, 128.6, 128.9, 129.5, 135.9, 137.7, 174.9. HRMS $[M+H]^+$ calcd 269.1648, found 269.1639.

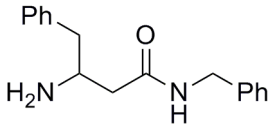

112

3-amino-*N*-benzyl-4-methyl-pentanamide 113

The procedure followed was the same as described in general procedure E to afford compound **109**. ^{1}H NMR ($CDCl_3/CD_3OD$) δ 0.87 (d, 6H, CH(C*H*$_3$)$_2$), 1.87 (m, 1H, C*H*(CH$_3$)$_2$), 2.48 (d, 2H, CHC*H*$_2$CO), 3.17 (m, 1H, NH$_2$C*H*CH$_2$), 4.23 (d, 2H, NHC*H*$_2$Ph), 7.10-7.17 (m, 5H, C$_6$*H*$_5$). ^{13}C NMR ($CDCl_3/CD_3OD$) δ 17.6, 30.0, 33.5, 43.0, 54.5, 127.1, 127.8, 128.2, 137.4, 173.3. HRMS $[M+H]^+$ calcd 221.1648, found 221.1656.

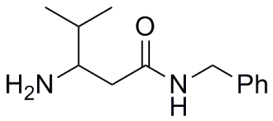

113

General Procedure F for Carbonylation of β-Amino Amides 109-112 to Form 109a-112a

To a 300 mL glass lined Parr high pressure vessel containing 20 mL of 1,2-dichloroethane were added α-amino amide **109** (99 mg, 0.55 mmol), $W(CO)_6$ (14 mg, 0.04 mmol), I_2 (98 mg, 0.39 mmol), and DBU (0.094 g, 0.61 mmol). The vessel was then charged with 80 atm CO and heated to 45 °C for 24 hours with constant stirring.

After cooling, the pressure was released and 20 mL of 95/5 (DCM:MeOH) was added. The organics were then washed immediately with Na_2SO_3 and separated. The aqueous layer was then extracted with 3:1 $CHCl_3$/EtOH solution (3 x 20 mL). The combined organic layers were then dried with $MgSO_4$, filtered, and concentrated. The resulting residue was then purified via flash column chromatography using DCM/EtOAc (80:20) to afford 3-benzyl-dihydropyrimidine-2,4(1*H*)-dione **109a**. ^{1}H NMR ($CDCl_3$/CD_3OD) δ 2.49 (t, 2H, $CH_2CH_2CONCH_2Ph$), 3.53 (q, 2H, $NHCH_2CH_2$), 4.39 (d, 2H, NCH_2Ph), 7.19-7.34 (m, 5H, C_6H_5). ^{13}C NMR ($CDCl_3$/CD_3OD) δ 43.11, 45.21, 62.10, 127.1, 127.4, 128.3, 137.9, 159.0, 170.9. IR (solid) v_{CO} 1726, 1678 cm^{-1}. The product was identified by comparison to literature values.[206]

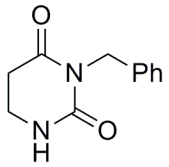

109a

Urea 110a

The procedure followed was the same as described in general procedure F to afford compound **110a**. ^{1}H NMR (DMSO) δ 1.01 (d, 3H, $CHCH_3$), 2.31 (d, 2H, $CHCH_2CO$), 3.92 (m, 1H, CH_3CHCH_2), 4.25 (d, 2H, NCH_2Ph), 7.21-7.29 (m, 5H, C_6H_5), 8.33 (s, 1H, NH). ^{13}C NMR (DMSO) δ 15.9, 31.8, 32.3, 57.9, 127.4, 127.9, 128.9, 134.8, 154.2, 171.0. IR (solid) v_{CO} 1651, 1687 cm^{-1}.

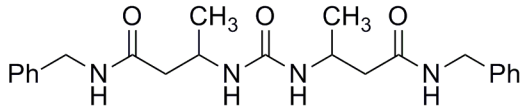

110a

Urea 111a

The procedure followed was the same as described in general procedure F to afford compound **111a**. ^{1}H NMR (DMSO) δ 2.62 (d, 2H, CHC*H*$_2$CO), 4.21 (t, 1H, PhC*H*CH$_2$), 5.10 (d, 2H, NC*H*$_2$Ph), 7.13-7.28 (m, 10H, C$_6$*H*$_5$). ^{13}C NMR (DMSO) δ 23.9, 43.9, 50.4, 126.2, 126.7, 126.9, 127.1, 127.6, 128.8, 132.1, 133.6, 153.0, 178.4. IR (solid) v_{CO} 1665, 1698 cm^{-1}.

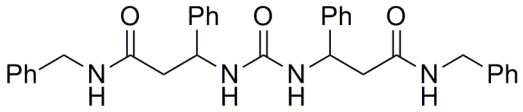

111a

Urea 112a

The procedure followed was the same as described in general procedure F to afford compound **112a**. ^{1}H NMR (CDCl$_3$/CD$_3$OD) δ 2.33 (d, 2H, CHC*H*$_2$CO), 2.81 (d, 2H, PhC*H*$_2$CH), 4.14 (quintet, 1H, PhCH$_2$C*H*CH$_2$), 4.36 (d, 2H, NC*H*$_2$Ph), 7.12-7.34 (m, 10H, aromatics), 7.71 (broad s, 1H, N*H*). ^{13}C NMR (CDCl$_3$/CD$_3$OD) δ 44.7, 44.8, 47.6, 53.2, 130.5, 131.4, 131.7, 132.4, 132.7, 133.4, 142.1, 142.3, 162.2, 175.9. IR (solid) v_{CO} 1637, 1684 cm^{-1}. HRMS [M+H]$^{+}$ calcd 563.3017, found 563.3013.

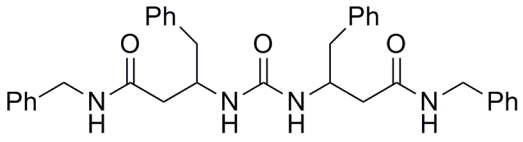

112a

APPENDIX A

CRYSTALLOGRAPHIC DATA AND STRUCTURE REFINEMENT OF **11**

Empirical formula	C_{36} H_{28} Zr
Formula weight	551.80
Temperature	173(2) K
Wavelength	0.71073 Å
Crystal system	Monoclinic
Space group	C2/c
Unit cell dimensions	a = 20.7551(14) Å α= 90° b = 8.6203(6) Å β= 116.0410(10)° c = 17.4685(11) Å γ = 90°
Volume	2808.1(3) $Å^3$
Z	4
Density (calculated)	1.305 Mg/m^3
Absorption coefficient	0.413 mm^{-1}
F(000)	1136
Crystal size	0.19 x 0.11 x 0.04 mm^3
Theta range for data collection	2.18 to 27.50°
Index ranges	-20≤h≤26, -11≤k≤11, -22≤l≤15
Reflections collected	9334
Independent reflections	3226 [R(int) = 0.0272]
Completeness to theta = 27.50°	99.8 %
Absorption correction	Integration
Max. and min. transmission	0.9861 and 0.9103
Refinement method	Full-matrix least-squares on F^2
Data / restraints / parameters	3226 / 0 / 168
Goodness-of-fit on F^2	1.065
Final R indices [I>2sigma(I)]	R1 = 0.0244, wR2 = 0.0676 [2730]
R indices (all data)	R1 = 0.0312, wR2 = 0.0700
Largest diff. peak and hole	0.300 and -0.346 $e.Å^{-3}$

$R1 = \Sigma(||F_O| - |F_C||) / \Sigma |F_O|$

$wR2 = [\Sigma [w(F_O^2 - F_C^2)^2] / \Sigma [wF_O^{22}]]^{1/2}$

$S = [\Sigma [w(F_O^2 - F_C^2)^2] / (n-p)]^{1/2}$

$w= 1/[\sigma^2(F_O^2)+(m*p)^2+n*p]$, $p = [max(F_O^2,0)+ 2* F_C^2]/3$, m and n are constants.

LIST OF REFERENCES

1. Parmeter, J. E.; Smith, D. C.; Healy, M. D. *J. Vac. Sci. Technol., A* **1994**, *12*, 2107-2113.

2. He, X.-M.; Shu, L.; Li, H.-B.; Weng, D. *J. Mater. Res.* **1999**, *14*, 615-618.

3. Mackie, W. A.; Xie, T. B.; Davis, P. R. *J. Vac. Sci. Technol. B* **1995**, *13*, 2459-2463.

4. Holmberg, K.; Matthews, A. *Coatings Tribology: Properties, Techniques, and Applications in Surface Engineering*; Elsevier: Amsterdam, 1994.

5. Reynolds, G. H. *J. Nucl. Mater.* **1974**, *50*, 215-216.

6. Xie, T.; Mackie, W. A.; Davis, P. R. *J. Vac. Sci. Technol., B.* **1996**, *14*, 2090.

7. D'Alessio, L.; Santagata, A.; Teghil, R.; Zaccagnino, M.; Zaccardo, I.; Marotta, V.; Ferro, D.; De Maria, G. *Appl. Surf. Sci.* **2000**, *168*, 284-287.

8. Zhang, Q.; He, J.; Liu, W.; Zhong, M. *Surf. Coat. Technol.* **2003**, *162*, 140-146.

9. Chen, C.-S.; Liu, C.-P.; Tsao, C.-Y. A. *Thin Solid Films* **2005**, *479*, 130-136.

10. Hollabaugh, C. M.; Wahman, L. A.; Reiswig, R. D.; White, R. W.; Wagner, P. *Nucl. Technol.* **1977**, *35*, 527-535.

11. Ogawa, T.; Ikawa, K.; Iwamoto, K. *J. Mater. Sci.* **1979**, *14*, 125-132.

12. Wagner, P.; Wahman, L. A.; White, R. W.; Hollabaugh, C. M.; Reiswig, R. D. *J. Nucl. Mater.* **1976**, *62*, 221-228.

13. Ducarroir, M.; Salles, P.; Bernard, C. *J. Electrochem. Soc.* **1985**, *132*, 221-228.

14. Liu, Q.; Zhang, L.; Cheng, L.; Wang, Y. *J. Coat. Technol. Res.* **2009**, *6*, 269-273.

15. Pattanaik, A. K.; Sarin, V. K. In *Chemical Vapor Deposition*; Park, J. H., Ed.; ASM International: Materials Park, 2001; Vol. 2, p 23.

16. Samoilenko, V. G.; Pereselentseva, L. N. *Powder Metall. Met. Ceram.* **1975**, *14*, 725-728.

17. Brüggert, M.; Hu, Z.; Hüttinger, K. J. *Carbon* **1999**, *37*, 2021-2030.

18. Pierson, H. O. *Handbook of Chemical Vapor Deposition (CVD): Principles, Technology, and Applications*; William Andrew Publishing: New York, 1992.

19. Ogawa, T.; Ikawa, K.; Iwamoto, K. *J. Nucl. Mater.* **1981**, *97*, 104-112.

20. Scussel, H. J. *ASM Handbook*; ASM Int.: New York, 1992; Vol. 18.

21. Glass, J. A., Jr.; Palmisiano, N., Jr.; Welsh, R. E. *Mater. Res. Soc. Symp. Proc.* **1999**, *555*, 185-190.

22. Blair, H. T.; Carroll, D. W.; Matthews, R. B. *AIP Conf. Proc.* **1991**, *217*, 1052-1058.

23. Wu, Y. D.; Peng, Z. H.; Chan, K. W. K.; Liu, X. Z.; Tuinman, A. A.; Xue, Z. L. *Organometallics* **1999**, *18*, 2081-2090.

24. Girolami, G. S.; Jensen, J. A.; Gozum, J. E.; Pollina, D. M. *Mater. Res. Soc. Symp. Proc.* **1988**, *121*, 429-438.

25. Smith, D. C.; Rubiano, R. R.; Healy, M. D.; Springer, R. W. *Proc. - Electrochem. Soc.* **1993**, *93-2*, 417-424.

26. Won, Y. S.; Varanasi, V. G.; Kryliouk, O.; Anderson, T. J.; McElwee-White, L.; Perez, R. J. *J. Cryst. Growth* **2007**, *307*, 302-308.

27. Won, Y. S.; Kim, Y. S.; Varanasi, V. G.; Kryliouk, O.; Anderson, T. J.; Sirimanne, C. T.; McElwee-White, L. *J. Cryst. Growth* **2007**, *304*, 324-332.

28. Sirimanne, C. T.; McElwee-White, L.; Won, Y. S.; Kryliouk, O.; Anderson, T. J. *Abstr. Pap. - Am. Chem. Soc.* **2005**, *230*, U2024-U2025.

29. Polk, J. *An Overview of JPL's Advanced Propulsion Concepts Research Program*, 2001.

30. Temple, D. *Mater. Sci. Eng., R.* **1999**, *24*, 185-239.

31. Smith, D. C.; Rubiano, R. R.; Healy, M. D.; Springer, R. W. *Mater. Res. Soc. Symp. Proc.* **1993**, *282*, 643-649.

32. Girolami, G. S.; Jensen, J. A.; Pollina, D. M.; Williams, W. S.; Kaloyeros, A. E.; Allocca, C. M. *J. Am. Chem. Soc.* **1987**, *109*, 1579-1580.

33. Cheon, J.; Rogers, D. M.; Girolami, G. S. *J. Am. Chem. Soc.* **1997**, *119*, 6804-6813.

34. Cheon, J.; Dubois, L. H.; Girolami, G. S. *J. Am. Chem. Soc.* **1997**, *119*, 6814-6820.

35. Wu, Y. D.; Peng, Z. H.; Xue, Z. L. *J. Am. Chem. Soc.* **1996**, *118*, 9772-9777.

36. Wojcicki, A. *Inorg. Chem. Commun.* **2002**, *5*, 82-97.

37. Pedly, J. B.; Naylor, R. D.; Kirby, S. P. *Thermochemical Data for Organic Compunds*; Chapman and Hall: London, 1986.

38. Doherty, S.; Corrigan, J. F.; Carty, A. J.; Sappa, E. *Adv. Organomet. Chem.* **1995**, *37*, 39-130.

39. Blosser, P. W.; Schimpff, D. G.; Gallucci, J. C.; Wojcicki, A. *Organometallics* **1993**, *12*, 1993-1995.

40. Casey, C. P.; Yi, C. S. *J. Am. Chem. Soc.* **1992**, *114*, 6597-6598.

41. Dewar, M. J. S.; Thiel, W. *J. Am. Chem. Soc.* **1977**, *99*, 4907-4917.

42. Hughes, A. K.; Kingsley, A. J. *J. Organomet. Chem.* **1997**, *539*, 109-114.

43. McAlexander, L. H.; Li, L.; Yang, Y.; Pollitte, J. L.; Xue, Z. *Inorg. Chem.* **1998**, *37*, 1423-1426.

44. Lai, T. Y. *Bull. Soc. Chim. Fr.* **1933**, *53*, 1533.

45. Lappin, G. R. *J. Am. Chem. Soc.* **1949**, *71*, 3966-3968.

46. Gaudemar, M. *Ann. Chim.* **1956**, *1*, 190-202.

47. Lewekebandara, T. S.; Sheridan, P. H.; Heeg, M. J.; Rheingold, A. L.; Winter, C. H. *Inorg. Chem.* **1994**, *33*, 5879-5889.

48. Interrante, L. V.; Sigel, G. A.; Garbauskas, M.; Hejna, C.; Slack, G. A. *Inorg. Chem.* **1989**, *28*, 252-257.

49. Bchir, O. J.; Green, K. M.; Hlad, M. S.; Anderson, T. J.; Brooks, B. C.; Wilder, C. B.; Powell, D. H.; McElwee-White, L. *J. Organomet. Chem.* **2003**, *684*, 338-350.

50. Blosser, P. W.; Gallucci, J. C.; Wojcicki, A. *J. Organomet. Chem.* **2000**, *597*, 125-132.

51. Costuas, K.; Saillard, J.-Y. *Chem. Commun.* **1998**, *18*, 2047-2048.

52. Gleiter, R.; Bethke, S.; Okubo, J.; Jonas, K. *Organometallics* **2001**, *20*, 4274-4278.

53. Bendjaballah, S.; Kahlal, S.; Costuas, K.; Bévillon, E.; Saillard, J.-Y. *Chem.--Eur. J.* **2006**, *12*, 2048-2065.

54. Summerscales, O. T.; Cloke, F. G. N. *Coord. Chem. Rev.* **2006**, *250*, 1122-1140.

55. Becke, A. D. *J. Chem. Phys.* **1993**, *98*, 5648-5652.

56. Lee, C.; Yang, W.; Parr, R. G. *Phys. Rev. B* **1988**, *37*, 785-789.

57. Vosko, S. H.; Wilk, L.; Nusair, M. *Can. J. Phys.* **1980**, *58*, 1200-1211.

58. Stephens, P. J.; Devlin, F. J.; Chabalowski, C. F.; Frisch, M. J. *J. Phys. Chem.* **1994**, *98*, 11623-11627.

59. Becconsall, J. K.; O'Brien, S. *Chem. Commun.* **1966**, 302-303.

60. Jennings, J. R. *J. Mol. Catal.* **1990**, *58*, 95-105.

61. Chrusciel, R. A.; Strohbach, J. W. *Curr. Top. Med. Chem.* **2004**, *4*, 1097-1114.

62. De Lucca, G. V.; Lam, P. Y. S. *Drugs Future* **1998**, *23*, 987-994.

63. Semple, G.; Ryder, H.; Rooker, D. P.; Batt, A. R.; Kendrick, D. A.; Szelke, M.; Ohta, M.; Satoh, M.; Nishida, A.; Akuzawa, S.; Miyata, K. *J. Med. Chem.* **1997**, *40*, 331-341.

64. Dragovich, P. S.; Barker, J. E.; French, J.; Imbacuan, M.; Kalish, V. J.; Kissinger, C. R.; Knighton, D. R.; Lewis, C. T.; Moomaw, E. W.; Parge, H. E.; Pelletier, L. A. K.; Prins, T. J.; Showalter, R. E.; Tatlock, J. H.; Tucker, K. D.; Villafranca, J. E. *J. Med. Chem.* **1996**, *39*, 1872-1884.

65. vonGeldern, T. W.; Kester, J. A.; Bal, R.; WuWong, J. R.; Chiou, W.; Dixon, D. B.; Opgenorth, T. J. *J. Med. Chem.* **1996**, *39*, 968-981.

66. Vishnyakova, T. P.; Golubeva, I. A.; Glebova, E. V. *Russ. Chem. Rev. (Engl. Transl.)* **1985**, *54*, 249-261.

67. DeLucca, G. V.; Liang, J.; Aldrich, P. E.; Calabrese, J.; Cordova, B.; Klabe, R. M.; Rayner, M. M.; Chang, C. H. *J. Med. Chem.* **1997**, *40*, 1707-1719.

68. Lam, P. Y.-S.; Jadhav, P. K.; Eyermann, C. J.; Hodge, C. N.; De, L. G. V.; Rodgers, J. D. WO Patent 9419329, 1994

69. Lam, P. Y. S.; Jadhav, P. K.; Eyermann, C. J.; Hodge, C. N.; Ru, Y.; Bacheler, L. T.; Meek, J. L.; Otto, M. J.; Rayner, M. M.; Wong, Y. N.; Chang, C. H.; Weber, P. C.; Jackson, D. A.; Sharpe, T. R.; Erickson-Viitanen, S. *Science* **1994**, *263*, 380-384.

70. Qian, F.; McCusker, J. E.; Zhang, Y.; Main, A. D.; Chlebowski, M.; Kokka, M.; McElwee-White, L. *J. Org. Chem.* **2002**, *67*, 4086-4092.

71. Ragaini, F. *Dalton Trans.* **2009**, 6251-6266.

72. Giannoccaro, P.; Tommasi, I.; Aresta, M. *J. Organomet. Chem.* **1994**, *476*, 13-18.

73. Sartori, G.; Maggi, R. In *Science of Synthesis*; Ley, S. V., Knight, J. G., Eds.; Thieme: Stuttgart, 2005; Vol. 18, pp 665-758.

74. Hegarty, A. F.; Drennan, L. J. In *Comprehensive Organic Functional Group Transformations*; Katritzky, A. R., Meth-Cohn, O., Rees, C. W., Eds.; Pergamon: Oxford, 1995; Vol. 6, pp 499-526.

75. Bigi, F.; Maggi, R.; Sartori, G. *Green Chem.* **2000**, *2*, 140-148.

76. Hylton, K.-G.; Main, A. D.; McElwee-White, L. *J. Org. Chem.* **2003**, *68*, 1615-1617.

77. Díaz, D. J.; Hylton, K. G.; McElwee-White, L. *J. Org. Chem.* **2006**, *71*, 734-738.

78. Trost, B. M. *Angew. Chem.-Int. Edit. Engl.* **1995**, *34*, 259-281.

79. Klausener, A.; Jentsch, J.-D. In *Applied Homogeneous Catalysis with Organometallic Compounds (2nd Edition)*; Cornils, B., Herrmann, W. A., Eds.; VCH: Weinheim, 2002; Vol. 1, pp 164-182.

80. Gabriele, B.; Salerno, G.; Costa, M. In *Catalytic Carbonylation Reactions*; Beller, M., Ed.; Springer: Heidelberg, 2006, pp 239-272.

81. McCusker, J. E.; Logan, J.; McElwee-White, L. *Organometallics* **1998**, *17*, 4037-4041.

82. McCusker, J. E.; Qian, F.; McElwee-White, L. *J. Mol. Catal. A-Chem.* **2000**, *159*, 11-17.

83. McCusker, J. E.; Grasso, C. A.; Main, A. D.; McElwee-White, L. *Org. Lett.* **1999**, *1*, 961-964.

84. McCusker, J. E.; Main, A. D.; Johnson, K. S.; Grasso, C. A.; McElwee-White, L. *J. Org. Chem.* **2000**, *65*, 5216-5222.

85. Li, K. T.; Peng, Y. J. *J. Catal.* **1993**, *143*, 631-634.

86. Srivastava, S. C.; Shrimal, A. K.; Srivastava, A. *J. Organomet. Chem.* **1991**, *414*, 65-69.

87. Dombek, B. D.; Angelici, R. J. *J. Catal.* **1977**, *48*, 433-435.

88. Li-Juan, C.; Fu-Ming, M.; Guang-Xing, L. *Catalysis Communications* **2009**, *10*, 981-985.

89. Park, J. H.; Yoon, J. C.; Chung, K. Y. *Adv. Synth. Catal.* **2009**, *351*, 1233-1237.

90. Bassoli, A.; Rindone, B.; Tollari, S.; Chioccara, F. *J. Mol. Catal.* **1990**, *60*, 41-48.

91. Benedini, F.; Nali, M.; Rindone, B.; Tollari, S.; Cenini, S.; Lamonica, G.; Porta, F. *J. Mol. Catal.* **1986**, *34*, 155-161.

92. Liu, J. M.; Peng, X. G.; Liu, J.-H.; Zheng, S. Z.; Sun, W.; Xia, C. G. *Tetrahedron Lett.* **2007**, *48*, 929-932.

93. Giannoccaro, P.; Nobile, C. F.; Mastrorilli, P.; Ravasio, N. *J. Organomet. Chem.* **1991**, *419*, 251-258.

94. Hoberg, H.; Fañanás, F. J.; Riegel, H. J. *J. Organomet. Chem.* **1983**, *254*, 267-271.

95. Kondo, T.; Kotachi, S.; Tsuji, Y.; Watanabe, Y.; Mitsudo, T. *Organometallics* **1997**, *16*, 2562-2570.

96. Kotachi, S.; Kondo, T.; Watanabe, Y. *Catal. Lett.* **1993**, *19*, 339-344.

97. Mulla, S. A. R.; Gupte, S. P.; Chaudhari, R. V. *J. Mol. Catal.* **1991**, *67*, L7-L10.

98. Mulla, S. A. R.; Rode, C. V.; Kelkar, A. A.; Gupte, S. P. *J. Mol. Catal. A-Chem.* **1997**, *122*, 103-109.

99. Durand, D.; Lassau, C. *Tetrahedron Lett.* **1969**, 2329-2330.

100. Alper, H.; Vasapollo, G.; Hartstock, F. W.; Mlekuz, M.; Smith, D. J. H.; Morris, G. E. *Organometallics* **1987**, *6*, 2391-2393.

101. Chiarotto, I.; Feroci, M. *J. Org. Chem.* **2003**, *68*, 7137-7139.

102. Choudary, B. M.; Rao, K. K.; Pirozhkov, S. D.; Lapidus, A. L. *Synth. Commun.* **1991**, *21*, 1923-1927.

103. Gabriele, B.; Salerno, G.; Mancuso, R.; Costa, M. *J. Org. Chem.* **2004**, *69*, 4741-4750.

104. Imada, Y.; Mitsue, Y.; Ike, K.; Washizuka, K.; Murahashi, S. *Bull. Chem. Soc. Jpn.* **1996**, *69*, 2079-2090.

105. Ozawa, F.; Soyama, H.; Yanagihara, H.; Aoyama, I.; Takino, H.; Izawa, K.; Yamamoto, T.; Yamamoto, A. *J. Am. Chem. Soc.* **1985**, *107*, 3235-3245.

106. Ozawa, F.; Sugimoto, T.; Yuasa, Y.; Santra, M.; Yamamoto, T.; Yamamoto, A. *Organometallics* **1984**, *3*, 683-692.

107. Shi, F.; Deng, Y. Q.; SiMa, T. L.; Yang, H. Z. *Tetrahedron Lett.* **2001**, *42*, 2161-2163.

108. Ozawa, F.; Yamamoto, A. *Chem. Lett.* **1982**, 865-868.

109. Tsuji, J.; Iwamoto, N. *Chem. Commun.* **1966**, 380.

110. Ronchin, L.; Vavasori, A.; Amadio, E.; Cavinato, G.; Toniolo, L. *J. Mol. Catal.* **2009**, *23*, 23-30.

111. Zhao, Y.; Jin, L.; Peng, L.; Lei, A. *J. Am. Chem. Soc.* **2008**, *130*, 9429-9433.

112. Grosjean, C.; Novakovic, K.; Scott, S. K.; Whiting, A.; Willis, M. J.; Wright, A. R. *J. Mol. Catal.* **2008**, *284*, 33-39.

113. McCusker, J. E.; Abboud, K. A.; McElwee-White, L. *Organometallics* **1997**, *16*, 3863-3866.

114. Fukuoka, S.; Chono, M.; Kohno, M. *J. Org. Chem.* **1984**, *49*, 1458-1460.

115. Shi, F.; Deng, Y. Q. *Chem. Commun.* **2001**, 443-444.

116. Shi, F.; Deng, Y. Q. *J. Catal.* **2002**, *211*, 548-551.

117. Waller, F. J. EP Patent 195515, 1986

118. Hiwatari, K.; Kayaki, Y.; Okita, K.; Ukai, T.; Shimizu, I.; Yamamoto, A. *Bull. Chem. Soc. Jap.* **2004**, *77*, 2237-2250.

119. Bitsi, G.; Jenner, G. *J. Organomet. Chem.* **1987**, *330*, 429-435.

120. Byerley, J. J.; Rempel, G. L.; Takebe, N.; James, B. R. *J. Chem. Soc. D.* **1971**, 1482-1483.

121. Jenner, G.; Bitsi, G. *Appl. Catal.* **1987**, *32*, 293-304.

122. Süss-Fink, G.; Langenbahn, M.; Jenke, T. *J. Organomet. Chem.* **1989**, *368*, 103-109.

123. Tsuji, Y.; Ohsumi, T.; Kondo, T.; Watanabe, Y. *J. Organomet. Chem.* **1986**, *309*, 333-344.

124. Chiusoli, G. P.; Costa, M.; Gabriele, B.; Salerno, G. *J. Mol. Catal. A-Chem.* **1999**, *143*, 297-310.

125. Giannoccaro, P. *J. Organomet. Chem.* **1987**, *336*, 271-278.

126. Gupte, S. P.; Chaudhari, R. V. *J. Catal.* **1988**, *114*, 246-258.

127. Sheludyakov, Y. L.; Golodov, V. A. *Bull. Chem. Soc. Jpn.* **1984**, *57*, 251-253.

128. Alper, H.; Hartstock, F. W. *J. Chem. Soc.-Chem. Commun.* **1985**, 1141-1142.

129. Pri-Bar, I.; Alper, H. *Can. J. Chem.-Rev. Can. Chim.* **1990**, *68*, 1544-1547.

130. Murahashi, S.; Mitsue, Y.; Ike, K. *J. Chem. Soc.-Chem. Commun.* **1987**, 125-127.

131. Tam, W. *J. Org. Chem.* **1986**, *51*, 2977-2981.

132. Fukuoka, S.; Chono, M.; Kohno, M. *J. Chem. Soc.-Chem. Commun.* **1984**, 399-400.

133. Kelkar, A. A.; Kolhe, D. S.; Kanagasabapathy, S.; Chaudhari, R. V. *Ind. Eng. Chem. Res.* **1992**, *31*, 172-176.

134. Gabriele, B.; Salerno, G.; Brindisi, D.; Costa, M.; Chiusoli, G. P. *Org. Lett.* **2000**, *2*, 625-627.

135. Gabriele, B.; Mancuso, R.; Salerno, G.; Costa, M. *Chem. Commun.* **2003**, 486-487.

136. Aresta, M.; Giannoccaro, P.; Tommasi, I.; Dibenedetto, A.; Lanfredi, A. M. M.; Ugozzoli, F. *Organometallics* **2000**, *19*, 3879-3889.

137. Stahl, S. S. *Angew. Chem. Int. Ed.* **2004**, *43*, 3400-3420.

138. Kanagasabapathy, S.; Gupte, S. P.; Chaudhari, R. V. *Ind. Eng. Chem. Res.* **1994**, *33*, 1-6.

139. Bolzacchini, E.; Meinardi, S.; Orlandi, M.; Rindone, B. *J. Mol. Catal. A-Chem.* **1996**, *111*, 281-287.

140. Orejón, A.; Castellanos, A.; Salagre, P.; Castillón, S.; Claver, C. *Can. J. Chem.* **2005**, *83*, 764-768.

141. Giannoccaro, P.; De Giglio, E.; Garganno, M.; Aresta, M.; Ferragina, C. *J. Mol. Catal. A-Chem.* **2000**, *157*, 131-141.

142. Presad, K. V.; Chaudhari, R. V. *J. Catal.* **1994**, *145*, 204-215.

143. Shi, F.; Zhang, Q.; Ma, Y.; He, Y.; Deng, Y. *J. Am. Chem. Soc.* **2005**, *127*, 4182-4183.

144. Jetz, W.; Angelici, R. J. *J. Am. Chem. Soc.* **1972**, *94*, 3799-3802.

145. Davies, S. G.; Mortlock, A. A. *Tetrahedron Lett.* **1991**, *32*, 4791-4794.

146. Smith, S. W.; Newman, M. S. *J. Am. Chem. Soc.* **1968**, *90*, 1249-1253.

147. De Lucca, G. V. *J. Org. Chem.* **1998**, *63*, 4755-4766.

148. Lam, P. Y. S.; Ru, Y.; Jadhav, P. K.; Aldrich, P. E.; DeLucca, G. V.; Eyermann, C. J.; Chang, C. H.; Emmett, G.; Holler, E. R.; Daneker, W. F.; Li, L. Z.; Confalone, P. N.; McHugh, R. J.; Han, Q.; Li, R. H.; Markwalder, J. A.; Seitz, S. P.; Sharpe, T. R.; Bacheler, L. T.; Rayner, M. M.; Klabe, R. M.; Shum, L. Y.; Winslow, D. L.; Kornhauser, D. M.; Jackson, D. A.; EricksonViitanen, S.; Hodge, C. N. *J. Med. Chem.* **1996**, *39*, 3514-3525.

149. Confalone, P. N.; Waltermire, R. E. In *Process Chemistry in the Pharmaceutical Industry*; Gadamasetti, K. G., Ed.; Marcel Dekker: New York, 1999, pp 201-219.

150. Lam, P. Y.; Jadhav, P. K.; Eyermann, C. J.; Hodge, C. N.; De Lucca, G. V.; Rodgers, J. D. US Patent 5,610,294, 1997

151. Nugiel, D. A.; Jacobs, K.; Worley, T.; Patel, M.; Kaltenbach, R. F.; Meyer, D. T.; Jadhav, P. K.; DeLucca, G. V.; Smyser, T. E.; Klabe, R. M.; Bacheler, L. T.; Rayner, M. M.; Seitz, S. P. *J. Med. Chem.* **1996**, *39*, 2156-2169.

152. Rossano, L. T.; Lo, Y. S.; Anzalone, L.; Lee, Y. C.; Meloni, D. J.; Moore, J. R.; Gale, T. M.; Arnett, J. F. *Tetrahedron Lett.* **1995**, *36*, 4967-4970.

153. Hodge, C. N.; Aldrich, P. E.; Bacheler, L. T.; Chang, C. H.; Eyermann, C. J.; Garber, S.; Grubb, M.; Jackson, D. A.; Jadhav, P. K.; Korant, B.; Lam, P. Y. S.; Maurin, M. B.; Meek, J. L.; Otto, M. J.; Rayner, M. M.; Reid, C.; Sharpe, T. R.; Shum, L.; Winslow, D. L.; EricksonViitanen, S. *Chem. Biol.* **1996**, *3*, 301-314.

154. Pierce, M. E.; Harris, G. D.; Islam, Q.; Radesca, L. A.; Storace, L.; Waltermire, R. E.; Wat, E.; Jadhav, P. K.; Emmett, G. C. *J. Org. Chem.* **1996**, *61*, 444-450.

155. DeClercq, P. J. *Chem. Rev.* **1997**, *97*, 1755-1792.

156. Zhang, Y.; Forinash, K.; Phillips, C. R.; McElwee-White, L. *Green Chem.* **2005**, *7*, 451-455.

157. Mehta, N. B.; Diuguid, C. A. R.; Soroko, F. E. *J. Med. Chem.* **1981**, *24*, 465-468.

158. Gutschow, M.; Hecker, T.; Eger, K. *Synthesis* **1999**, 410-414.

159. Wessels, F. L.; Schwan, T. J.; Pong, S. F. *J. Pharm. Sci.* **1980**, *69*, 1102-1104.

160. Caldwell, A. G.; Harris, C. J.; Stepney, R.; Whittaker, N. *J. Chem. Soc.-Perkin Trans. 1* **1980**, 495-505.

161. Sarges, R.; Bordner, J.; Dominy, B. W.; Peterson, M. J.; Whipple, E. B. *J. Med. Chem.* **1985**, *28*, 1716-1720.

162. Smith, R. J.; Bratovanov, S.; Bienz, S. *Tetrahedron* **1997**, *53*, 13695-13702.

163. LeTiran, A.; Stables, J. P.; Kohn, H. *Bioorg. Med. Chem.* **2001**, *9*, 2693-2708.

164. Hulme, C.; Ma, L.; Romano, J. J.; Morton, G.; Tang, S. Y.; Cherrier, M. P.; Choi, S.; Salvino, J.; Labaudiniere, R. *Tetrahedron Lett.* **2000**, *41*, 1889-1893.

165. Zhang, D.; Xing, X. C.; Cuny, G. D. *J. Org. Chem.* **2006**, *71*, 1750-1753.

166. Meusel, M.; Gutschow, M. *Org. Prep. Proced. Int.* **2004**, *36*, 391-443.

167. Beller, M.; Eckert, M.; Moradi, W. A.; Neumann, H. *Angew. Chem. Int. Ed.* **1999**, *38*, 1454-1457.

168. Talaty, E. R.; Yusoff, M. M.; Ismail, S. A.; Gomez, J. A.; Keller, C. E.; Younger, J. M. *Synlett* **1997**, 683-684.

169. Choi, D.; Stables, J. P.; Kohn, H. *J. Med. Chem.* **1996**, *39*, 1907-1916.

170. Andurkar, S. V.; Stables, J. P.; Kohn, H. *Tetrahedron: Asymm.* **1998**, *9*, 3841-3854.

171. Bailey, P. D.; Bannister, N.; Bernad, M.; Blanchard, S.; Boa, A. N. *J. Chem. Soc., Perkin Trans. 1* **2001**, 3245-3251.

172. Wolin, R. L.; Venkatesan, H.; Tang, L.; Santillan Jr., A.; Barclay, T.; Wilson, S.; Lee, D. H.; Lovenberg, T. W. *Bioorg. Med. Chem.* **2004**, *12*, 4477-4492.

173. Zhao, M.-X. W. S.-M. *Tetrahedron: Asymm.* **2002**, *13*, 1695-1702.

174. Diaz, D. J. PhD Dissertation, Department of Chemistry, University of Florida, 2007

175. Mills, J. E.; Maryanoff, C. A.; Cosgrove, R. M.; Scott, L.; McComsey, D. F. *Org. Prep. Proced. Int.* **1984**, *16*, 97-114.

176. Hannon, S. J.; Kundu, N. G.; Hertzberg, R. P.; Bhatt, R. S.; Heidelberger, C. *Tetrahedron Lett.* **1980**, *21*, 1105-1108.

177. Chaudhuri, N. K.; Mukherjee, K. L.; Heidelberger, C. *Biochem. Pharmacol.* **1959**, *1*, 328-341.

178. Mukherjee, K. L.; Heidelberger, C. *J. Biol. Chem.* **1960**, *235*, 433-437.

179. Suto, A.; Kubota, T.; Fukushima, M.; Ikeda, T.; Takeshita, T.; Ohmiya, H.; Kitajima, M. *Oncolo. Rep.* **2006**, *15*, 1517-1522.

180. LaFrate, A. L.; Katzenellenbogen, J. A. *J. Org. Chem.* **2007**, *72*, 8573-8576.

181. Kolodziej, S. A.; Hamper, B. C. *Tetrahedron Lett.* **1996**, *37*, 5277-5280.

182. Takano, M.; Mishima, H. Patent EP 1095935, 2001

183. Embrey, M. W.; Wai, J. S.; Funk, T. W.; Homnick, C. F.; Perlow, D. S.; Young, S. D.; Vacca, J. P.; Hazuda, D. J.; Felock, P. J.; Stillmock, K. A.; Witmer, M. V.; Moyer, G.; Schleif, W. A.; Gabryelski, L. J.; Jin, L.; Chen, I. W.; Ellis, J. D.; Wong, B. K.; Lin, J. H.; Leonard, Y. M.; Tsou, N. N.; Zhuang, L. *Bioorg. Med. Chem. Lett.* **2005**, *15*, 4550-4554.

184. Bocci, G.; Danesi, R.; Allegrini, G.; Innocenti, F.; Di Paolo, A.; Falcone, A.; Conte, P. F.; Del Tacca, M. *Eur. J. Clin. Pharmacol.* **2002**, *58*, 593-595.

185. Katritzky, A. R.; Nesbit, M. R.; Kurtev, B. J.; Lyapova, M.; Pojarlieff, I. G. *Tetrahedron* **1969**, *25*, 3807-3824.

186. Rouillier, P.; Delmau, J.; Duplan, J.; Nofre, C. *Tetrahedron Lett.* **1966**, *7*, 4189-4194.

187. Lee, C. K.; Shim, J. Y. *Bull. Korean Chem. Soc.* **1991**, *12*, 343-347.

188. Zee-Cheng, K.-Y.; Robins, R. K.; Cheng, C. C. *J. Org. Chem.* **1961**, *26*, 1877-1884.

189. Delpiccolo, C. M. L.; Albericio, F.; Schiksnis, R. A.; Michelotti, E. L. *Tetrahedron* **2007**, *63*, 8949-8953.

190. Bhat, K. S.; Rao, A. S. *Org. Prep. Proced. Int.* **1983**, *15*, 303-312.

191. Kondo, Y.; Witkop, B. *J. Am. Chem. Soc.* **1969**, *91*, 5264-5270.

192. Duschinsky, R.; Pleven, E.; Heidelberger, C. *J. Am. Chem. Soc.* **1957**, *79*, 4559-4560.

193. Paryzek, Z.; Tabaczka, B. *Org. Prep. Proced. Int.* **2001**, *33*, 400-405.

194. Kundu, N. G.; Sikdar, S.; Hertzberg, R. P.; Schmitz, S. A.; Khatri, S. G. *J. Chem. Soc.-Perkin Trans. 1* **1985**, 1295-1300.

195. Yamamoto, I.; Fukui, K. I.; Yamamoto, S.; Ohta, K.; Matsuzaki, K. *Synthesis* **1985**, 686-688.

196. Deck, L. M.; Papadopoulos, E. P. *J. Heterocyclic Chem.* **2000**, *37*, 675-686.

197. Guemmout, F. E.; Foucaud, A. *Synth. Commun.* **1993**, *23*, 2065-2070.

198. Zhang, C.; Moran, E. J.; Woiwode, T. F.; Short, K. M.; Mjalli, A. M. M. *Tetrahedron Lett.* **1996**, *37*, 751-754.

199. Marzinzik, A. L.; Felder, E. R. *Tetrahedron Lett.* **1996**, *37*, 1003-1006.

200. Gordeev, M. F.; Patel, D. V.; Gordon, E. M. *J. Org. Chem.* **1996**, *61*, 924-928.

201. Goff, D. A.; Zuckerman, R. J. *J. Org. Chem.* **1995**, *60*, 5748-5749.

202. Wipf, P.; Cunningham, A. *Tetrahedron Lett.* **1995**, *36*, 7819-7822.

203. Wu, S.; Janusz, J. M. *Tetrahedron Lett.* **2000**, *41*, 1165-1169.

204. Yang, T.; Lin, C.; Fu, H.; Jiang, Y.; Zhao, Y. *Org. Lett.* **2005**, *7*, 4781-4784.

205. Pretsch, E.; Buhlmann, P.; Badertscher, M. *Structure Determination of Organic Compounds*; 4th ed.; Springer: Berlin, 2009.

206. Beckwith, A. L. J.; Hickman, R. J. *J. Chem. Soc. C.* **1968**, 2756-2759.

207. Eliel, E. L.; Wilen, S. H.; Mander, L. N. *Stereochemistry of Organic Compounds*; Wiley Interscience: New York, 1994.

208. Vogel, A. I.; Tatchell, A. R.; Furnis, B. S.; Hannaford, A. J.; P.W.G., S. *Vogel's Textbook of Practical Organic Chemistry*; 5th ed.; Wiley: New York, 1996.

209. *SHELXTL6*; Bruker-AXS:·Madison, Wisconsin, 2000

210. Frisch, M. J.; Trucks, G. W.; Schlegel, H. B.; Scuseria, G. E.; Robb, M. A.; Cheeseman, J. R.; Montgomery, J. J. A.; Vreven, T.; Kudin, K. N.; Burant, J. C.; Millam, J. M.; Iyengar, S. S.; Tomasi, J.; Barone, V.; Mennucci, B.; Cossi, M.; Scalmani, G.; Rega, N.; Petersson, G. A.; Nakatsuji, H.; Hada, M.; Ehara, M.; Toyota, K.; Fukuda, R.; Hasegawa, J.; Ishida, M.; Nakajima, T.; Honda, Y.; Kitao, O.; Nakai, H.; Klene, M.; Li, X.; Knox, J. E.; Hratchian, H. P.; Cross, J. B.; Bakken, V.; Adamo, C.; Jaramillo, J.; Gomperts, R.; Stratmann, R. E.; Yazyev, O.; Austin, A. J.; Cammi, R.; Pomelli, C.; Ochterski, J. W.; Ayala, P. Y.; Morokuma, K.; Voth, G. A.; Salvador, P.; Dannenberg, J. J.; Zakrzewski, V. G.; Dapprich, S.; Daniels, A. D.; Strain, M. C.; Farkas, O.; Malick, D. K.; Rabuck, A. D.; Raghavachari, K.; Foresman, J. B.; Ortiz, J. V.; Cui, Q.; Baboul, A. G.; Clifford, S.; Cioslowski, J.; Stefanov, B. B.; Liu, G.; Liashenko, A.; Piskorz, P.; Komaromi, I.; Martin, R. L.; Fox, D. J.; Keith, T.; Al-Laham, M. A.; Peng, C. Y.; Nanayakkara, A.; Challacombe, M.; Gill, P. M. W.; Johnson, B.; Chen, W.; Wong, M. W.; Gonzalez, C.; Pople, J. A. *Gaussian 03, Revision B.04*, 2004

211. Gorelsky, S. I.; Lever, A. B. P. *J. Organomet. Chem.* **2001**, *635*, 187-196.

212. Gorelsky, S. I. *AOMix: Program for Molecular Orbital Analysis*; University of Ottawa, 2009

213. Edward, J. T.; Lantos, I. *Can. J. Chem.* **1967**, 1925-1934.

214. Lazarus, R. A. *J. Org. Chem.* **1990**, *15*, 4755-4757.

215. Pham, T. Q.; Pyne, S. G.; Skelton, B. W.; White, A. H. *J. Org. Chem.* **2005**, *16*, 6369-6377.

216. Sanders, M. L.; Donkor, I. O. *Synthetic Commun.* **2002**, *7*, 1015-1021.

217. Banjac, N.; Uscumlic, G.; Valentic, N.; Mijin, D. *J. Solution Chem.* **2007**, *36*, 869-878.

BIOGRAPHICAL SKETCH

Seth M. Dumbris was born in Evansville, Indiana February 22, 1982. He graduated from Model Laboratory High School in 2000. His undergraduate studies were conducted at Western Kentucky University as he was awarded a B.S. in chemistry in May of 2004.